

Ammonium Attenuation and Nitrogen Dynamics in Groundwater Impacted by
a Poultry Manure Lagoon

by

Brent Lazenby

A thesis
presented to the University of Waterloo
in fulfillment of the
thesis requirement for the degree of
Master of Science
in
Earth Sciences

Waterloo, Ontario, Canada, 2011

© Brent Lazenby 2011

Author's Declaration

I hereby declare that I am the sole author of this thesis. This is a true copy of the thesis, including any required final revisions, as accepted by my examiners.

I understand that my thesis may be made electronically available to the public.

Brent K.E. Lazenby

Abstract

Fertilizer application and manure use practice in agriculture has become one of the most common sources of dissolved nitrogen species to both ground and surface waters. Nitrogen, released as nitrate (NO_3^-), ammonium (NH_4^+) and/or organic nitrogen (DON) is subject to a variety of transformation and attenuation processes in groundwater, including sorption, nitrification, denitrification, dissimilatory nitrate reduction to ammonium (DNRA), ammonification and anaerobic ammonium oxidation (anammox). Of these, only denitrification and anammox represent complete attenuation of nitrogen, releasing nitrogen gas (N_2). This study examines the occurrence and mechanisms of nitrogen attenuation in groundwater affected by a manure lagoon. Lagoon effluent is in strong contrast to background water with elevated chemical constituents including NH_4^+ (mean = 121 mg N/L) and DON (218 mg N/L), which are transported through a fast moving groundwater flow system. The NH_4^+ rich plume interacts with NO_3^- rich background water at an interface ~3 m below ground surface. Over 100 m of groundwater transport from the source, total nitrogen (TN) was consistently reduced by 90% over two years of study. This reduction can be largely attributed to dilution (~ 80%), but the remaining 10% reflects a component of nitrogen loss due to attenuation, reflecting 32 mg N/L in attenuation and a TN degradation rate of 0.4 mg/L/day. Localized zones of nitrification and denitrification are evidenced by loss of NO_3^- accompanied by elevated N_2O emissions. Anammox is implicated by localized enrichment of $\delta^{15}\text{N}$ with according decreases in both NO_3^- and NH_4^+ at the plume-background interface and through corroborating microbiological study. Ammonification of DON along the flow path, something not observed in similar studies, is conjectured to have a confounding effect on a detailed isotopic investigation by introducing a second source of NH_4^+ that is depleted in $\delta^{15}\text{N}$ - NH_4^+ .

Acknowledgements

I would like to thank my supervisor, Dr. Will Robertson, and committee members Dr. Sherry Schiff, Dr. Ramon Aravena and Dr. John Spoelstra for their advice and assistance over the course of my degree. I would also like to thank the research group at the University of Ottawa and our colleagues in the Department of Biology here at UW for their collaboration in anammox research.

Thanks to everyone who helped with field work over the years: crafting and installing piezometers, surveying well elevations and groundwater sampling; especially when dealing with pesky mosquitoes, interesting aromas from the lagoon and swampy conditions. Your help was appreciated and I couldn't have completed this work without you all! Special thanks to Bob Ingleton and Paul Johnson for help during well installations and to Jon Gingerich and Tom who helped make things run a bit more smoothly at the field site.

The utmost thanks are due to everyone who has been in and out of the Environmental Geochemistry Laboratory at UW. Days in the field followed by days of running samples and helping me find my way around the lab were invaluable to this research. Thanks in particular to Justin Harbin, who was always willing to lend a hand and patient enough to teach me a technique or two and above all thanks to Richard Elgood without whom many students like me would not make it through their first months, let alone reach graduation.

Finally, thanks to my friends and family for their continued support through this adventure. Be it for a relaxing beverage, game of hockey, coffee run, couch to sleep on, BBQ or even a trip to Brazil (thanks Habibis!), the people I met over these years were always around to support me through the best and worst of times and I'll always be grateful to every one of them. It's been quite an adventure, thank you all!

Table of Contents	Page
List of Tables	viii
List of Figures	ix
1.0 Introduction	
1.1 Agricultural Nitrogen Contamination	1
1.2 Manure Composting	7
1.3 Research in NH_4^+ Attenuation	8
1.4 Field Site	12
1.5 Research Objectives	13
2.0 Methods	
2.1 Field Methods	14
2.1.1 Monitoring Well Installation	
2.1.2 Aquifer Characterization	
2.1.3 Groundwater Sampling	
2.1.4 NO_3^- , NH_4^+ , DO	
2.1.5 EC, DO, E_o , pH	
2.2 Laboratory Methods	17
2.2.1 Cations	
2.2.2 Anions	
2.2.3 N_2O	
2.2.4 Total Nitrogen, TKN, NO_2^-	
2.2.5 $\delta^{18}\text{O}\text{-H}_2\text{O}$	
2.2.6 $\delta^{15}\text{N}\text{-NO}_3^-$	
2.2.7 $\delta^{15}\text{N}\text{-NH}_4^+$	
2.2.8 Ammonification Experiments	
3.0 Results	
3.1 Aquifer Description	23
3.2 Groundwater Flow System	23

3.3 Lagoon Geochemistry	25
3.3.1 Redox Setting	
3.4 Plume Indicator Parameters	27
3.4.1 Electrical Conductivity	
3.4.2 Cl^-	
3.4.3 Na^+	
3.4.4 K^+	
3.4.5 Plume Extent using Conservative Tracers	
3.5 Nitrogen Distribution	30
3.5.1 NH_4^+	
3.5.2 NO_3^-	
3.5.3 DON	
3.5.4 NO_2^-	
3.5.5 N_2O	
3.5.6 Total Nitrogen	
3.5.7 $\delta^{15}\text{N-NO}_3^-$	
3.5.8 $\delta^{15}\text{N-NH}_4^+$	
3.6 Other Parameters	34
3.6.1 pH	
3.6.2 DO	
3.6.3 Ca^{2+}	
3.6.4 Fe^{2+}	
3.6.5 DOC	
3.7 Ammonification Experiments	35
4.0 Discussion	
4.1 Plume Comparison to Other Sites	37
4.2 Nitrogen Synthesis, Zorra Site	38
4.3 Nitrogen Attenuation in the Zorra Plume	39
4.4 Mechanisms of Nitrogen Attenuation	41
4.4.1 Sorption	
4.4.2 Nitrification	

4.4.3 Denitrification	
4.4.4 Anammox	
4.4.5 Ammonification	
5.0 Summary & Conclusions	52
References	56
Appendices	
Appendix A: Well Construction Details & Water Levels	112
Appendix B: Borehole Logs and Grain Size Analysis	117
Appendix C: Geochemical Data August 2008 – November 2009	129
Appendix D: Ammonification Experiments	146
Appendix E: Additional Figures	149

List of Tables

Table 1	Hydraulic Conductivities and Groundwater Velocity	66
Table 2	Lagoon Geochemistry August 28, 2008 – January 7, 2010	67
Table 3	Lagoon and Background Chemical Parameters	68
Table 4	Percent Composition of Total Nitrogen	69
Table 5	NH ₄ ⁺ -N and TN Reduction Along the Centre Line	71
Table 6	Percent Reduction of NH ₄ ⁺ -N and TN Through Time Along the Fenceline	72
Table 7	Ammonification Experiment Results	73

List of Figures

Figure 1	Major Pathways of NH_4^+ and NO_3^- Reactions	74
Figure 2	Zorra Site Regional Site Map	75
Figure 3	Zorra Site Monitoring Well Locations and Transects	76
Figure 4	Generalized Geology Along the Site Centre Line	77
Figure 5	Hydraulic Conductivity Depth Profiles	78
Figure 6	Water Table Maps for Zorra Site	79
Figure 7	Geochemistry at Lagoon and Background Locations	80
Figure 8	Site Distribution of Cl^- (Plan View) August 2008	81
Figure 9	Site Distribution of EC (Plan View) August 2008	82
Figure 10	Distribution of EC Along the Centre Line August, October 2009	83
Figure 11	Distribution of DO in Plan View and Along the Centre Line August 2009	84
Figure 12	Site Distribution of Na^+ (Plan View) August 2008, July 2009	85
Figure 13	Na^+ Distribution Along Transects A-E July 15, 2009	86
Figure 14	Distribution of Na^+ Along the Centre Line August, November 2009	88
Figure 15	Site Distribution of K^+ (Plan View) August 2008, July 2009	89
Figure 16	Distribution of K^+ Along the Centre Line August, November 2009	90
Figure 17	Site Distribution of NH_4^+ -N (Plan View) August 2008, July 2009	91
Figure 18	Site Distribution of NO_3^- -N (Plan View) August 2008, July 2009	92
Figure 19	Distribution of N_2O in Plan View & Along the Centre Line August 2009	93
Figure 20	Distribution of NO_3^- , NH_4^+ and N_2O Along Transect A July 2009	94
Figure 21	Distribution of NO_3^- , NH_4^+ and N_2O Along Transect B July 2009	95
Figure 22	Distribution of NO_3^- , NH_4^+ and N_2O Along Transect C July 2009	96
Figure 23	Distribution of NO_3^- , NH_4^+ and N_2O Along Transect D July 2009	97
Figure 24	Distribution of NO_3^- , NH_4^+ and N_2O Along Transect E July 2009	98

Figure 25	Distribution of NH_4^+ , NO_3^- , DON and TN Along the Centre Line August 20, 2009	99
Figure 26	Distribution of NH_4^+ , NO_3^- , DON and TN Along the Centre Line November 13, 2009	100
Figure 27	$\delta^{15}\text{N}$ of NH_4^+ and NO_3^- Along the Centre Line August 2009	101
Figure 28	Distribution of Ca^{2+} Along the Centre Line August, November 2009	102
Figure 29	Distribution of Fe^{2+} Along the Centre Line August, November 2009	103
Figure 30	Distribution of pH and DOC Along the Centre Line August 2009	104
Figure 31	Ratio of $\text{NH}_4^+ / \text{Na}^+$ Along the Centre Line August, November 2009	105
Figure 32	Ratio of TN/ Na^+ Along the Centre Line August, November 2009	106
Figure 33	$\delta^{15}\text{N}$ of NH_4^+ and NO_3^- and Concentrations	107
Figure 34	Breakthrough Curves	108
Figure 35	Depth Profiles for Nitrogen Species at PU124, 92 & 125	109
Figure 36	Nitrogen Loss Along the Centre Line August, November 2009	110
Figure 37	Ammonification Experiment Results	111

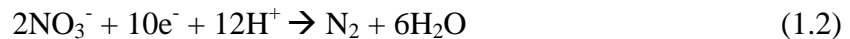
1.0 Introduction

1.1 Agricultural Nitrogen

Over the last three decades annual poultry production in Ontario has nearly doubled from almost 106 000 to 203 000 individuals (Statistics Canada, 2007). The amount of poultry waste has thus increased and is a preferred source for fertilizer use due to its high nitrogen content of 4-5% (Amanullah et al., 2010). Increases in anthropogenic nitrogen loading has led to increasing nitrogen concentrations in ground and surface waters, such as a threefold increase in nitrate (NO_3^-) in the lower Mississippi River over the last thirty years (Goolsby et al., 2001). Such observations have been prompting policy makers to look at ways of controlling fertilizer application rates (Kaiser et al., 2010; de Vries et. al., 2003; Mallin and Cahoon, 2003; Goss et. al., 2001). Nitrate, and its reduced form nitrite (NO_2^-), have been associated with methaemoglobinaemia in infants (Health Canada, 1992) and as a result, a drinking water guideline of 10 mg/L NO_3^- -N (Ontario MOE, 2003) has been developed. Ammonium (NH_4^+) in groundwater has received less attention as a contaminant because levels normally found in drinking water supplies are not considered a cause for human health concern (Health Canada, 1987). However, elevated NH_4^+ in drinking water supplies can decrease the efficiency of disinfection systems by interfering with chlorine effectiveness as well as adversely affecting aesthetic factors, such as the taste and odour, at concentrations above 0.2 mg/L (World Health Organization, 2003). In surface water environments NH_4^+ is assumed to volatilize as ammonia gas (NH_3), to nitrify to NO_3^- in the presence of oxygen or to be taken up by aquatic plants. When NH_4^+ volatilization does not reach completion, dissolved un-ionized ammonia ($\text{NH}_{3(\text{aq})}$) can contribute to fish mortality and other adverse ecosystem effects at low concentrations (Buss et

al., 2004) . As such, the province of Ontario recommends a maximum concentration of 20 ug/L un-ionized ammonia in surface waters for the protection of aquatic life (CCME, 1998).

Upon release into the environment, NH_4^+ can be biologically converted to NO_3^- or NO_2^- through nitrification (Eq. 1.1). Subsequently, one way in which reactive NO_3^- can be eliminated from the environment is by denitrification which ultimately yields only dinitrogen gas (N_2) as a product (Eq. 1.2). However, denitrification is known to produce nitrous and nitric oxides (N_2O and NO) as intermediate byproducts (Eq. 1.3) which are greenhouse gases and can ‘leak’ from the reaction pathway into the environment (Pérez et al., 2006). In groundwater environments, the overall elimination of nitrogen has been most frequently attributed to a combination of nitrification, which oxidizes any NH_4^+ present (Eq. 1.1) and denitrification, which sequentially reduces NO_3^- to N_2 in anaerobic conditions (Payne, 1976; Korom, 1992; Zumft, 1997) (Eq. 1.3).



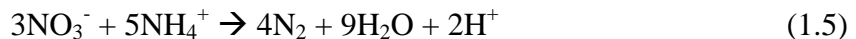
Key intermediates in both nitrification and denitrification reactions include hydroxylamine (NH_2OH), N_2O and NO_2^- (Buss et al., 2004). From Eq. 1.1, any NH_4^+ that has been eliminated is merely transformed to NO_3^- , but once conditions become anaerobic in the subsurface, denitrification can take over using a variety of possible electron donors including organic carbon (Trudell et al., 1986; Lu et al., 2009; Robertson et al., 2008), reduced sulphur (Postma et al., 1991; Aravena and Robertson, 1998; Torrento et al., 2010) and reduced forms of dissolved metals iron (Fe^{2+}) and manganese (Mn^{2+}) (Straub et al., 1996; Saunders et al., 1997;

Penny et al., 2003). Incomplete denitrification can allow the release of any of the intermediate products shown in Eq. 1.3, which can each have their own environmental effects.

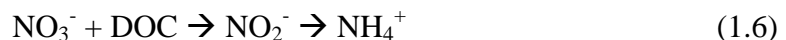
An alternative to the nitrification/denitrification pathway for elimination of nitrogen from a groundwater system is anaerobic ammonium oxidation (anammox). Bacteria responsible for this reaction have been shown to be active in groundwater systems (Moore et al., 2010; Robertson et al., 2010) while geochemical and isotopic evidence have also indicated their activity in industrially impacted groundwater (Clark et al., 2008). Concurrent with this study, two of the four known genera of anammox bacteria have been positively identified on site and comprise up to 5% of the total bacterial community at the current study site (Zorra site, Moore et al., 2010). In its most basic form, anammox is the reaction between NH_4^+ and NO_2^- with N_2 as the reaction product (Thamdrup and Dalsgaard, 2002) (Eq. 1.4):



Alternatively the reaction is expressed by embedding the reduction of NO_3^- to NO_2^- as part of the reaction (Mulder et. al., 1995) (Eq.1.5):



Although nitrification, denitrification and anammox are normally considered the major pathways of nitrogen transformation in most aquatic environments, NO_3^- can also be reduced to NH_4^+ in environments that have low NO_3^- and high dissolved organic carbon (DOC). This is referred to as dissimilatory nitrate reduction to ammonium (DNRA; Eq. 1.6) (Smith et al., 1991; Kelso et al., 1997; Silver et al., 2001).



Additional NH_4^+ can also be produced in organic rich environments through the process of ammonification, whereby dissolved organic nitrogen (DON) is mineralized into biologically available NH_4^+ (Eq. 1.7); a process that is influenced by pH, temperature, dissolved oxygen and moisture content (Nahm, 2003).



This less considered reaction has been largely unstudied in groundwater. Normally, ammonification is not considered significant in groundwater studies because dissolved organic matter (DOM) values are usually low in groundwater systems (eg. < 2.5 mg/L, Smith et al., 1991; < 8 mg/L, Aravena and Robertson, 1998; < 1 mg/L, Loveless and Oldham, 2010), although isotopic evidence has suggested that ammonification may play a role in aquifer nitrogen conversions where DON is high (Karr et al., 2001). Ammonification is often implicated as an important process in constructed wetlands, occurring in both oxygenated and anaerobic zones (Lee et. al, 2009), where the process occurs in a wide range of pH, temperature and substrate conditions (Vymazal, 2002). The discovery of nitrogen reactions in groundwater such as DNRA, and more recently chemolithotrophic denitrification and anammox has created a nitrogen cycle that is becoming increasingly complex. Fig. 1 shows a conceptual view of the range of nitrogen cycle reaction pathways that are possible within a groundwater environment.

Denitrification has previously been considered the dominant reactive nitrogen attenuation process in groundwater and surface water environments, although this notion is changing (Burgin and Hamilton, 2007; de Vries et al., 2003). In marine (Thamdrup and Dalsgaard, 2002; Jensen et al., 2008; Kuenen et al., 2008), sediment (Rysgaard et al., 2004) and aqueous systems (Hamersley et al., 2009; Schubert et al., 2008), the anammox reaction has been found to

dominate over denitrification in some environments. The problem remains however, that specific conditions which drive anammox rather than denitrification are poorly understood. Dissolved O₂ (DO), substrate concentrations (NH₄⁺, NO₃⁻, NO₂⁻), DOC and environmental conditions (pH, E_h and temperature) are all expected to have significant impacts on the potential reactions that dominate. In groundwater systems, anammox has recently been investigated as a potential reactive mechanism (Bohlke et. al., 2006; Clark et. al., 2008; Robertson et al., 2010) and anammox bacteria have been positively identified in groundwater at several sites in Ontario (Moore et al., 2010).

In addition to biological reactions, the nitrogen cycle is influenced by abiotic factors such as sorption (in groundwater) and volatilization (in surface water and near the unsaturated zone). The effects of cation exchange are most often summarized in terms of the retardation factor (R) of a chemical component. This parameter is simply the ratio of the groundwater velocity of a given dissolved species to the velocity of a conservative tracer (Eq. 1.8).

$$R = \frac{v_{tracer}}{v_{species}} \quad (1.8)$$

Cation exchange and sorption can influence the movement of cations, including NH₄⁺, through solution. NH₄⁺ has a similar affinity to that of potassium (K⁺) for cation exchange sites (R = 1-4 Dance and Reardon, 1983; Ceazan et al., 1989; DeSimone et al., 1997; Nuñez-Delgado et al., 1997; Böhlke et al., 2006). The sorption of these ions is most often accompanied by the displacement of existing sodium (Na⁺), calcium (Ca²⁺) and magnesium (Mg²⁺) ions on exchange sites (Dance and Reardon, 1983; Bjerg and Christensen, 1993). Sorption is considered a significant process particularly in clay dominated sediments, with sand and gravel dominated aquifers having a much lower cation exchange capacity, although sorption can still play an

important role at such sites (Dance and Reardon, 1983; Ceazan et al., 1989). Conversion of NH_4^+ to NH_3 and then volatile loss to the atmosphere is possible near the water table, but this reaction is controlled by the NH_4^+ pK_a of 9.25 (Lide and Haynes, 2010) and thus may become more important only in high pH environments. Also, because this reaction relies on the interface between the saturated and unsaturated zone, nitrification may be the more likely reaction pathway for NH_4^+ loss (Christensen et al., 2001). Rarely, either NH_4^+ or NO_3^- can form complexes with other ions including dissolved metals or anions, but the solubility products (K_{sp}) of these compounds is less than the dissolved species (Lide and Haynes 2010), thus these compounds are less mobile in groundwater systems, but do not commonly occur in groundwater environments.

In differentiating biological reactions from abiotic reactions, or from one another, environmental isotope techniques are often employed. Nitrogen exists most commonly as two isotopes: ^{14}N (most abundant) and ^{15}N (0.366% abundant in air). The ways in which the ratio of $^{15}\text{N}:^{14}\text{N}$ in NH_4^+ , NO_3^- , N_2O and DON changes along a flow path is a reflection of the processes acting upon these constituents. Most commonly, $^{15}\text{N}/^{14}\text{N}$ of a compound is expressed as a ‘permil’ value, calculated by Eq. 1.9 with the reference abundance ratio coming from atmospheric N_2 (Clark and Fritz, 1997).

$$\delta^{15}\text{N}_{sample} = \left(\frac{(^{15}\text{N}/^{14}\text{N})_{sample}}{(^{15}\text{N}/^{14}\text{N})_{reference}} - 1 \right) * 1000\text{‰ AIR} \quad (1.9)$$

1.2 Manure Composting

Poultry manure is typically very high in nutrients, including nitrogen (N; 4-5%), phosphorus (P; 1%), K^+ (1%), Ca^{2+} (5%) and a number of metals such as zinc (Zn^{2+}), copper (Cu^{2+}) and manganese (Mn^{2+}); all of which stimulate plant growth (Brown, 2005; Amanullah et al., 2010). Composting of manure is a common practice as it concentrates nutrients and minimizes mass (Larney et al., 2006). For effective composting, high nitrogen manure must be combined with a carbon source to develop a mixture with an appropriate carbon to nitrogen (C:N) ratio, be sufficiently exposed to O_2 and kept appropriately moist (Rynk, 1992). The need to mix manure with a carbon source is especially pronounced in the composting of poultry manure, which is extremely high in nitrogen compared to other manure sources (Nahm, 2003). A common composting technique is the use of windrows; a series of long, shallow rows of manure that can be easily turned. During windrow composting, nitrogen as NH_4^+ can be readily lost from the system due to volatilization as NH_3 in basic pH conditions (Sheppard et al., 2008). Additionally, partial nitrification during composting can yield an abundance of gaseous N_2O , which is a greenhouse gas (IPCC, 2007; Hayakawa et al., 2009; Avrahami et al., 2009).

Windrow composting requires a significant amount of time for completion. Regular turning of material is required to maintain air exposure and aerobic conditions and to maintain adequate moisture levels. Compost piles are normally maintained for about six months for complete conversion of the raw manure to a commercially viable product (Moon, 1997). A common strategy to have irrigation water available for maintaining adequate moisture content is to construct a holding pond or manure 'lagoon' at the downgradient edge of windrows to collect liquid runoff. To minimize impacts on underlying groundwater and downgradient surface water systems, holding ponds are recommended to be situated over at least 1 m of hydraulically secure

soil and 50 m away from any surface water bodies (Ward and Johnson, 2009). Additionally, lagoon systems may develop bottom sludge layers, which over time can improve the effectiveness of existing hydraulic barriers (Meyer et al., 1972). Such layers are never entirely impermeable to prevent leakage to the adjacent groundwater system, and so, some infiltration can be expected in most cases.

1.3 Research in NH_4^+ Attenuation

Research specifically in the area of NH_4^+ attenuation in groundwater is scattered and far between (Ceazan et al., 1989; Karr et al., 2001; Fernando et al., 2005; Böhlke et al., 2006; Sills, 2006; Loveless and Oldham, 2010) while consideration of NH_4^+ dynamics is often a secondary piece to the story of NO_3^- movement and attenuation through a system. A detailed study of the attenuation of all major nitrogen components, including NO_3^- , NH_4^+ and DON, incorporating investigation of all possible nitrogen cycle components (including reactions such as anammox, DNRA and ammonification) is lacking in groundwater literature. Instead, typically one or two components of the cycle are examined in detail, with ‘minor’ contributors left untouched. Research investigating these newer processes however, should open the door for a greater understanding of the complete nitrogen cycle in groundwater.

Manure lagoon effluents have been the focus of a number of studies, although few of these studies focus on the complete attenuation cycle of nitrogen from the source. Existing focussed studies include investigating the behaviour of lagoon seepage to the water table (McNab et al., 2007), determining typical $\delta^{15}\text{N-NH}_4^+$ values for manure lagoons across the United States (Mariappan et al., 2010), researching the geochemical effects of lagoon spills on surface waters (Mallin et al., 1991) and studying the behaviour of NO_3^- as a component of lagoon

plumes (Karr et al., 2001). Sills (2006; field based) and Fernando et al. (2005; laboratory based) both investigated the fate of NH_4^+ in groundwater affected by a manure lagoon. Both studies identified sorption (based on $\delta^{15}\text{N-NH}_4^+$ trends and equilibration experiments in the field and laboratory respectively) as the main mode of NH_4^+ attenuation, but did not go into detail about the ultimate fate of nitrogen as a whole. The system described by Sills (2006) was an anaerobic ($\text{DO} < 1 \text{ mg/L}$) NH_4^+ dominated system with little to no NO_3^- or DON. NH_4^+ -N up to 3700 mg/L occurred in the source manure lagoon, and ranged from 300-1500 mg/L in proximal groundwater along the plume. The majority of these concentrations decreased to $< 1 \text{ mg/L}$ where clay layers were present in the geological system. NO_3^- -N concentrations were typically $< 1.0 \text{ mg/L}$ throughout the system and absent in the plume core zone coincident with NH_4^+ . Total Kjeldahl nitrogen (TKN) analysis from the Sills study identified NH_4^+ as the primary nitrogen component, with DON concentrations assumed to be within the range of analytical error (unspecified). Sorption was determined to be the main mode of attenuation with $\delta^{15}\text{N-NH}_4^+$ ranging from 5.7-12.2 ‰; varying slightly amongst wells and showing slight depletion from a mean of 12‰ to 6‰ along the centre line in accordance with a decrease in NH_4^+ -N from above 2500 mg/L to less than 10 mg/L.

Mariappan et al. (2010) performed a survey of surficial $\delta^{15}\text{N-NH}_4^+$ values at 13 lagoons throughout the state of Nebraska, citing a range of 2.0-59.1‰. This variability emphasizes the need to consider the source characteristics when assessing subsurface nitrogen evolution. The study notes that as lagoons mature, higher $\delta^{15}\text{N-NH}_4^+$ values are measured. The highest $\delta^{15}\text{N-NH}_4^+$ values were attributed to the effect of NH_4^+ -N volatilization, which leaves a $^{15}\text{N}/^{14}\text{N}$ enriched pool of NH_4^+ in open lagoons. This volatilization effect was minimized in lagoons that were frequently fed new wastewater.

Fernando et al. (2005) explored cation exchange characteristics of a swine manure slurry ($\text{NH}_4^+\text{-N} = 475 \text{ mg/L}$) through a silty sand loam in the laboratory. Compared to an ammonium sulphate control, higher sorption effects were observed for the slurry solution. The study postulates that the high DOC (1232 mg/L) in the slurry increased the affinity for NH_4^+ sorption, although the potential for desorption of cations over time remained.

Karr et al. (2002) also investigated a manure lagoon source, focussing on using $\delta^{15}\text{N-NO}_3^-$ as a fingerprinting tool for NO_3^- in groundwater. Other aspects of the source lagoon were not investigated in detail. A lagoon concentration of 742 mg/L $\text{NH}_4^+\text{-N}$ with a corresponding $\delta^{15}\text{N-NH}_4^+$ of 15.0 ‰ was reported, which was consistent with the general range of $^{15}\text{N-NO}_3^-$ (13.0 - 16.0 ‰) along the groundwater plume. Lagoon DON was reported as 30 mg N/L, while concentrations dropped to below 2 mg/L elsewhere within the monitoring network whereas $\text{NH}_4^+\text{-N}$ values ranged from 1-21 mg/L in the same areas.

NH_4^+ attenuation in general has been addressed in some other groundwater settings. The majority of groundwater studies examining NH_4^+ attenuation deal with concentrations on the low mg/L to $\mu\text{g/L}$ scale, which makes it difficult to compare with manure lagoon studies. Typically, NH_4^+ attenuation in groundwater has been attributed to coupled nitrification/denitrification and sorption, although recent research has considered anammox as a viable attenuation pathway (Buss et al., 2002; Böhlke et al., 2006). Studies by Böhlke et al. (2006) and Loveless and Oldman (2010) examined anaerobic aquifer systems (a wastewater plume and coastal aquifer respectively) where $\text{NH}_4^+\text{-N}$ and $\text{NO}_3^-\text{-N}$ coexisted with maximum concentrations of 1.4 mg/L and 0.2 mg/L respectively. Observations at the 1 mg/L scale can be difficult to compare to those in studies by Sills (2006) and Fernando et al. (2005) where $\text{NH}_4^+\text{-N}$ concentrations are often above 400 mg/L.

Böhlke et al. (2006) used the isotopic composition of nitrogen species and spatial trends to conclude that anammox was of minimal significance in NH_4^+ attenuation at a septic field site. Instead NH_4^+ was attenuated by nitrification in the shallow zone and sorption in the waste water plume core. Samples analyzed from the plume core ranged from 10.0-13.0‰ for $\delta^{15}\text{N-NH}_4^+$ (with NH_4^+ -N concentrations ranging from 30-700 $\mu\text{g/L}$), while substantial isotopic enrichment ($\delta^{15}\text{N-NH}_4^+$ up to 30.0‰) was observed exclusively along the upper fringe of the plume where nitrification was occurring. A study of industrially affected groundwater examined by Clark et al. (2008) used isotopic composition and enrichment of $\delta^{15}\text{N}$ in NO_3^- and NH_4^+ to suggest that anammox was occurring. With NH_4^+ -N (500-700 mg/L) at one source zone able to interact with NO_3^- -N (150-300 mg/L) from a second source, isotopic changes provided evidence for anammox inclusive attenuation along the flow path. $\delta^{15}\text{N-NO}_3^-$ values ranged widely from 12.0-24.0 ‰, while $\delta^{15}\text{N-NH}_4^+$ ranged from 5.0-20.0 ‰, changing within the source and along the plume flow path. In this case, changes in $\delta^{15}\text{N-NO}_3^-$ and $\delta^{15}\text{N-NH}_4^+$ could not be explained by a combination of nitrification/denitrification, suggesting anammox as an attenuation alternative.

Most recently, a study at a septic plume site by Robertson et al. (2010) revealed anammox to be an important attenuation mechanism in a zone where both NH_4^+ -N and NO_3^- -N were present together (both >5 mg/L). Reduction in mean NH_4^+ -N concentration values from 48 to 8 mg/L was accompanied by enrichment of $\delta^{15}\text{N-NH}_4^+$ in the proximal zone of 7.8‰ to an average of 15.7‰ in the distal zone. This change was also supported by positive identification of anammox-performing organisms to suggest reduction due to anammox activity. Total nitrogen removal by anammox at the site was estimated at 1-2 mg N/L per day.

1.4 Field Site

The field site of interest in this study is a poultry manure composting operation located in Zorra Township in southwestern Ontario. The site has a shallow unconfined aquifer system comprised of glaciofluvial outwash consisting of everything from fine silts/clays to very coarse gravel (Robertson and Schiff, 2008). Downgradient of the manure composting windrows is a runoff control lagoon (manure lagoon), approximately 20 m x 50 m in surface area and varying from about 1 to 2 m in depth. The 'shoreline' of the lagoon varies by tens of metres over a season; hence its surface area is also seasonally variable. The lagoon was constructed with a low permeability clay berm at its downgradient end to prevent surface runoff. The lagoon water level can vary seasonally by more than a metre. The facility accepts poultry manure from a number of farms and is considered a relatively large scale composting operation. The geochemistry of the lagoon water is seasonally variable, but consistently has elevated NH_4^+ , DOC, DON, chloride (Cl^-), Na^+ , K^+ and electrical conductivity (EC). The Thames River is located ~ 200m downgradient from the lagoon. A second compost yard is located ~300 m west of the lagoon, while active sand and gravel pits are within 50 m of the lagoon. Previous work at this site has included the testing of permeable reactive barriers (PRBs) to promote denitrification of groundwater NO_3^- (McLean, 2007; Robertson et al., 2007) and investigation of the fate of groundwater nitrogen in an adjacent riparian zone (Robertson and Schiff, 2008). A regional shallow unconfined aquifer is present that is heavily influenced by agriculture (mostly corn production) and consequently, background groundwater is elevated in NO_3^- (Robertson and Schiff, 2008). The monitoring network at the site (Fig. 2, 3) was designed to incorporate a series of five monitoring well transects extending downgradient from the lagoon transverse to

groundwater flow, from which a plume centre line was identified for more detailed sampling focus.

1.5 Research Objectives

The main objective of the current study was to investigate the fate and possible attenuation of the elevated nitrogen concentrations associated with the manure lagoon. Nitrogen in the lagoon occurs primarily as NH_4^+ and organic nitrogen, but nitrification could occur in the 1-2 m thick, oxygenated vadose zone underlying the lagoon. Also, groundwater under the adjacent fields is NO_3^- rich (Robertson and Schiff, 2008). Thus the possibility exists that both NH_4^+ and NO_3^- may coexist in the plume water at this site. This then opens the possibility that anammox may also be an important component of nitrogen attenuation, in addition to denitrification, at this site. The study approach was to use geochemical and isotopic tracers to identify nitrogen derived from the manure lagoon and to infer if nitrogen attenuation reactions were active.

2.0 Methods

2.1 Field Methods

2.1.1 Monitoring Well Installation

Multi-level monitoring wells were constructed using 1.2 cm diameter PVC pipe for the centre pipe with additional 3 mm diameter polyethylene tubes screened with Nitex screen at variable depths (construction details in Appendix A; Table A-1). These were installed first in August 2008, using a hand auger and then subsequently, using removable steel casing driven into the ground, using a percussive hammer. Wells were backfilled using clean sand from the nearby sand pit. After August 2008, monitoring wells were installed using a Geoprobe direct push remote controlled drill rig. Using this method, some wells (PU103, PU106, and PU122-125) were installed to depths between 7.5 and 9 m. During the drilling process, continuous soil cores were extracted for microbiological sampling and geological characterization. Prior to use as groundwater sampling points, sampling ports were purged using a peristaltic pump for 15 minutes.

2.1.2 Aquifer Characterization

Water level measurements (from the top of the PVC pipe, ± 1.0 cm) were routinely measured throughout the monitoring network using Solinst Water Level Meter tapes (Solinst Georgetown, ON). Borehole logs were constructed based on continuous core samples retrieved from ground surface to up to 9.0 m depth (Appendix B; Fig. B-2-B-7). Samples were taken at ~ 0.5 m depth intervals for grain size analysis. The sediments were shaken through a series of sieves 0.075 – 4.0 mm using a Meinzer ii Sieve Shaker (CSC Scientific, Fairfax VA), for 15

minutes per sample. Estimated hydraulic conductivity (K) values were calculated according to the Hazen method (Hazen, 1911; Eq 2.1).

$$K = C d_{10}^2 \quad (2.1)$$

Where $C = 1.0$ (for input units of mm and output of cm/s) and d_{10} is the grain size diameter for which 90% of the sediments are coarser; determined graphically (Appendix B; Table B-1, Fig. B-1).

A pumping test was conducted at PU104 in October 2008 (screened ~ 7.5- 9.0 m below ground surface) at a pumping rate of 110 L/min. Pumping test response data for PU104 and proximal wells is available in Appendix B, Table B-2.

2.1.3 Groundwater Sampling

Field samples were collected using peristaltic pumps from multi-level piezometers. Prior to sampling, monitoring points were purged for 3-5 minutes. Samples for cation and anion (including DOC, DON and TN) analysis were each collected in a 30 mL Nalgene bottle filtered using a 0.45 μm in-line filter prior to atmospheric exposure, when possible. Some 'dirty' samples were filtered in the laboratory using either a syringe tip or a vacuum filter apparatus. Cations were preserved to a pH of 2 using concentrated nitric acid (HNO_3), while anion samples were filtered but not preserved. A third 30 mL Nalgene bottle was used to collect an unfiltered sample for NH_4^+ analysis, which was preserved to pH of 2-4 using sulphuric acid (H_2SO_4). Samples for N_2O analysis were collected in duplicate in 60 mL (isotope) and 160 mL (concentration) Wheaton serum bottles. These bottles were filled completely, with no headspace and sealed with a serum stopper (Vacutainer brand) with an injected hypodermic needle to allow any overflow to escape. These bottles were then sealed around the cap with electrical tape

and injected with 2 or 4 mL (for 60mL and 160 mL size bottles respectively) of mercuric chloride (HgCl_2) to preserve the sample. Additionally, samples for $^{15}\text{N}/^{14}\text{N}$ of NH_4^+ isotopic analysis were collected identically to NH_4^+ samples (in 30-125 mL Nalgene bottles, unfiltered and preserved with H_2SO_4). Samples for $^{15}\text{N}/^{14}\text{N}$ of NO_3^- were collected in large volume (500 mL – 1L) Nalgene bottles and typically filtered in the laboratory using a vacuum flask apparatus. All samples collected were stored promptly in a large cooler filled with ice for transport back to the University of Waterloo. Samples that were not immediately analyzed were frozen during storage.

2.1.4 NO_3^- , NH_4^+ , DO

Semi-quantitative field measurements of NO_3^- , NH_4^+ and DO were determined (approximately) using CHEMets™ colorimetric analysis kits. Pre-filled reagent ampoules were submerged within a sample of groundwater and the glass tip was broken, introducing and containing sample within the ampoule by vacuum.

2.1.5 EC, DO, E_0 , pH

Field measurements were periodically performed for the electrical conductivity (EC), dissolved oxygen (DO), reduction potential (E_h) and pH of groundwater. EC ($\mu\text{S}/\text{cm}$) and temperature ($^\circ\text{C}$) were measured in the field using a calibrated Oakton Acorn CON 6 Conductivity/ $^\circ\text{C}$ meter (Oakton Instruments, Vernon, IL). A Barnant 20 brand digital pH meter (Barnant, Barrington, IL) was used to determine *in situ* pH and E_0 of groundwater after being calibrated to buffers of pH 4, 7 and 10 and checking against a Zobell's solution. DO was measured using an HQ20d Dissolved Oxygen meter (Hach Company, Loveland, CO) which also

gave corroborating measurements of EC and temperature using interchangeable probes on the same meter.

2.2 Laboratory Methods

2.2.1 Cations

Major cation (Al^{3+} , Ca^{2+} , Fe^{2+} , K^{+} , Mg^{2+} , Na^{+}) concentrations were determined by inductively coupled plasma-atomic emission spectroscopy using a Horiba Jobin Yvon Ultima 2 ICP (Horiba Jobin Yvon) with a detection limit of 0.005-0.01 mg/L at the National Water Research Institute, Environment Canada, Burlington ON. Sample concentrations were calibrated against multi-ion standards that were included within each run of samples. When necessary, samples were diluted with Milli-Q water to bring their concentration within the working range of the standards.

NH_4^{+} concentrations were determined colorimetrically using a Beckman D600 UV-Vis Spectrophotometer (Beckman Coulter Canada, Mississauga, ON) (650-660 nm) after reaction with Indophenol Blue indicator solution at the Environmental Geochemistry Laboratory (EGL), University of Waterloo. Samples were routinely diluted on a 1:100 or 1:20 basis as determined by the colour of sample (indicative of organic and NH_4^{+} concentration) to prevent interference with colorimetry and keep sample concentrations within the range of standards.

2.2.2 Anions

NO_3^{-} -N analyses were performed at the Soil and Nutrient Laboratory (SNL), University of Guelph, Guelph, ON according to the USEPA method 353.2 for inorganic substances (USEPA, 1993). Nitrate is reduced by copperized cadmium to nitrite, which reacts with sulphanilamide to form a diazonium compound which, in dilute phosphoric acid couples with N-

(1-naphthyl)-ethylenediamine dihydrochloride to form a reddish-purple azo dye. This is measured spectrophotometrically at 520 nm, using a Seal AQ2 (Seal Analytical) with a detection limit of 0.1 mg/L (Barr, 2010). For uncoloured samples containing lower DOC content, NO_3^- -N concentrations were determined by ion chromatography at the EGL at the University of Waterloo using a Dionex ICS-90 (Dionex, Sunnyvale, CA) which provided a detection limit of 0.5 mg/L.

Other anions (Cl^- , SO_4^{2-} , Br^- , PO_4^{3-} , F^-), were also analyzed by ion chromatography in the EGL at the University of Waterloo, with a detection limit of < 0.5 mg/L. DOC was measured using a Dohrman DC-190 total carbon analyzer (Dohrman, Santa Clara, CA) also at the EGL. For anion analyses, dilutions were undertaken for highly coloured and concentrated samples. Standards were included in all analyses.

2.2.3 N_2O

N_2O analyses were performed at the EGL using a headspace equilibrium technique and a gas chromatograph. Thus (2008) describes this technique as follows: headspace is created to produce positive pressure inside bottles by injecting 10ml of He into the samples while removing 5mL of samples, then sample bottles were shaken for about 90 minutes until dissolved N_2O reaches equilibrium with headspace. The N_2O concentrations were then determined with an Electron Capture Detector (ECD) on a Varian CP 3800 greenhouse gas analyzer (Varian Canada, Inc.). Dissolved N_2O concentrations were then calculated according to Henry's Law which provided a detection limit of 0.2 $\mu\text{g/L}$

2.2.4 Total Nitrogen, TKN, NO_2^-

NO_2^- -N analyses were performed at the SNL according to the USEPA method 354.1. Nitrite ions in solution react with sulphanilamide to form a diazonium compound which, at the

acidic pH of an acetate buffer, couples with N-(1-naphthyl)-ethylenediamine dihydrochloride to form a reddish-purple azo dye. The absorbance of this complex is measured spectrophotometrically at 520nm using a Seal AQ2 (Seal Analytical) with a detection limit of 0.1 mg/L (Barr, 2010).

Total Kjeldahl Nitrogen (TKN) analysis at the SNL follows a modified Kjeldahl digestion (Thomas et al., 1967), with the concentrations of nitrogen measured by Technicon Auto Analyzer. DON was calculated from TKN as the difference between TKN and $\text{NH}_4^+\text{-N}$. TN was determined at the EGL using a Dohrmann Apollo Carbon Analyzer with TN Module (Dohrman, Santa Clara, CA). In this case, DON was calculated as the difference between TN and $(\text{NH}_4^+\text{-N} + \text{NO}_3^-\text{N})$.

2.2.5 $\delta^{18}\text{O-H}_2\text{O}$

The measurement of $^{18}\text{O}/^{16}\text{O}$ of H_2O was carried out by a CO_2 equilibration method described in Heemskerk (1993). The procedure follows the method outlined in Fritz et al. (1986) with the aqueous sample shaken for a minimum of 3 hours to degas and equilibrate with injected CO_2 . Upon equilibration, the gaseous sample is run through a Fisons Instrument Isochrom-EA mass spectrometer (GV Instruments, Manchester, UK). The results are reported as $\delta^{18}\text{O-H}_2\text{O}$ values (permil difference) referenced to Vienna Standard Mean Ocean Water (VSMOW), within an analytical error of 0.2‰.

2.2.6 $\delta^{15}\text{N-NO}_3^-$

$^{15}\text{N}/^{14}\text{N}$ ratios of NO_3^- were evaluated at the EGL. The method of preparation is similar to that described in Silva et al. (2000). The method is appropriate for samples low in organic matter and concentrations down to 1 mg/L $\text{NO}_3^-\text{-N}$. For preparation, samples are filtered

(0.45 μ m) using a vacuum flask setup if not field filtered. SO_4^{2-} is removed from solution using barium chloride (BaCl_2) as a reagent to precipitate out SO_4^{2-} as barium sulphate (BaSO_4), since SO_4^{2-} can interfere with the isolation of NO_3^- . Samples are eluted through a reactive resin column (Bio Rad AG 1-X8) to isolate NO_3^- within the column. NO_3^- is removed from the column by reaction with aliquots of a 3M hydrochloric acid (HCl) solution. The resultant mixture is dosed with reactive silver oxide (Ag_2O) to yield a solution of silver nitrate (AgNO_3). This is then freeze dried and combusted at the EGL using a Carlo Erba 1108 CNOS Elemental Analyzer coupled to a Fisons Instrument Isochrom-EA mass spectrometer (GV Instruments, Manchester, UK). Isotopic results are expressed as standard $\delta^{15}\text{N-NO}_3^-$ units (per mil difference) relative to the reference standards of atmospheric N_2 for $^{15}\text{N}/^{14}\text{N}$.

2.2.7 $\delta^{15}\text{N-NH}_4^+$

Preparation for determination of $^{15}\text{N}/^{14}\text{N}$ of NH_4^+ was performed at the EGL according to the methods in Spoelstra et al. (2006). This is a modified version of the standard ammonium diffusion technique for $^{15}\text{N}/^{14}\text{N}$ determination (Sørensen and Jensen, 1991; Holmes et al., 1998; Sebilo et al., 2004). Unfiltered, preserved samples with concentrations as low as 0.6 mg/L NH_4^+ -N are prepared, in duplicate, with a solution of 4M potassium chloride (KCl) so that the total volume in a 50 mL Wheaton serum bottle is 20 mL and the mass of NH_4^+ -N contained in the bottle is at least 20 μ g. Separately, diffusion ‘traps’ are made by sealing an acidified (10 μ L 0.2M H_2SO_4) quartz filter disk (Whatman 4.7cm QMA filters, baked at 550 $^\circ\text{C}$) in a section of polytetrafluoroethylene (PTFE) tape (‘T-Tape’), which allows gas, but not water, diffusion across the membrane. After the addition of a magnetic stir bar (Fisherbrand, 1’’) each solution containing the nitrogen and KCl mixture is made basic (as indicated by the addition of a phenolphthalein indicator) by the addition of 0.2M sodium hydroxide (NaOH) and buffered to a

pH of ~ 9.3 by the addition of 2 mL of a sodium tetraborate ($\text{Na}_2\text{B}_4\text{O}_7$) solution, at which time the PTFE traps are added to the solution and bottles are capped with 20 mm butyl blue septum stoppers (Belco Glass Co.). Bottles are left to stir (using a magnetic stir plate) for a minimum of 10 days, during which time the dissolved NH_4^+ progressively volatilizes to gaseous NH_3 in the bottle headspace and then precipitates on the acidified filter disk as ammonium sulphate ($(\text{NH}_4)_2\text{SO}_4$). At the conclusion of the diffusion period, PTFE traps are removed and the filter disks placed in vials (Fisherbrand 1 dr.) that are frozen, then freeze dried. The disks are then combusted and the vapour produced is analyzed on a Varian CP-3800 Gas Chromatograph at the EGL. Isotopic results are expressed in the standard $\delta^{15}\text{N-NH}_4^+$ units (per mil difference) relative to the reference standards of atmospheric N_2 for $^{15}\text{N}/^{14}\text{N}$.

2.2.8 Ammonification Experiments

Two sets of laboratory experiments were performed to determine the potential for ammonification of groundwater samples with significant organic content along the plume core zone. The first was set up with 3 samples in parallel using groundwater from wells PU125, PU121 and PU92. Four 160 mL diffusion bottles with 120 mL of each respective sample (twelve bottles total) were set to stir on a stir plate each with a magnetic stir bar, closed off to the atmosphere. In this instance, samples were exposed to whatever amount of oxygen remained in the bottle headspace; but were not exposed to the atmosphere afterwards. Bottles were then sampled destructively at 0, 5 and 12 days and analyzed for NH_4^+ , NO_3^- and TN.

The second experiment was conducted in a strictly anaerobic environment in four 1L Pyrex jars. In this scenario, 300 mL of sediment, taken from cores near well PU92, was placed in each jar and 700 mL of groundwater from one of each of wells PU122, PU95, PU92 and

PU115 was added to each jar respectively. Jars were capped with a septum to allow for periodic sampling, were degassed with helium while capped, then set to shake. Samples for NH_4^+ , NO_3^- and TN analyses were taken 1, 2, 3, 4, 5 and 11 days from each jar, with helium gas replacing the removed sample volume to maintain anaerobic conditions.

3.0 Results

3.1 Aquifer Description

The shallow aquifer is assumed to be hydrologically connected to the overlying manure lagoon to some extent since there is no evidence of a confining layer between the two. The geology at the site is a heterogeneous mix of glacio-fluvial outwash consisting of gravel and sand layers with thin discontinuous layers of clay and silt present also (Fig. 4, Appendix B; Fig.B-2-B-7). The stratigraphy in a gravel pit, located just north of the lagoon, shows this variability as well as general substrate heterogeneity. Generalized geology along the plume centre line, based on four continuously cored boreholes is shown in Fig. 4. These holes show coarse grained sands and gravels with increasing particle size at depth (Fig. 5). Proximal to the lagoon, a layer of silt exists at mid-depths (~2-4 m below ground surface) and also a clay birm is installed at the edge of the lagoon. The predominance of permeable heterogeneous gravel below 6-8 m depth allows the possibility for very fast groundwater velocities. Shallower depths are dominated by comparatively homogeneous medium-coarse grained sand, with silt (~ 3 m below surface at PU122, 123) present proximal to the lagoon. Off centreline boreholes (PU103, 106), also show gravelly sands predominantly, with sporadic observations of silt and clay at mid depths (Appendix B; Fig.B-2, B-3).

3.2 Groundwater Flow System

The water table at the Zorra site fluctuates seasonally by ~1 m (Fig. 6). The relative elevation of the water table ranged between 7.6 and 9.0 m over the two years of study. Generally, a ~10 cm drop occurs in the water table level over ~60 m distance (Fig. 6) from transect B to E giving an average horizontal gradient of 0.002 at 3 m depth (ranging between

0.0017 and 0.0025 seasonally) . Highly variable water table measurements along transect A made it difficult to determine the hydraulic gradient along the entire plume core. The level of the lagoon itself changed by more than 1 m annually (Fig. 6), implying a change in vertical gradient to the water table throughout the two years of monitoring. A strong vertical gradient in geochemistry between the bottom of the lagoon and ~7.5 m depth is observed proximal to the lagoon (Fig. 10, 14 for example) but is not seen downgradient of the lagoon where the plume core is restricted to a maximum of approximately 3 m depth. This plume shape is largely due to a density driven gradient near the lagoon. Lagoon waters are denser than pristine water; in the range of 1.010-1.015 g/cm³.

Hydraulic conductivities (K) were determined from a pumping test and from grain size analyses. Hydraulic conductivity estimates are summarized in Table 1, along with estimates of groundwater velocity. Three relatively distinct geological units along the centre line cross section were determined with increasing hydraulic conductivity at depth (Fig. 5). The shallowest component of the aquifer (~0-4 m below surface) consisted of sand with some silt, with K values ranging from 0.0001 (in the clay lens near the lagoon) to 0.04 cm/s. At mid depth (4-6 m), the sandy aquifer has a significant gravel content, giving a range of K from 0.06-0.2 cm/s. At depths > 6 m K values of up to 2.2 cm/s occur in clean heterogeneous gravel. A pumping test undertaken at 7.5-9 m depth in well PU104 confirmed this highly permeable material, yielding a K of 10 cm/s. In all, K ranges over 5 orders of magnitude, emphasizing the significant heterogeneity at the site. With these K ranges and observed hydraulic gradients, the Darcy equation yields increasing groundwater velocities with depth ranging from 50-7000 m/year (Table 1). The downward migration of tracer parameters below 7.5 m (section 3.4) near to the lagoon (PU122) confirms downward movement of the plume below the lagoon, but further along

the centre line the plume appears to be confined to the shallower zone at 0-2 m below the water table. It is possible that some lagoon movement at depth has been missed proximal to the lagoon since no confining layer was directly observed at the deepest drilling points (9 m below ground surface). Because of the extremely high K values present, hydraulic gradients are relatively very low, bordering on measurement error. Therefore it is difficult to predict plume movement precisely using hydraulic gradients. Rather the plume appears to be responding primarily to geologic heterogeneity which is considerable at this site. Nonetheless, the general plume migration direction follows the hydraulic gradient southward toward the Thames River (Fig. 6).

Average annual rainfall in the area is nearly 840 mm in the surrounding area (Environment Canada, 2011). This precipitation could influence the shallow groundwater plume by providing a source of uncontaminated, oxygenated water along the water table boundary throughout the year, potentially promoting nitrification and the formation of NO_3^- along this upper boundary as well as contributing to dilution of the plume.

3.3 Lagoon Geochemistry

The lagoon has high organic nitrogen content (218 ± 67 mg/L DON) and high K^+ concentrations (1130 ± 250 mg/L), characteristic of poultry waste, as well as elevated Na^+ (219 ± 64 mg/L), EC (5500 ± 1800 $\mu\text{S}/\text{cm}$) and $\text{NH}_4^+\text{-N}$ (121 ± 98 mg/L) (Table 2, Fig. 7). The composition of the lagoon changes seasonally, shown in Fig. 7. Also, liquid from the lagoon is recycled by pumping it back onto the compost piles during periods of low rainfall to maintain a specific moisture content range. This likely has a considerable effect on the concentration and isotopic signature of NH_4^+ as this will cause volatilization of dissolved NH_3 at the lagoon pH of 7.5-8.0 (Table 2). NH_4^+ loss through volatilization will enrich the $\delta^{15}\text{N-NH}_4^+$ in solution

signature because the process ($\text{NH}_4^+ \rightarrow \text{NH}_{3(\text{aq})} \rightarrow \text{NH}_{3(\text{g})}$) has a significant enrichment factor (ϵ) of ~30‰ at 25 °C (Kirschenbaum et al., 1947; Urey, 1947). The amount of recharge from the lagoon to the shallow aquifer system is presumed to be seasonally variable because the water level in the lagoon, and hence the lagoon surface area is seasonally variable (Fig. 6).

Fig. 7 and Table 3 illustrate the contrast between lagoon and background groundwater chemistry for $\text{NH}_4^+\text{-N}$, $\text{NO}_3^-\text{-N}$, K^+ , Na^+ and EC as indicated from the background well (PU86; Fig. 3). Input from the lagoon varies strongly through time, but K^+ , Na^+ and EC are distinctly higher in the lagoon compared to background waters on a consistent basis. K^+ is up to 1300 mg/L in the lagoon compared to 9 mg/L in the background well. Na^+ is also much lower in background water (mean of 6.0 mg/L) compared to the lagoon (mean of 219 mg/L). All three of Na^+ , K^+ and EC show substantial variability in concentrations throughout the two years that are not seasonally consistent, reflecting changes in evaporation, rainfall dilution, compositional variability of the compost and frequency of rewatering the compost piles. Fig. 7 also illustrates the considerable variability in the $\delta^{15}\text{N-NH}_4^+$ signature in the lagoon; ranging from 28.2 to 72.1‰ (mean = 43.7 ‰). Table 2 also shows the wide range of available total nitrogen concentrations (260-520 mg/L). Based on these concentrations, organic nitrogen is a considerable portion of the total nitrogen in the lagoon (mean of 60% of total nitrogen, Table 4). It is important to keep in mind that with such a variable input function, observations based along the plume centreline are based on mean values.

3.3.1 Redox Setting

The lagoon represents an anaerobic source that is a relatively reducing environment. DO and NO_3^- are strongly depleted, with $\text{DO} < 0.5\text{mg/L}$ and NO_3^- constituting only 1% of the total

nitrogen in the lagoon on average (Table 4). Dissolved Fe^{2+} is much higher in the lagoon than what is seen in background water (16 mg/L and below detection limit respectively), suggesting reduction of ferric oxyhydroxides. Background water represents a less reducing environment, where, although DO remains relatively low (approximately 1.5-2 mg/L), NO_3^- is available consistently at 10 mg/L while Fe^{2+} is absent in solution.

3.4 Plume Indicator Parameters

Due to the seasonal variability of the lagoon chemistry (Table 2), the considerable heterogeneity of aquifer sediments and the variable degree of dilution that occurs within the groundwater flow system, delineation of the plume core zone is not straight forward. Consequently, a suite of plume tracers (K^+ , Na^+ and EC) has been used to identify the groundwater plume influenced by recharge from the lagoon.

3.4.1 Electrical Conductivity

The mean EC value of the lagoon is 5500 (± 1800) $\mu\text{S}/\text{cm}$, compared to 600 $\mu\text{S}/\text{cm}$ in the background wells (Fig. 9). Within the plume core, EC ranges between 1200 to 3800 $\mu\text{S}/\text{cm}$ (Fig. 10). The 1500 $\mu\text{S}/\text{cm}$ contour which is indicative of the plume core is ~ 70 m in width and extends nearly 80 m downgradient from the source (Fig. 9). The range of EC along the centre line of the plume was similar in August and November 2009 (Fig. 10), peaking at 4800 $\mu\text{S}/\text{cm}$ in August and 5500 $\mu\text{S}/\text{cm}$ in November. The vertical extent of the EC plume was similar in both snapshots, but values >1000 $\mu\text{S}/\text{cm}$ extended ~ 1.5 m deeper in October compared to August.

3.4.2 Cl⁻

Plume Cl⁻ values range from a peak in of 690 mg/L near to the lagoon, decreasing to ~200 mg/L 20 m downgradient of the lagoon (Fig. 8). Cl⁻ averages 697 (± 261) mg/L in the lagoon, but the concentrations are much lower in the plume, as high as 690 mg/L proximal to the lagoon, but with few locations exceeding 100 mg/L downgradient (Fig. 8). In general, distal piezometers approach background values of 20 mg/L. Similar Cl⁻ values were observed in October 2008 (Appendix E, Fig. E-2).

3.4.3 Na⁺

Fig. 12 shows the plan view distribution of Na⁺ in the summer of 2008 and 2009. Groundwater concentrations in the plume zone range from 20-170 mg/L compared to the lagoon mean value of 220 (± 60) mg/L. In the distal piezometers for both years, vertical averages of Na⁺ decrease to < 25 mg/L (Fig. 12). The range of values and distribution was similar in 2008 to 2009, with the highest core values (>100 mg/L) present near the lagoon in both years.

Fig. 13 shows the distribution of Na⁺ along transects A through E, which are ‘fences’ transverse to the flow direction. Concentrations decrease downgradient from > 100 mg/L to a maximum of ~50 mg/L at the distal transect E-E’. PU95 and PU92 show unusually low Na⁺ concentrations between two higher nests (Fig. 13), but these nests were still included as centre line wells based on NH₄⁺ distribution (Fig. 21,22).

Na⁺ distribution along the designated plume centre line in August 2009 and November 2009 (Fig. 14) show an elevated core proximal to the lagoon of >100 mg/L. The Na⁺ plume extent is similar in August and November, with the plume core zone defined where Na⁺ >30 mg/L.

3.4.4 K⁺

The distribution of K⁺ is generally similar to that of Na⁺. The mean concentration of the lagoon is 1150 (± 250) mg/L, greatly above the background mean value of 2.6 mg/L (Table 3, Fig. 7). Centre line plume core values range from ~600 mg/L near the lagoon to < 100 mg/L at the most distal location ~100 m downgradient (Fig. 15). Relative concentrations are similar to the Na⁺ distribution and K⁺ was consistent from year to year (Fig. 15)

Two snapshots of K⁺ along the centre line are shown in Fig. 16, showing a similar relative distribution within the plume core to that of Na⁺, with a similar plume core zone boundary present where K⁺ > 100 mg/L.

3.4.5 Plume Extent using Conservative Parameters

The extent of a contaminant plume is most accurately defined by the distribution of conservative tracers that are elevated compared to background water. The most common candidate is Cl⁻, however, at the Zorra site there is not a significant contrast between the values in the plume core zone and the groundwater outside the core which shows relatively high Cl⁻ of 50-100 mg/L (Appendix E, Fig. E-2). As such, Cl⁻ is not considered an appropriate tracer for the manure lagoon plume at this site.

The lagoon water has a number of distinct parameters compared to background groundwater (Table 3). Most contrasting (of non-nitrogenous compounds) are the concentrations of Na⁺, K⁺ and EC. The problem with using K⁺ or EC as tracers is that they are somewhat less conservative parameters. K⁺ is readily sorbed, and EC is a parameter that depends on the total dissolved solids (TDS) content that can be influenced in many ways. However, in plan view and along the centre line transects these parameters show very similar distributions to that of Na⁺

(Fig. 9, 10, 12, 14-16). Na^+ is less strongly affected by sorption (Nicholson et al., 1983; Dance and Reardon, 1983) and has been used previously as a ‘conservative’ plume tracer for septic system plumes (Robertson et al., 1989). These three parameters present a consistent distribution of the plume’s core zone location, which has changed little in shape over the study period and starkly contrasts with background groundwater. The variation in plume extent comparing 2008 to 2009 (Fig. 12) in plan view is an effect of the more extensive monitoring network that was installed between the two snapshots. For the purposes of this study, monitoring points with $\text{Na}^+ > 30 \text{ mg/L}$ are considered to be in the plume core zone.

3.5 Nitrogen Distribution

3.5.1 NH_4^+

The concentration of $\text{NH}_4^+\text{-N}$ in the lagoon varies strongly over time, with a mean of 121 ($\pm 98 \text{ mg/L}$). $\text{NH}_4^+\text{-N}$ is also highly variable in the plume ($< 0.01\text{-}107 \text{ mg/L}$), decreasing steadily downgradient from the lagoon (Fig. 17, 25-26). In general, high concentrations were constrained to 1-1.5 m below the water table except for piezometer PU122, where elevated $\text{NH}_4^+\text{-N}$ extended to 7.5 m depth (Fig. 25). The NH_4^+ zone was widest in the middle transects (B and C), with proximal and distal transects (A, D and E) showing a much more constrained distribution (Fig. 20-24).

Fig. 34 shows a series of breakthrough curves for $\text{NH}_4^+\text{-N}$ over two years for piezometers along the centreline. $\text{NH}_4^+\text{-N}$ decreases overall from a mean of 32 (± 3) mg/L proximal to the lagoon to 2 (± 3) mg/L at the most distal (101 m away) piezometer downgradient. In between, concentrations vary more strongly, averaging 17 (± 23) mg/L and 29 (± 33) mg/L at piezometers 40 and 60 m from the lagoon respectively. Concentrations remain relatively high 88 m from the

lagoon, but are much less variable (28 ± 4 mg/L). Variations in NH_4^+ -N do not appear to follow a seasonal trend and instead likely reflect the varying input of manure primarily.

3.5.3 NO_3^-

Lagoon NO_3^- -N values have remained low (3.0 ± 1.0 mg/L) throughout the study period. Plume values on the other hand are variably higher ranging from <0.01 mg/L to > 100 mg/L in local areas (Figs. 18, 20-26). However NO_3^- -N is frequently below detection in the plume core zone whereas the highest values generally occur around the periphery of the NH_4^+ plume. Background values contrast the lack of NO_3^- -N in the core zone, averaging 10 ± 1 mg/L (Table 3). Breakthrough curves in Fig. 34 show generally low NO_3^- -N for all sampling points with periodic spikes in concentration that do not reflect seasonal trends. Proximal piezometer PU122 in the core zone shows the lowest NO_3^- -N (0.3 ± 0.3 mg/L), with downgradient values increasing variably to $11 (\pm 13)$, $9 (\pm 18)$ and $8 (\pm 6)$ mg/L at 40, 60 and 100 m from the lagoon respectively. The most distal concentrations are a close reflection of background values, while the mid-distance observations show much higher variability, implying sporadic nitrification.

3.5.3 DON

DON averages $218 (\pm 67)$ mg/L in the lagoon, while background values are consistently <1 mg/L (Table 3). The distribution of DON along the centre line transect for August 2009 is shown on Fig. 25. Similarly to NH_4^+ , total DON diminishes rapidly along the groundwater flow system from peak values of 75 mg/L near the lagoon to < 10 mg/L at the distal piezometers consistently in August and November 2009 (Fig. 24, 25). In general, DON remains above 20 mg/L throughout the plume core with the exception of a few local points: < 5 mg/L below 4.0 m at PU124 & 125; at the shallowest monitoring point at PU96 (5 mg/L); and at the distal

piezometer PU121 (< 10 mg/L). DON is similarly elevated (>75 mg/L) proximal to the lagoon, but quickly decreases to ~20mg/L throughout the rest of the core zone (Fig. 26). Throughout the plume core zone, DON contributes on average ~40% to total nitrogen (Table 4).

3.5.4 NO₂⁻

Groundwater NO₂⁻-N concentrations ranged from 0.1-1.5 mg/L during sampling on July 15, 2009 (Appendix C). This represents < 1 % of total nitrogen. NO₂⁻ is a relatively unstable form of nitrogen in the aquatic environment because it is quickly converted to other forms of nitrogen such as NO₃⁻ in oxidizing environments, or N₂ in reducing environments.

3.5.5 N₂O

N₂O concentrations peak in the range of 50-100 µg/L at locations along the periphery of the core zone (Fig. 20-24), while core locations generally show lower N₂O values of <10 µg/L (Fig. 19). Proximal concentrations are generally lower in N₂O than are mid-distance points along the centre line, including PU95 peaking at 28 µg/L 40 m from the source (Fig. 19). Similarly localized maxima typically occur off of the centre line along transverse transects A-E (Fig. 20-24), which again show centre line wells typically with < 10 µg/L N₂O.

3.5.6 Total Nitrogen

Fig. 25 shows the distribution of total nitrogen (sum of DON, NO₃⁻-N, NH₄⁺-N and NO₂⁻-N) in August 2009. Total nitrogen concentrations peak above 200 mg/L, with a core of concentrations typically exceeding 100 mg/L. A zone of TN >50 mg/L reaches to a moderate depth (~2.2 m) at PU96. TN is depleted to < 20 mg/L at some locations along the plume core (eg. PU124 and 125 at 4 m depth as well as upgradient of the lagoon). The upgradient well and

> 4 m depths mentioned consist almost entirely of NO_3^- . Otherwise, NO_3^- is a more minor component of TN compared to NH_4^+ and DON (Table 4), except where associated with sharp drops in NH_4^+ -N. DON dominates TN on average in August (46% vs. 33% for NH_4^+) while NH_4^+ and DON are approximately equal components of the total nitrogen in November 2009 (40% for NH_4^+ vs. 37% for DON). The distal piezometer locations, particularly at shallow depths have significantly lower TN (<10 mg/L), which is only about 5% of the source amount.

3.5.7 $\delta^{15}\text{N-NO}_3^-$

$\delta^{15}\text{N-NO}_3^-$ values were not determined in most of the plume core zone samples due to insufficient NO_3^- -N concentrations, and/or due to high organic contents. Fig. 27 shows $\delta^{15}\text{N-NO}_3^-$ ranged from 20.6 – 40.2 ‰ in the plume periphery zone. In general, the permil values of locations downgradient (> 27‰) from the lagoon are enriched compared to the upgradient area (20.6‰, Fig. 27). At wells PU124 and PU125, $\delta^{15}\text{N-NO}_3^-$ is enriched in the shallow sampling points bordering on the plume core zone (Fig. 35).

3.5.8 $\delta^{15}\text{N-NH}_4^+$

Fig. 27 also shows the distribution of $\delta^{15}\text{N-NH}_4^+$ along the centre line transect. Values range from 17.5 to 39.6 ‰ in the groundwater compared to 43.7 (\pm 13.2) ‰ in the source zone. Values peak (36-39‰) ~20 m downgradient from the lagoon before dropping and ranging between 23-27‰ further downgradient. Local enrichment of a few permil is noted in several nests near the periphery of the plume core where NH_4^+ -N concentrations decline abruptly (Fig. 35). A significant number of monitoring points show $\delta^{15}\text{N-NH}_4^+$ values below the minimum value observed in the lagoon (28‰).

3.6 Other parameters

3.6.1 pH

Along the centreline flow path pH decreases abruptly from the lagoon (7.7) to PU122 (~6.5), including to depths of 9 m (Fig. 30). By the next monitoring well downgradient (PU95), pH has risen back to >7.0. A core zone of pH > 7.0 is seen at moderate depths along the centre line, peaking at 7.9 at PU115 located 60 m downgradient. pH drops slightly below 7.00 at depth at PU125 and PU124, and at the shallow monitoring points from PU92 and PU96. Background pH values are ~7.5 (Table 3).

3.6.2 DO

Dissolved oxygen is generally below 2.0 mg/L throughout the centreline transect and the plume has an anaerobic core that can be seen in plan view and along the centreline (<1.0 mg/L, Fig. 11). This anaerobic core is in contrast to background values of ~8.0 mg/L (Table 3).

3.6.3 Ca²⁺

Fig. 28 shows the distribution of Ca²⁺ along the centreline during August and November, 2009. Both snapshots show substantial increases between the lagoon and the proximal piezometer PU122, from the lagoon average of ~ 70 mg/L Ca²⁺ (Table 2) to >150 mg/L in PU122 (Fig. 28)

3.6.4 Fe²⁺

The distribution of Fe²⁺ is shown in Fig. 29 for August and November 2009. Both snapshots show a similar trend of Fe²⁺ with peak values at PU122 as high as 61 mg/L. Farther downgradient Fe²⁺ values gradually decrease in the plume core to <0.1 mg/L (Fig. 29). Fe²⁺

levels are also below detection limit at depth below the plume core zone (Fig. 29). A difference between the two time periods is the extent to which elevated Fe^{2+} occurs along the centre line. During the August snapshot, concentrations > 5 mg/L extend 60 m downgradient whereas in November $\text{Fe}^{2+} > 5$ mg/L extends only ~20m from the lagoon.

3.6.5 Dissolved Organic Carbon

Dissolved organic carbon (DOC) ranged from 6-690 mg/L within the plume core zone in August 2009 (Fig. 30). A previous survey from July 15, 2009 from within the core zone and the periphery gave a wide range of 25-1800 mg/L (Table C-3).

3.7 Ammonification Experiments

The results from the first of the two ammonification experiments are given in Table 7 and Fig. 37, while the results from the second experiment are shown in Appendix D. The experiments were designed to determine whether or not ammonification may be occurring in groundwater with high DON and low NH_4^+ -N concentrations. For the first experiment in the batch with PU125 groundwater, a significant drop in DON concentrations occurred between day 0 and 5 (45 to 12 mg/L) which was accompanied by a rise in NO_3^- -N from 0.4-35 mg/L. The presumed order of reaction was DON being mineralized to NH_4^+ followed by oxidation to NO_3^- . Experiment 2 was designed with more frequent temporal resolution, and to be completely anoxic. A problem arose when field measurements of NH_4^+ -N did not agree with lab results. Each jar in this case more or less maintained its nitrogen composition over 11 days.

Results from the first experiment indicated a loss of 33 mg/L of DON and 4 mg/L of NH_4^+ -N (Table 7). This loss corresponded with a gain of 36 mg/L of NO_3^- -N, suggesting that in an environment with limited oxygen supply, the complete mineralization of DON can occur,

with ammonification as an intermediate reaction. This experiment more or less represents the environment along the periphery of the groundwater plume through the unsaturated zone, where some oxygen may be supplied.

4.0 Discussion

4.1 Plume Comparison to Other Sites

The Zorra plume has some similarities, but also contrasts with other NH_4^+ rich manure and septic plumes. One major difference is the physical geology of the site which is very permeable and highly heterogeneous. This contrasts with the manure storage site near Saskatoon, SK described by Sills (2006) where cation exchange is largely implicated in the fate of the NH_4^+ plume. Stratigraphy at that field site consisted primarily of a silty sand aquifer and confining clay aquitard, with a maximum groundwater velocity of 30 m/yr; orders of magnitude below the 400 m/yr in the sand and gravel zone at Zorra. The source at the Sills site had NH_4^+ -N concentrations above 3000 mg/L, with plume concentrations >1000 mg/L proximal to the source. A major difference was the low concentrations of DON in the plume groundwater (TKN > 95% NH_4^+ -N) at the Sills site, while at the Zorra site a high proportion of TN is DON (~40%, Table 4). The site in the Sills study has similarly low NO_3^- (~3 mg/L N) in the source and a NO_3^- deficient core zone. The Sills plume uses Cl^- as a conservative tracer, while at the Zorra site this was deemed less useful. Based on the Cl^- plume movement, site stratigraphy and soil coring, > 1000 mg/L of groundwater NH_4^+ was determined to be attenuated by cation exchange over 20 m distance, with a retardation factor for NH_4^+ of 2.2-6.0.

The attenuation study by Ceazan et al. (1989) describes the Otis, MA septic plume, with a source consisting largely of NH_4^+ (up to 11 mg N/L) with coexisting NO_3^- (~2 mg N/L) concentrations that disappear in the NH_4^+ rich (~6 mg N/L) plume core, much like at the Zorra site. The main difference there was that the NH_4^+ plume is significantly retarded compared to the NO_3^- distribution, reaching only 2 km, compared to more than double that distance for the

extent of the NO_3^- plume. A study of NH_4^+ attenuation in the same plume by Böhlke et al. (2006) showed similar NH_4^+ & NO_3^- coexistence, but at much lower concentrations (~ 1.0 mg/L). Isotopic ranges, particularly for $\delta^{15}\text{N-NH}_4^+$ also showed strong differences between the two plumes, with Böhlke showing a relatively consistent $\delta^{15}\text{N-NH}_4^+$ values ($12.6 \pm 0.4\%$) along the plume whereas the Zorra plume has a wide range. The biggest contrast between the Zorra site and the previous plume studies is the elevated DON proportion (218 ± 67 mg/L, $\sim 40\%$ of TN). This makes isotopic methods for tracing process more difficult due to the uncertainty associated with $\delta^{15}\text{N}$ transformations from the organic component. The high propagation of DON in this plume is most likely a result of the fast flowing groundwater system; thus plume ages are relatively young (0.5-1 year) along the centre line transect compared to many years to decades in the Otis and Sills plumes.

4.2 Nitrogen Synthesis, Zorra Plume

Nitrogen enters the shallow aquifer system from two sources in the Zorra field site: as NH_4^+ mineralized from organic nitrogen in the composting piles, or as NO_3^- from ambient groundwater flow. Elevated NO_3^- -N is also seen in some of the shallow depths along the plume core line. NH_4^+ concentrations remain elevated along the majority of the centre line of the plume, with fluctuations largely dependent on the incoming load of NH_4^+ based on the variations over the study time period (Fig. 34). In general, mid depth locations (0-2 m below the water table) in the plume core have the highest NH_4^+ concentrations. The exception to this is the proximal well, PU122, which consistently shows a strong plume influence (elevated Na^+ , EC, K^+) and also elevated NH_4^+ down to 9 m. The deeper plume position at PU122 is attributed to the stratigraphic, and hence the flow system heterogeneity and the high density source recharge.

NO_3^- is present along the peripheries of the plume core zone, suggesting influences of nitrification and background water. A vadose zone ~1-2 m thick between the lagoon bottom and the water table poses the possibility for substantial nitrification along the periphery of the manure plume. Nitrification is also evidenced at very shallow depths. At depth (> 4.5 m below the ground surface) along the plume centre line, background NO_3^- seen along the plume boundary has the potential to interact with plume NH_4^+ .

DON shows a very similar distribution as NH_4^+ , peaking at mid depths, while decreasing along the flow path to less than 10% of the incoming concentration by the most distal piezometer. The plume is within appropriate dissolved oxygen, pH and temperature conditions for ammonification to occur as the mechanism of DON loss.

NO_2^- is typically a minor component when compared to other forms of nitrogen dissolved in the system (typically <1% of total nitrogen), but is present and measureable (0.1-1.5 mg N/L) in many locations, suggesting it is generated intermittently as an intermediate of nitrogen transformation reactions.

4.3 Nitrogen Attenuation in the Zorra Plume

A case for nitrogen attenuation can be made based on comparing to the distribution of the conservative tracer Na^+ . Na^+ represents a reasonably conservative tracer at the Zorra site since it has a relatively low retardation value (~1, DeSimone et al., 1997; Nuñez-Delgado et al., 1997) and many pore volumes (at least 16) have passed through the sediment, suggesting cation exchange may not be a significant factor. Also, K^+ is the major cation in solution (Table 2), and would more likely become sorbed first. As such, any changes in Na^+ concentration should primarily reflect dilution since background concentrations are relatively low (< 10 mg/L)

compared to the lagoon value of 219 (\pm 64) mg/L. If the changes in NH_4^+ along the centre line were due exclusively to dilution as well, then the proportion of NH_4^+ compared to Na^+ ($\text{NH}_4^+/\text{Na}^+$) should vary similarly. Fig. 31 shows the distribution of this ratio along the centre line for August and November 2009. Within the lagoon itself, this ratio's mean value is 0.55. The proximal plume values deviate both above and below this ratio, but then decline to as low as 0.001 in the downgradient zone. Similarly, the ratio of TN/Na^+ shows a gradual decline from a mean lagoon value of 1.65 to below 0.5 downgradient (Fig. 32). The TN is not expected to be 100% attenuated based on the presence of background NO_3^- . Additionally, DON is a very significant component of the TN (Table 4), thus it exerts a strong influence on the nitrogen budget. The variable N/Na^+ ratios suggest that nitrogen, particularly NH_4^+ , is affected by processes other than just dilution.

Since the lagoon is the dominant source of both K^+ and Na^+ , a simple mixing calculation can be used to model or predict the concentrations of other parameters that should be present in the plume core if other attenuation reactions were not active. For this calculation Na^+ is considered more conservative (less affected by sorption). Table 5 and Fig. 36 give the predicted values of N based on such a Na^+ ratio along the centre line summarizing the difference between measured and predicted values of NH_4^+ -N and TN along the centre line and showing that a substantial amount of the TN reduction cannot be accounted for based on dilution alone. Thus total nitrogen loss must be occurring along the plume. Table 6 gives a comparison of measured and predicted NH_4^+ -N and TN values for the most distal transect during 5 sampling events in 2009 and 2010. On average, TN is reduced by 93% over 100 m distance, with 84% of this explained by dilution and the remaining 9% presumably indicating a nitrogen loss reaction. Considering the mean TN of 361 mg/L in the lagoon, this 9% represents a loss of 32 mg N/L that

is presumed to be attenuated along the flow path. Assuming this loss over the 100 m flow path, assuming a representative groundwater velocity of 400 m/year, the total nitrogen loss rate would be on the order of 0.4 mg N/L/day.

This figure is likely an underestimation of the true nitrogen loss at the field site. In addition to the nitrogen strictly within the plume itself, along the boundary of the plume, background waters, with NO_3^- -N of 10 mg/L on average interacts with the plume nitrogen and is likely incorporated into the total loss through the system.

4.4 Mechanisms of Nitrogen Attenuation

With a dynamic source function and heterogeneous groundwater flow system, the Zorra plume provides a complex setting for assessment of nitrogen attenuation. The flow system and geochemistry offers the possibility that a suite of attenuation/transformation mechanisms occur including sorption, ammonification, nitrification, denitrification and anammox. This chapter examines the evidence for these mechanisms.

4.4.1 Sorption

Although sorption retards the migration of certain cations, it is a temporary mechanism, which is fully reversible (Ceazan et al., 1989, Böhlke et al., 2006). In the lagoon plume, cations with strong sorption affinity including K^+ and NH_4^+ may displace existing cations such as Ca^{2+} and Mg^{2+} from sorption sites (Dance and Reardon, 1983). Although clay sediments have the most potent sorption sites, in sand, NH_4^+ and K^+ retardation factors in the range of 2-4 have been reported (Bjerg and Christensen, 1983; Dance and Reardon, 1983; Ceazan et al., 1989). At the Zorra site, sorption could be important between wells PU96 and PU121, where there is a rapid transition from gravelly sand to a more sand dominated medium. However, with continuous

input from a source such as the manure lagoon a saturation of sorption sites will occur, primarily by K^+ , which is the major cation in solution from the lagoon. Considering a groundwater velocity of ~ 400 m/year (Table 1), the 100 m long plume is flushed by four pore volumes per year. With the manure lagoon being in operation since 2006, this means that at least 16 pore volumes have passed through the system, thus most sorption sites are likely filled. Active sorption/desorption cycling however may act to dampen the effects of seasonally variable input from the lagoon. Fig.34 shows a series of breakthrough curves showing the seasonal variability of NH_4^+ -N at points along the centre line. Variability in the NH_4^+ -N at these points along the plume centreline is a subdued reflection of the large variability seen in the pond. If sorption/desorption cycles were playing a prominent role at the Zorra site, the variability of NH_4^+ -N should be dampened through time. However, a number of sharp peaks and/or valleys can be seen through time, further suggesting that sorption is a minor process.

Isotopically, sorption is characterized by a very low fractionation factor in the range of only 2-4 permil for $\delta^{15}N-NH_4^+$ (Delwiche & Steyn 1970, Karamanos & Rennie 1978) with partitioning of the *heavier* ^{15}N isotope favoured onto the solid phase, which is contrary to biological tendencies. Böhlke (2006) and Sills (2006) observed little change in the range of $\delta^{15}N-NH_4^+$ along their respective plume flow paths where sorption was the dominant mechanism of attenuation. In the Zorra plume there is a considerable range of $\delta^{15}N-NH_4^+$ values along the flow path (18-40‰, Fig, 27 Table 2) most of which fall within the variability of the source. A few values are lower than the lowest source value of 28‰.

Due to the large number of pore volumes that have influenced the plume zone, sorption probably has little effect on overall NH_4^+ attenuation, but could dampen the effects of seasonal variation.

4.4.2 Nitrification

Nitrification (Eq. 1.1) consumes O_2 and NH_4^+ while producing NO_3^- and H^+ and includes N_2O and/or NO_2^- as intermediates. Thus, the primary geochemical evidence for nitrification would include a zone where DO is available, NH_4^+ is lost, and NO_3^- increases. This process also has a significant isotopic effect which enriches residual $\delta^{15}N-NH_4^+$ and generates depleted $\delta^{15}N-NO_3^-$ ($\epsilon = 14.2-38.2$ ‰ Mariotti et al., 1981; Casciotti et al., 2003). A decrease in pH also occurs with the release of H^+ during the oxidation of NH_4^+ (Eq. 1.1) which is buffered at this site by $CaCO_3$ dissolution (Eq. 4.1).



Nitrification is considered to be the primary mechanism of NH_4^+ attenuation in septic systems (Wilhelm et al., 1996; Hinkle et al., 2008; Meile et al., 2010) where the vadose zone below the tile bed normally allows for active oxidation. The migration of the lagoon effluent through an unsaturated zone at the Zorra site (~ 2 m thick) suggests that substantial nitrification should be possible in that zone.

Along the water table, O_2 diffusion into the plume might also occur, possibly leading to nitrification along the upper fringe of the plume. This possibility is illustrated along the NO_3^- centre line profile from August and November 2009 (Fig. 25, 26) where elevated concentrations occur at shallow points (up to 47 mg N/L). The fact that these concentrations peak above 40 mg N/L, far above background levels (5-10 mg/L), indicate that there is an internal source of NO_3^- generation within the plume. This provides strong evidence for nitrification activity, which appears focussed primarily along the margins of the plume (Fig. 25, 26). Böhlke et al. (2006) observed similar active nitrification along the upper boundary of the septic system NH_4^+ plume

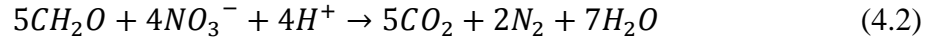
at Cape Cod. An additional influence on this area along the water table is the infiltration of rain water; an uncontaminated source of oxygenated water, further promoting nitrification as well as dilution of the plume itself.

Evidence for nitrification occurring in the vadose zone below the lagoon is not as clear-cut. Although a decrease in NH_4^+ -N is seen between the source (121 mg N/L) and the first well, PU122 (up to a 50% reduction; Fig. 25, 26), elevated NO_3^- -N is not present (≤ 5 mg/L). However, the production of NO_3^- can be inferred indirectly by assessing the evolution of H^+ and resulting increase in Ca^{2+} between the lagoon and PU122 (ignoring all other H^+ producing reactions). Based on Eq. 1.1 (nitrification) and Eq. 4.1 (CaCO_3 dissolution), one mole (14 g) of NO_3^- -N production will cause an associated 2 moles (80 g) of Ca^{2+} increase in solution. Between the lagoon and the first well, the average Ca^{2+} increase was 3.8 mmoles/L Ca^{2+} in August 2009 and 5.5 mmoles/L in November 2009 (Fig. 28), indicating production of 27-38 mg/L NO_3^- -N, which is within the range of NH_4^+ -N loss that cannot be attributed to dilution between these points (Fig. 36, Table 5). These suggestions likely represent an overestimation of nitrogen reaction since the oxidation of DOC through the same zone is likely responsible for the majority of the Ca^{2+} and pH effects seen.

Further evidence of nitrification is provided by the presence of N_2O , an intermediate in the nitrification reaction, along the plume and along the transverse transects (Fig. 19-24). Concentrations of N_2O are elevated at the shallow points (> 10 $\mu\text{g/L}$) for example in wells PU117 and PU113, where NO_3^- -N is elevated (10-150 mg N/L) whereas the plume core has much lower N_2O concentrations of 0.3-1 $\mu\text{g/L}$.

4.4.3 Denitrification

Denitrification is the reduction of NO_3^- to N_2 in the absence of DO and with the existence of appropriate electron donors, most commonly DOC (Eq. 4.2) and also pyrite (Aravena and Robertson, 1998).



Denitrification is inactivated by small amounts of DO and may be compromised in favour of DNRA in high DOC environments (Silver et al., 2001; Nizzoli et al., 2010). Evidence for denitrification is also seen through the production of intermediates including NO and N_2O . The denitrification process is associated with a large isotopic enrichment factor ($\epsilon = -15.9\text{—}29.4\%$; Mariotti et al., 1981; Böttcher et al., 1990), so isotopic evidence can be useful in delineating zones of denitrification. The denitrification process, using DOC as the electron donor, is also a net H^+ consuming reaction (Eq. 4.2), so the pH of the system should increase when denitrification is active.

Some observations provide evidence for denitrification at the Zorra site. The core is anaerobic ($\text{DO} < 1.0 \text{ mg/L}$), DOC in the plume core can be very high ($> 100 \text{ mg/L}$; Fig. 30, Appendix C), suggesting that a source of electron donors is available. Loss of DOC along the centreline could indicate denitrification. Denitrification could be attenuating the shallow NO_3^- present along the plume upper fringe since elevated NO_3^- does not persist in the shallow zone downgradient (Fig. 25, 26) and sufficient DOC is present to allow for the reaction to take place. Denitrification was previously shown to be an active process in an adjacent field area at the Zorra site that was less affected by NH_4^+ contamination (Robertson and Schiff, 2008). N_2O

peaks occur primarily outside of the plume core (Fig. 19-24) suggesting N₂O production at depth and some shallow locations and at downgradient piezometers.

One line of evidence for denitrification is isotopic enrichment of residual $\delta^{15}\text{N-NO}_3^-$. The progressive enrichment of $\delta^{15}\text{N-NO}_3^-$ along a flow path as the concentration of NO_3^- decreases, with no additional nitrogen inputs, is an indicator of denitrification (Aravena and Robertson, 1998; Karr et al., 2001). Such a relationship is only somewhat apparent at the Zorra site (Fig. 27, 33). However, the $\delta^{15}\text{N-NO}_3^-$ data do show slight enrichment of $\sim 6\%$ at 3-4.5 m depth at PU124 and 125 along with decreasing NO_3^- concentrations compared to the deeper background values. The most enriched $\delta^{15}\text{N-NO}_3^-$ values ($\sim 40\%$) occur closest to the plume interface zone, where NH_4^+ and NO_3^- coexist. There is also potential for denitrification near the plume's upper fringe zone, where nitrification appears to be active, since DOC remains (> 15 mg/L; Fig.30).

Finally, at this site where NO_3^- -N values are low but DOC concentrations are very high, competition for the NO_3^- could induce some organisms to perform DNRA rather than denitrification (Smith et al., 1991). Little is known of this process in groundwater, but terrestrial studies suggest that similar conditions would be conducive to DNRA reactions (Silver et al., 2001; Nizzoli et al., 2010).

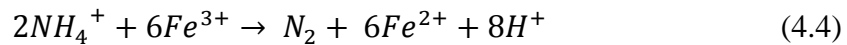
4.4.4 Anammox

The anammox reaction has been implicated in nitrogen attenuation observed in a variety of marine and aquatic environments (Thamdrup and Dalsgaard, 2002; Rysgaard et al., 2004; Jensen et al., 2008; Kuenen et al., 2008; Hamersley et al., 2009) and recently in groundwater environments (Clark et al., 2008; Robertson et al., 2010). The stoichiometry of the reaction is a 5:3 NH_4^+ to NO_3^- molar ratio with a release of H^+ (Eq. 1.5). While denitrification is

characterized by the loss of only NO_3^- , anammox shows the coincidental loss of both NO_3^- and NH_4^+ . The same loss of both NO_3^- and NH_4^+ can occur during coupled nitrification/denitrification reaction sequences. However, N_2O production, which occurs during both nitrification and denitrification does not occur during anammox, thus a lack of N_2O is one possible distinguishing characteristic of anammox (Bulow et al., 2010). Anammox may be more tolerant of mid-level DO concentrations, while denitrifiers can be inhibited completely at very low DO concentrations (Galán et al., 2009; Bulow et al., 2010). Also, denitrification increases pH whereas anammox decreases the pH (Eq. 1.5, 4.2). Denitrification is thought to dominate in high DOC environments, but a number of waste water treatment systems that include anammox occur in relatively high DOC slurries ($> 100 \text{ mg C/L}$; Pynaert et al., 1997; Sliemers et al., 2002). Other constituents such as Fe^{3+} and Mn^{4+} have also been implicated as potential electron acceptors for the anammox reaction (Strous et al., 2006; van Niftrik et al., 2008). The increase of reduced forms of these metals (Fe^{2+} and Mn^{2+} respectively) in solution *could* thus also indicate anammox activity. The most likely cause of the appearance of these dissolved metals is from organic matter oxidation, but with no rigorous DOC trends available, some of the production could be attributable to other reactions. Although little is known of isotopic evolution in the anammox reaction, a progressive enrichment of $^{15}\text{N}/^{14}\text{N}$ in both NO_3^- and NH_4^+ would be expected. Clark et al. (2008) observed $\delta^{15}\text{N-NH}_4^+$ a fractionation factor of -4% during NH_4^+ -N attenuation observed in groundwater at an industrially contaminated site. Similarly, Robertson et al. (2010) observed enrichment of $\delta^{15}\text{N-NH}_4^+$ from $\sim 8\%$ to $> 20\%$ as concentrations decreased in a septic system plume, also suggesting a fractionation factor of -4% . Moreover, this enrichment was more evident at depth, which is in contrast to what would be expected if NH_4^+ loss was due to nitrification at the water table.

In the Zorra plume, the core is largely deficient of NO_3^- -N (<1 mg/L), however elevated NO_3^- -N is present (19-40 mg/L) in the overlying shallow water table zone, intermittently, and in the underlying background water (~10 mg/L; Fig. 25, 26). The core is elevated in NH_4^+ -N but is deficient in NO_3^- -N which suggests that the boundary zones in particular, could be locations for anammox activity. Moderately low DO (1.4-1.8 mg/L) occurs in the background groundwater, while the plume core zone has DO concentrations of < 1 mg/L, conducive to anammox (Fig. 11). Note that the anammox reaction (Eq. 1.5) generates acidity (at a lower rate than nitrification) that could also contribute to CaCO_3 dissolution and the observed Ca^{2+} increases within the plume (Fig. 28). However, profiles of Ca^{2+} concentrations along the plume (Fig. 28) show that the Ca^{2+} increase occurs most sharply in immediate proximity to the lagoon, thus this is most likely a result of acidity generated during organic matter mineralization and possibly some nitrification.

In the absence of sufficient NO_3^- , Fe^{3+} is an alternative electron acceptor for anammox (Strous et al., 2006; van Niftrik et al., 2008) Eq. 4.4.



Fe^{2+} increases along the plume up to 61 mg/L (Fig. 28) compared to a lagoon value of 16 ± 5 mg/L, indicating the presence of reactive Fe^{3+} possibly associated with ferric-oxyhydroxide mineral coatings on the sediment grains. An Fe^{2+} increase of 45 mg/L could indicate NH_4^+ -N consumption of ~4.0 mg/L by Fe^{2+} associated anammox if no other reactions are considered. DOC can also act as an electron acceptor and could play a role in degradation along the centre line.

Although there is little evidence of systematic $\delta^{15}\text{N}$ - NH_4^+ enrichment along the flowpath (Fig. 27) or at decreased NH_4^+ concentrations (Fig. 33), previous studies suggest that isotopic

fractionation during anammox NH_4^+ consumption in groundwater is relatively low ($\epsilon \sim -4\text{‰}$ Clark et al., 2008; Robertson et al., 2010). Considering this low fractionation, it is likely that the extremely large seasonal variability of the lagoon $\delta^{15}\text{N-NH}_4^+$ signature (28-72‰ Table 2) would mask any anammox isotope effect. However, depth profiles of isotopic behaviour, particularly in the boundary zones where both NH_4^+ and NO_3^- occur together, does provide some evidence for anammox activity. Fig. 35 shows that $^{15}\text{N}/^{14}\text{N}$ in both NH_4^+ and NO_3^- become slightly enriched across the boundary zone by 3-6‰ for $\delta^{15}\text{N-NH}_4^+$ and 4-11 ‰ for $\delta^{15}\text{N-NO}_3^-$ at PU124, 92 & 125. The effect is most pronounced at PU124, where $^{15}\text{N}/^{14}\text{N}$ becomes enriched as concentrations of both NH_4^+ and NO_3^- decrease.

The most compelling evidence to support anammox activity at the Zorra site is presented by Moore et al (2010). DNA-based microbiological techniques (PCR) were used to show that anammox performing bacteria were present at the Zorra site, particularly at PU103 and PU106, comprising up to 5% of the total groundwater bacterial population. The presence of anammox bacteria in the site groundwater, coupled with laboratory batch tests using isotopically tagged $\delta^{15}\text{N-NH}_4^+$ and $\delta^{15}\text{N-NO}_3^-$ showed that anammox was responsible for up to 29% of inorganic nitrogen loss at the Zorra site versus 71% for denitrification.

4.4.5 Ammonification

Organic nitrogen is a common constituent in manure lagoon waters and in the underlying sediment material at concentrations often above 100 mg DON/L (DeSutter et al., 2005; Vaillant et al., 2009). However, the organic nitrogen typically ammonifies (mineralizes to NH_4^+) in the vadose zone or during slow groundwater migration. However, in the Zorra plume DON is a dominant component of the TN, accounting for up to 90% in the lagoon, and averaging ~40% as

far as 100 m downgradient (Fig. 25, 26). It is possible that this large organic nitrogen component ammonifies along the groundwater flow path, generating additional NH_4^+ . Ammonification is characterized simply by a loss of organic N and gain of NH_4^+ in solution. The process is tolerant to many pH, DO, temperature and substrate conditions, operating optimally between pH of 6.5-8.5 (Vymazal, 2002; Lee et. al, 2009). Ammonification occurs in both oxygenated and anaerobic zones; competing with the nitrification reaction for oxygen in aerobic zones. Kinetically, ammonification is a faster reaction than nitrification and may dominate over nitrification at low temperatures (Lee et. al, 2009). Since DON is continually lost through the plume core zone (Fig. 25, 26, Table 6), conversion to either NH_4^+ or NO_3^- (where DO is available) must be occurring, as evidenced through rough ammonification lab batch experiments (Fig. 37, Table 7). Consistent loss of DON averaging 96% (Table 6) along the plume, declining from mean values of 218 mg/L to < 10 mg/L over the 100 m plume flow path suggests active ammonification. Assuming ammonification is primarily leading to NH_4^+ production, the dilution adjusted DON loss can be converted to NH_4^+ . This added NH_4^+ input could also substantially influence the NH_4^+ isotopic signature. Initially, the $^{15}\text{N}/^{14}\text{N}$ of both DON and NH_4^+ that is formed initially should be the same since they both derive from the same poultry manure source. However, NH_4^+ is prone to volatilization, enriching the residual $\delta^{15}\text{N-NH}_4^+$, whereas the $\delta^{15}\text{N-DON}$ would remain more constant in the lagoon. NH_4^+ and DON from the lagoon reaching the water table could then have two different $\delta^{15}\text{N}$ signatures. Since the process of ammonification is not associated with a large fractionation (Kendall, 1998; Mariappan et al. 2009), any NH_4^+ derived through ammonification could then alter the $\delta^{15}\text{N-NH}_4^+$ in groundwater. The effect could be determined if both ^{15}N values are known and the percent influence of ammonification could then be quantified via a mixing calculation Eq. 4.5, where the fraction of ammonification (AMM)

derived NH_4^+ could be determined knowing the measured (meas.) and lagoon derived (L) $\delta^{15}\text{N}$ - NH_4^+ permil values :

$$f_{AMM} = \frac{\%Meas - \%L}{\%AMM - \%L} \quad (4.5)$$

Ammonification is suggested to occur based on the results of lab batch ammonification experiments, whereby DON loss is coupled to the gain of NO_3^- in solution (Table 7). The intermediate step, conversion of DON to NH_4^+ -N is not seen due to the sampling time and abundant O_2 available to the solution. However, both the $\delta^{15}\text{N}$ -DON, and the rates of ammonification are unknown at the Zorra site, and both of these aspects are unstudied in groundwater settings. If ammonification is active, predictions of nitrogen transformation processes based on expected enrichment schemes may be perturbed. Thus, ammonification may be a component of the nitrogen story in the Zorra plume that requires further attention and additional studies should be undertaken.

5.0 Conclusions & Summary

5.1 Overall Nitrogen Attenuation

The lagoon input at the Zorra site is seasonally variable and the aquifer is highly heterogeneous and permeable. DON is a substantial component of the plume TN (~40% on average) and the plume is extensively mixed with background groundwater, diluted by an average of 85%. All of these factors make resolving the fate of nitrogen along the plume flow path very difficult. However, despite these issues, the fact remains that through a combination of dilution (no doubt assisted by the heterogeneous and variable flow path) and biological reaction, plume concentrations of total nitrogen decrease by 93% (on average) through 100 m of groundwater flow from the source over two years of monitoring. Although only ~ 10% can be attributable to degradation reactions, this represents a mean total nitrogen consumption of 36 mg/L which is substantial. Considering a representative groundwater velocity of 400 m/yr (Table 1) and the 100 m plume length monitored, this consumption occurs over a period of ~3 months. This equates to a degradation rate of ~0.4 mg/L/day. Although modest, this rate could allow for very substantial nitrogen attenuation over time considering the multiyear ages of many groundwater plumes.

One question to be answered in regards to the 32 mg/L of attenuated total nitrogen is: what portion of this is attributable to denitrification, and how much to anammox? Since denitrification and anammox represent the only complete elimination pathways, determining the influence of each would be a valuable activity in advancing our knowledge of the anammox process in groundwater. At this site the two processes may operate concurrently, with the dominance of one process over the other changing depending on changes in substrate concentrations and the microbiological community composition along the way.

Nitrification/denitrification pathways are suggested through the production of N_2O with loss of nitrogen, while geochemical evidence for anammox is strongly supported by microbiological and laboratory tracer studies (Moore et al., 2010). Further isotopic studies have the potential to help unravel this uncertainty, but can only be properly interpreted with a thorough understanding of the dynamics of ammonification along the flow path. DON is an understudied component of the nitrogen cycle in groundwater, but at sites such as the Zorra site it is very important and should be the focus of further work.

5.2 Anammox

While the exact proportion of nitrogen loss attributable to anammox is a difficult to estimate, the geochemical evidence supports the likelihood that anammox is indeed an active process at the Zorra site, which puts it among the first field studies to illustrate this newly discovered natural attenuation process for reactive nitrogen removal in groundwater. The concurrent disappearance of NO_3^- and NH_4^+ in an anoxic plume core, with a dearth of N_2O , contrary to what would be expected from the nitrification/denitrification cycle is supported by the concurrent, although slight enrichment of $^{15}N/^{14}N$ of both NO_3^- and NH_4^+ where the two coexist. This process is also strongly supported by a predominant portion of microbiological samples taken by Moore et al (2010) showing anammox performing bacteria present and active. Additionally, laboratory studies within the Moore et al. study suggest that anammox contributes ~29% of the nitrogen attenuation through the use of isotopically tagged $\delta^{15}N$ in batch tests. Having the foundations of a geochemical interpretation is an important step in supporting the evidence for anammox at this site.

5.3 Next Steps

Furthering the understanding of the contribution of anammox at the Zorra site requires a greater comprehension of the entire nitrogen cycle; particularly ammonification. The substantial loss of DON along the flow path along with confounding $\delta^{15}\text{N-NH}_4^+$ results well below the range of the source suggest ammonification is an active process on site. To confirm, $\delta^{15}\text{N-DON}$ should be determined in future study to confirm or deny the effects of this process. This could be achieved through the collection of a suite of samples along the plume core zone analyzed for NO_3^- , NH_4^+ and DON concentrations, as well as respective isotopes. Further to this, more reliable and a greater distribution of DOC concentrations can help determine the presence of ammonification through the changing ratios of C:N. DON is such a significant component of the total nitrogen through the flow path that it cannot be ignored. Since the persistence of DON along a plume is so uncommon, little information exists about the rates or effects of ammonification, which opens the door for some novel investigations.

Aside from investigation of ammonification, soil coring, to determine more precisely the role of sorption at the site should be undertaken. Coring over two time snapshots in similar locations would provide insight into the possibility for continuing sorption. However, the considerable heterogeneity of the site would have to be kept in mind during such an investigation.

Once ammonification can be understood, a thorough characterization of the centreline in-situ to investigate the utility of isotopic enrichment as a tracer for anammox can be undertaken. Such an investigation would be time and labour intensive, but could enlighten further researchers into acceptable or even ideal conditions for groundwater anammox to take place. Knowing

through biological and lab incubation experiments that anammox is a player at the Zorra site gives a great deal of support to continue such research at Zorra. Keys to continued success lie in keeping track of the highly variable source, and the dynamics of ammonification. If the source were to be discontinued at some point in the future, this in particular would present a unique opportunity to investigate the effects of sorption, nitrification, denitrification and anammox as the plume eventually dissipates.

References

- Amanullah, M.M., S. Sekar and P. Muthukrishnan. 2010. Prospects and potential of poultry manure. *A. J. Plant Sci.* 9: 172-182.
- Aravena, R. and W.D. Robertson. 1998. Use of multiple isotope tracers to evaluate denitrification in ground water: study of nitrate from a large-flux septic system plume. *Ground Water* 36: 975-982.
- Avrahami, S., R. Conrad and G. Braker. 2002. Effect of ammonium concentration on N₂O release and on the community structure of ammonia oxidizers and denitrifiers. *Appl. Environ. Microbiol.* 68: 5685-5692.
- Bjerg P.L. & T.H. Christensen. 1993. A field experiment on cation exchange-affected multi-component solute transport in a sandy aquifer. *J. Contam. Hydrol.* 12: 269-290.
- Böhlke, J.K., R.L. Smith and D.N. Miller. 2006. Ammonium transport and reaction in contaminated groundwater: application of isotope tracers and isotope fractionation studies. *Water Resour. Res.* 42: W05411.
- Böttcher, J., O. Strelbel, S. Voerkelius and H.L. Schmidt. 1990. Using isotope fractionation of nitrate-nitrogen and nitrate-oxygen for evaluation of microbial denitrification in a sandy aquifer. *J. Hydrol.* 114: 413-424.
- Brad, T., B.M. van Breukelen, M. Braster, N.M. van Straalen and W.F.M. Röling. 2008. Spatial heterogeneity in sediment-associated bacterial and eukaryotic communities in a landfill leachate-contaminated aquifer. *FEMS Microbiol. Ecol.* 65: 534-543
- Brown, C. 2005. Available nutrients for manure from various livestock types. Ontario Ministry of Agriculture Food and Rural Affairs. available [online]:
http://www.omafra.gov.on.ca/english/crops/field/news/croptalk/2005/ct_1105a6.htm
- Bulow, S.E., J.J. Rich, H.S. Naik, A.K. Pratihary and B.B. Ward. 2010. Denitrification exceeds anammox as a nitrogen loss pathway in the Arabian Sea oxygen minimum zone. *Deep Sea Res. I* 57:384-393.

Burgin, A.J. and S.K. Hamilton. 2007. Have we overemphasized the role of denitrification in aquatic ecosystems? A review of nitrate removal pathways. *Front. Ecol. Environ.* 5: 89-96.

Burr, C. 2010. Personal communication regarding analytical methods. Soil and Nutrient Laboratory, University of Guelph, Guelph, ON.

Buss, S.R., A.W. Herbert, P. Morgan, S.F. Thornton and J.W.N. Smith. 2004. A review of ammonium attenuation in soil and groundwater. *Q. J. Eng. Hydrol. Hydrogeol.* 37: 347-359

Canadian Council of Ministers of the Environment. 1998. Canadian Environmental Quality Guidelines,

Chapter 4: Canadian water quality guidelines for the protection of aquatic life. CCME, Winnipeg, MB.

Casciotti, K.L., D.M. Sigman and B.B. Ward. 2003. Linking diversity and stable isotope fractionation in ammonia-oxidizing bacteria. *Geomicrobiol. J.* 20: 335-353.

Ceazan, M.L., E.M. Thurman, R.L. Smith. 1989. Retardation of ammonium and potassium transport through a contaminated sand and gravel aquifer: the role of cation exchange. *Environ. Sci. Technol.* 23: 1402-1408.

Christensen, T.H., P. Kjedsen, P.L. Bjerg, D.L. Jensen, J.B. Christensen, A. Baun, H. J. Albrechtsen and G. Heron. 2001. Biogeochemistry of landfill leachate plumes. *Appl. Geochem.* 16: 659-718

Clark, I. And P. Fritz. 1997. *Environmental isotopes in hydrogeology.* CRC Press, New York, New York.

Clark, I., R. Timlin, A. Bourbonnais, K. Jones, D. Lafleur, K. Wickens. 2008. Origin and fate of industrial ammonium in anoxic ground water – ¹⁵N evidence for anaerobic oxidation (anammox), *Ground Water Monit. Rem.* 28:73-82.

Dance, J.T. & E.J. Reardon. 1983. Migration of contaminants in groundwater at a landfill: a case study. 5. Cation migration in the dispersion test. *J. Hydrol.* 63: 109-130.

- DeSimone, L.A., B.L. Howes & P.M. Barlow. 1997. Mass-balance analysis of reactive transport and cation exchange in a plume of wastewater-contaminated groundwater. *J. Hydrol.* 203: 228-249.
- de Vries, W., J. Kros, O. Oenema and J. de Klein. 2003. Uncertainties in the fate of nitrogen II: A quantitative assessment of the uncertainties in major nitrogen fluxes in the Netherlands. *Nutr. Cycling Agroecosyst.* 66: 71-102.
- Delwiche, C.C. and P.L. Steyn. 1970. Nitrogen isotope fractionation in soils and microbial reactions. *Environ. Sci. Technol.* 4: 929-935.
- Denver, J.M., A.J. Tesoriero and J.R. Barbaro. 2010. Trends and transformations of nutrients and pesticides in a coastal plain aquifer system. *J. Environ. Qual.* 39: 154-167.
- DeSutter, T.M., G.M. Pierzynski and J.M. Ham. 2005. Movement of lagoon-liquor constituents below four animal waste lagoons. *J. Environ. Qual.* 34: 1234-1232.
- Environment Canada. 2011. Canadian Climate Normals 1971-2000 for Woodstock, ON. Available [online]: http://www.climate.weatheroffice.gc.ca/climate_normals/index_e.html
- Fernando, W.A.R.N., K. Xia and C.W. Rice. 2005. Sorption and desorption of ammonium from liquid swine waste in soils. *Soil Sci. Soc. Am. J.* 69: 1057-1065.
- Fritz, P., S.K. Frappe, R.J. Drimmie and A.R. Heemskerk. 1986. Reply to comments by Grabczak et al. On 'Water-rock interaction and chemistry of groundwaters from the Canadian Shield'. *Geochim. Cosmochim. Acta.* 50: 1561-1563.
- Galán, A., V. Molina, B. Thamdrup, D. Woebken, G.Lavik, M.M.M. Kuypers and O. Ulloa. 2009. Anammox bacteria and the anaerobic oxidation of ammonium in the oxygen minimum zone off northern Chile. *Deep Sea Res. II* 56:1125-1135.
- Goolsby, D.A., W.A. Battaglin, B.T. Aulenbach and R.P. Hooper. 2001. Nitrogen input to the Gulf of Mexico. *J. Environ. Qual.* 30: 329-336.
- Goss, M.J., K.S. Rollins, K. McEwan, J.R. Shaw and H. Lammers-Helps. 2001. The management of manure in Ontario with respect to water quality. University of Guelph, ON.

Available [online]:

http://agrienvarchive.ca/bioenergy/download/manure_man_ONT_waterquality2001.pdf

Hamersley, M.R., G. Lavik, D. Woebken, J.E. Rattray, P. Lam, E.C. Hopmans, J.S.S. Damsté, S. Krüger, M. Graco, D. Gutiérrez and M.M.M. Kuypers. 2007. Anaerobic ammonium oxidation in the Peruvian oxygen minimum zone. *Limnol. Oceanogr.* 52:923-933.

Hayakawa, A., H. Akiyama, S. Sudo and K. Yagi. 2009. N₂O and NO emissions from an Andisol field as influenced by pelleted poultry manure. *Soil Biol. Biochem.* 41: 521-529.

Hazen, A., 1911: Discussion of "dams on sand foundations", by A.C. Koenig, *Transactions of the American Society of Civil Engineers*, v. 73, pp. 199-200.

Health Canada. 1987. Ammonia (Guidelines for Canadian Drinking Water Quality – Technical Documents). Available [online]: <http://www.hc-sc.gc.ca/ewh-semt/pubs/water-eau/ammonia-ammoni/index-eng.php>

Health Canada. 1992. Nitrate/Nitrite(Guidelines for Canadian Drinking Water Quality – Technical Documents). Available: [online] http://www.hc-sc.gc.ca/ewh-semt/pubs/water-eau/nitrate_nitrite/index-eng.php

Heemskerk, R. 1993. Water ¹⁸O by CO₂ Equilibration. Environmental Isotope Laboratory, technical procedure 13.0. Waterloo, ON.

Hinkle, S.R., J.K. Böhlke and L.H. Fisher. 2008. Mass balance and isotope effects during nitrogen transport through septic tank systems with packed-bed (sand) filters. *Sci. Total Environ.* 407:324-332.

Holmes, R.M., J.W. McClelland, D.M. Sigman, B. Fry and B.J. Peterson. 1998. Measuring ¹⁵N-NH₄⁺ in marine, estuarine and fresh waters: an adaptation of the ammonia diffusion method for samples with low ammonium concentrations. *Mar. Chem.* 60: 235-243.

IPCC, 2007: Summary for Policymakers. In: *Climate Change 2007: The Physical Science Basis. Contribution of Working Group I to the Fourth Assessment Report of the Intergovernmental Panel on Climate Change* [Solomon, S., D. Qin, M. Manning, Z. Chen, M. Marquis, K.B.

Averyt, M.Tignor and H.L. Miller (eds.)]. Cambridge University Press, Cambridge, United Kingdom and New York, NY, USA.

Jensen, M. M., M.M.M. Kuypers, G. Lavik and B. Thamdrup. 2008. Rates and regulation of anaerobic ammonium oxidation and denitrification in the Black Sea. *Limnol. Oceanogr.* 53:23-36.

Kaiser, D.R., D.J. Reinert, J.M. Reichert, C.A. Streck and A. Pellegrini. 2010. Nitrate and ammonium in soil solution in tobacco management systems. *R. Bras. Ci. Solo.* 34: 379-387

Karamanos, R.E. and D.A. Rennie. 1978. Nitrogen isotope fractionation during ammonium exchange reactions with soil clay. *Can. J. Soil Sci.* 58: 53-60.

Karr, J.D., W.J. Showers, J.W. Gilliam and A.S. Andres. 2001. Tracing nitrate transport and environmental impact from intensive swine farming using delta nitrogen-15. *J. Environ. Qual.* 30: 1163-1175.

Karr, J.D., W.J. Showers and T.H. Hinson. 2002. Nitrate source identification using $\delta^{15}\text{N}$ in a ground water plume near an intensive swine operation. *Ground Water Monit. Rem.* 22: 68-75.

Kelso, B.H.L., R.V. Smith, R.J. Laughlin and S.D. Lennox. 1997. Dissimilatory nitrate reduction in anaerobic sediments leading to river nitrate accumulation. *Appl. Environ. Microbiol.* 63: 4679-4685

Kirschenbaum, I., J.S. Smith and T. Crowell. 1947. Separation of the nitrogen isotopes by the exchange reaction between ammonia and solutions of ammonium nitrate. *J. Chem. Phys.* 15:440-446.

Korom, S.F. 1992. Natural denitrification in the saturated zone: a review. *Water Resour. Res.* 28: 1657-1668.

Larney, F.J., K.E. Buckley, X. Hao and W.P. McCaughey. 2006. Fresh, stockpiled and composted beef cattle feedlot manure: nutrient levels and mass balance estimates in Alberta and Manitoba. *J. Environ. Qual.* 35: 1844-1854.

Lee, C., T.D. Fletcher and G. Sun. 2009. Nitrogen removal in constructed wetland systems. *Eng. Life Sci.* 9: 11-22.

Lide DR and W.M. Haynes. 2010. *CRC Handbook of Chemistry and Physics*, 90th ed. Available at: <http://www.hbcnpnetbase.com>.

Loveless, A.M. and C.E. Oldham. 2010. Natural attenuation of nitrogen in groundwater discharging through a sandy beach. *Biogeochemistry* 98: 75-87.

Lu, S., H. Hu, Y. Sun and J. Yang. 2009. Effect of carbon source on the denitrification in constructed wetlands. *J. Environ. Sci.* 21: 1036-1043

Mallin, M.A. and L.B. Cahoon. 2003. Industrialized animal production – a major source of nutrient and microbial pollution to aquatic ecosystems. *Popul. Environ.* 24: 369-385.

Mariappan, S., M.E. Exner, G.E. Martin and R.F. Spalding. 2009. Variability of anaerobic animal waste lagoon delta¹⁵N source signatures. *Environ. Forensics* 10: 18-25.

Mariotti, A., J.C. Germon, P. Hubert, P. Kaiser, R. Letolle, A. Tardieux and P. Tardieux. 1981. Experimental determination of nitrogen kinetic isotope fractionation: some principles; illustration for the denitrification and nitrification processes. *Plant Soil* 62: 413-430

McNab, W.W., M.J. Singleton, J.E. Moran and B.K. Esser. 2007. Assessing the impact of animal waste lagoon seepage on the geochemistry of an underlying shallow aquifer. *Environ. Sci. Technol.* 41: 753-758.

McLean, N. 2007. Use of drains for passive control of flow through a permeable reactive barrier. MSc. Thesis, Dept. of Earth Sciences, University of Waterloo, Waterloo, ON.

Meile, C., W.P. Porubsky, R.L. Walker and K. Payne. 2010. Natural attenuation of nitrogen loading from septic effluents: spatial and environmental controls. *Wat. Res.* 44: 1399-1408.

Moon, P.E. 1997. *Basic On-Farm Composting Manual (Report CM-97-3)*. Clean Washington Centre. Seattle, Washington. Available [online]: <http://www.cwc.org/wood/wd973rpt.pdf>

Moore, T., B. Lazenby, S. Schiff, W. Robertson, D. Fortin, R. Timlin, S. Ladia, C. Ryan, R. Aravena, I. Clark and J.D. Neufeld. 2010. Anammox bacteria are predominant microbial

community members in ammonium-contaminated groundwater. Abstract presented at Canadian Soc. Microbiol. meeting, Hamilton, ON, June 15, 2010.

Mulder A., A.A. van de Graaf, L.A. Robertson, J.G. Kuenen. 1995. Anaerobic ammonium oxidation discovered in a denitrifying fluidized bed reactor, *FEMS Microbiol. Ecol.* 16:177-184.

Nahm, K.H. 2003. Evaluation of the nitrogen content in poultry manure. *World Poultry Sci. J.* 59: 77-88.

Nicholson, R.V., J.A. Cherry and E.J. Reardon. 1983. Migration of contaminants in groundwater at a landfill: A case study 6. Hydrogeochemistry. *J. Hydrol.* 63: 131-176.

Nizzoli, D., E. Carraro, V. Nigro and P. Viaroli. 2010. Effect of organic enrichment and thermal regime on denitrification and dissimilatory nitrate reduction to ammonium (DNRA) in hypolimnetic sediments of two lowland lakes. *Wat. Res.* 44: 2715-2724.

Núñez-Delgado, A., E. Lopez-Periago and F. Diaz-Fierros-Viqueira. 1997. Breakthrough of inorganic ions present in cattle slurry: soil column trials. *Wat. Res.* 31: 2892-2898.

Ontario Ministry of the Environment. 2006. Technical support document for Ontario drinking water standards, objectives and guidelines. Available [online]: <http://www.ene.gov.on.ca/envision/gp/4449e01.pdf>

Payne, W.J. 1976. Denitrification. *Trends Biochem. Sci.* 1: 220-222.

Penny, E., M.K. Lee and C. Morton. 2003. Groundwater and microbial processes of Alabama coastal plain aquifers. *Water Resour. Res.* 39:HWC2-1-HWC2-17

Pérez, T., D. Garcia-Montiel, S. Trumbore, S. Tyler, P. de Camargo, M. Moreira, M. Piccolo and C. Cerri. 2006. Nitrous oxide nitrification and denitrification ^{15}N enrichment factors from Amazon forest soils. *Ecol. Appl.* 16: 2153-2167.

Postma, D., C. Boesen, H. Kristiansen and F. Larsen. 1991. Nitrate reduction in an unconfined sandy aquifer: water chemistry, reduction processes, and geochemical modelling. *Water Resour. Res.* 27:2027-2045.

Pynaert K., B.F. Smets, D. Beheydt and W.Verstraete. 1997. Start-up of autotrophic nitrogen removal reactors via sequential biocatalyst addition, *Environ. Sci. Technol.* 35:111-120.

Robertson, W.D., E.A. Sudicky, J.A. Cherry, R.A. Rapaport and R.J. Shrimp. 1989. Impact of a domestic septic system on an unconfined sand aquifer. Contaminant transport in groundwater: symposium proceedings, Stuttgart, pg. 105-112.

Robertson, W.D., C.J. Ptacek and S.J. Brown. 2007. Geochemical and hydrogeological impacts of a wood particle barrier treating nitrate and perchlorate in ground water. *Ground Water Monit. Rem.* 27: 85-95.

Robertson, W.D. and S.L. Schiff. 2008. Persistent elevated nitrate in a riparian zone aquifer. *J. Environ. Qual.* 37: 669-679.

Robertson, W.D., J.L. Vogan and P.S. Lombardo. 2008. Nitrate removal rates in a 15-year-old permeable reactive barrier treating septic system nitrate. *Ground Water Monit. Rem.* 28: 65-72.

Robertson, W.D., J. Spoelstra, L. Li, R. Elgood, I.D. Clark, S.L. Schiff, R. Aravena and J.D. Neufeld. 2010. Natural attenuation of septic system nitrogen by anammox.

Rynk, R. 1992. Northeast Regional Agricultural Engineering Service. On-farm Composting Handbook.

NRAS-54. Northeast Regional Agricultural Engineering Service. Ithaca, NY

Rysgaard, S., R.N. Glud, N. Risgaard-Petersen and T. Dalsgaard. 2004. Denitrification and anammox activity in Arctic marine sediments. *Limnol. Oceanogr.* 49:1493-1502.

Saunders, J.A., M.A. Pritchett and R.B. Cook. 1997. Geochemistry of biogenic pyrite and ferromanganese coatings from a small watershed: a bacterial connection? *Geomicrobiol. J.* 14:203-217

Schubert, C.J., E. Durisch-Kaiser, B. Wehrli, B. Thamdrup, P. Lam, and M.M.M. Kuypers 2008. Anaerobic ammonium oxidation in a tropical freshwater system (Lake Tanganyika). *Environ. Microbiol.* 8:1857-1863.

Sebilo, M., B. Mayer, M. Grably, D. Billiou and A. Mariotti. 2004. The use of the ammonium diffusion method for $^{15}\text{N-NH}_4^+$ and $^{15}\text{N-NO}_3^-$ measurements: comparison with other techniques. *Environ. Chem.* 1:99-103

Sheppard, S.C., S. Bittman and J. Tait. 2008. Monthly NH_3 emissions from poultry in 12 ecoregions of Canada. *Can. J. Anim. Sci.* 89: 21-35.

Sills, A.R. 2006. The fate of a groundwater ammonium plume from an earthen manure storage tank. MSc. Thesis, Dept. Of Earth Sciences, University of Waterloo, Waterloo, ON.

Silva, S.R., C. Kendall, D.H. Wilkison, A.C. Zeigler, C.C.Y. Chang, and R.J. Avanzino. 2000. A new method for collection and analysis of nitrate from dilute water for nitrogen and oxygen isotopes. *J. Hydrol.* 228: 22-36.

Silver, W.L., D.J. Herman and M.K. Firestone. 2001. Dissimilatory nitrate reduction to ammonium in upland tropical forest soils. *Ecology* 82: 2410-2416.

Sliekers, A.O., N. Derwort, J.L.C Gomez, M. Strous, J.G. Kuenen, M.S.M. Jetten. 2002. Completely autotrophic nitrogen removal over nitrite in one single reactor, *Water Res.* 36:2475-2482.

Smith, R.L., Howes, B.L. and J.H. Duff. 1991. Denitrification in nitrate-contaminated groundwater: occurrence in steep vertical geochemical gradients. *Geochim. Cosmochim. Acta* 55: 1815-1825.

Sørensen, P. and E.S. Jensen. 1991. Sequential diffusion of ammonium and nitrate from soil extracts to a polytetrafluoroethylene trap for ^{15}N determination. *Anal. Chim. Acta* 252: 201-203.

Spoelstra, J., M. Murray and R.J. Elgood. 2006. A simplified diffusion method for delta ^{15}N analysis of NH_4^+ . Environmental Geochemistry Lab Technical Procedure 20. Department of Earth and Environmental Sciences, University of Waterloo. 10 pp.

Spoelstra, J. 2010. Personal communication regarding analytical methods of groundwater cations. National Water Research Institute, Environment Canada. Burlington, ON.

Statistics Canada 2007. Canadian environmental sustainability indicators: socio-economic information. (Catalogue number 16-253-X). Ottawa, ON. Statistics Canada. Environment

Accounts and Statistics Division. Retrieved January 15, 2011 from
<http://www.statcan.gc.ca/bsolc/olc-cel/olc-cel?catno=16-253-X&lang=eng>

Straub, K.L., M. Benz, B. Schink and F. Widdel. 1996. Anaerobic, nitrate-dependent microbial oxidation of ferrous iron. *Appl. Environ. Microbiol.* 62:1458-1460.

Strous, M., E. Pelletier, S. Mangenot, T. Rattei, A. Lehner, M.W. Taylor, M. Horn, H. Daims, D. Bartol-Mavel, P. Wincker, V. Barbe, N. Fonknechten, D. Vallenet, B. Segurens, C. Schenowitz-Truong, C. Médingue, A. Collingro, B. Snel, B.E. Dutilh, H.J.M. Op den Camp, C. Van der Drift, I. Cirpus, K.T. van de Pas-Schoonen, H.R. Harhangi, L. van Niftrik, M. Schmid, J. Keltjens, J. van de Vossenberg, B. Kartal, H. Meier, D. Frishman, M.A. Huynen, H.W. Mewes, J. Weissenbach, M.S.M. Jetten, M. Wagner and D. Le Paslier. 2006. Deciphering the evolution and metabolism of an anammox bacterium from a community genome. *Nature* 440:790-794.

Thamdrup, B. and T. Dalsgaard. 2002. Production of N₂ through anaerobic ammonium oxidation coupled to nitrate reduction in marine sediments. *Appl. Environ. Microbiol.* 60:1312-1318.

Thomas R.L., R.W. Sheard and J.R. Moyer. 1967. Comparison of conventional and automated procedures for N, P and K analysis of plant material using a single digestion. *Agron. J.* 59:240-243.

Torrentó, C., J. Cama, J. Urmeneta, N. Otero and A. Soler. 2010. Denitrification of groundwater with pyrite and *Thiobacillus denitrificans*. *Chem. Geol.* 278:80-91.

Thuss, S. J., 2008. Nitrous oxide production in the Grand River, Ontario, Canada: new insights from stable isotope analysis of dissolved nitrous oxide. M.Sc. thesis, Department of Earth Sciences. Univ. of Waterloo, Waterloo, ON

Trudell, M.R., R.W. Gillham and J.A. Cherry. 1986. An in-situ study of the occurrence and rate of denitrification in a shallow unconfined sand aquifer. *J. Hydrol.* 83: 251-268.

United States Environmental Protection Agency. 1993. Methods for the Determination of Inorganic Substances in Environmental samples. EPA/600/R-93/100: Method 353.2

Urey, H.C. 1947. The thermodynamic properties of isotopic substances. *J. Chem. Soc.* 1947: 562-581.

Vaillant, G.C., G.M. Pierzynski, J.M. Ham and J. DeRouche. 2009. Nutrient accumulation below cattle feedlot pens in Kansas. *J. Environ. Qual.* 38: 909-918.

van Niftrik, L., W.J.C. Geerts, E.G. van Donselaar, B.M. Humbel, A. Yakushevskaya, A.J. Verkleij, M.S.M. Jetten and M. Strous. 2008. Combined structural and chemical analysis of the anammoxosome: a membrane-bounded intracytoplasmic compartment in anammox bacteria. *J. Struct. Biol.* 161:401-410.

Vymazal, J. 2002. The use of sub-surface constructed wetlands for wastewater treatment in the Czech Republic: 10 years experience. *Ecol. Eng.* 18: 633-646.

Ward, D. and J. Johnson. 2009. Siting regulations for manure storage facilities (Document 09-061) Ontario Ministry of Agriculture Food and Rural Affairs. Available [online]: <http://www.omafra.gov.on.ca/english/engineer/facts/09-061.pdf>

Wilhelm, S.R., S.L. Schiff and W.D. Robertson. 1996. Biogeochemical evolution of domestic waste water in septic systems: 2. Application of conceptual model in sandy aquifers. *Groundwater.* 34: 853-864.

Williams, C.M. 2009. Development of environmentally superior technologies in the US and policy. *Biores. Technol.* 100: 5512-5518.

World Health Organization. 2003. Ammonia in drinking water. Geneva. (Originally published in: *Guidelines for Drinking Water Quality*, 2nd ed. Vol. 2. Health criteria and other supporting information. WHO Geneva, 1996.)

Zumft, W.G. 1997. Cell biology and molecular basis of denitrification. *Microbiol. Mol. Biol. R.* 61: 533-596

Table 1. a) Hydraulic conductivity (K) at selected monitoring points as determined by grain size analysis from borehole core samples **b)** Darcy velocity (q) and groundwater velocity (v) calculated for each unit using a representative K and hydraulic gradient (i) where $q=KI$ and $v = q/\eta$, using a porosity (η) of 0.3.

a)

Unit	Sample	K (cm/s)
Gravel	PU124-6.5	2.25
	PU122-6.5	1.0
	PU123-7.5	0.16
	PU122-7.5	0.16
	¹ PU104 6.0-7.5 m	10
Sand/ Gravel	PU124-4.5	0.2
	PU124-3.0	0.2
	PU122-5.5	0.1
	PU125-5.5	0.06
	PU123-3.5	0.16
	PU123-5.5	0.16
	PU123-0.5	0.2
Sand	PU124-0.5	0.02
	PU124-1.5	0.02
	PU122-4.5	0.01
	PU122-3.0	0.001
	PU122-2.0	0.01
	PU122-0.5	0.01
	PU125-0.5	0.01
	PU125-2.5	0.04
	PU125-4.5	0.04
	PU125-7.0	0.04
	PU123-2.0	0.0001

b)

Unit	K (cm/s)	i	q (m/yr)	v (m/yr)
Gravel	2.7	0.0025	2100	7000
Sand & Gravel	0.15	0.0025	120	400
Sand	0.018	0.0025	15	50

¹ determined by pumping test; all data available in Appendix B

Table 2. Geochemistry at the lagoon between August 28, 2008 and January 7, 2010. Number of samples (n), mean, and standard deviation (S.D.) are given for each parameter. Samples were taken from the south shore of the lagoon, near PU99 (Figure 3).

Date	NH ₄ ⁺ -N mg/L	NO ₃ ⁻ -N mg/L	Total N mg/L	DON mg/L	Cl ⁻ mg/L	EC μS/cm	pH	Ca ²⁺ mg/L	Fe ²⁺ mg/L	K ⁺ mg/L	Mg ²⁺ mg/L	Na ⁺ mg/L	δ ¹⁵ N-NH ₄ ⁺ ‰
Aug. 28/08	58.5	3.5			815			74.0	20.6	1309	102	243	45.5
Sept. 3/08	53.7	3.8			926	5570							
Sept. 11/08	44					8620	7.8						
Sept. 23/08	87.1	2.6			718								
Oct. 31/08	150	3.4				7500	7.9 8	71.0	18.9	1343	67.1	336	33.6
Dec. 1/08	67.8	1.4			327			41.0	8.2	624	36.9	127	29.4
Mar.3/09	43												
Mar. 31/09	236												
May 11/09	268					4200							34.7
June 15/09	131		450	315		5180		76.9	19.8	1215	47.8	208	45.2
July 15/09	112	2.94						62.2	12.6	1213	52.9	214	48.2
Aug 20/09	80.1	4	290	205		5110	7.6 6	72.1	21.2	1234	67.1	226	53.0
Sept. 25/09	79.8	3	260	180		3150							47.4
Oct. 31/09						4440							
Nov. 13/09	32.0	2.83	285	250				88.9	10.8	970	74.3	182	72.1
Jan. 7/10	374		520	140									28.2
Mean	121	3.1	361	218	697	5470	7.8	69.4	16.0	1130	64.0	219	43.7
S.D.	98.5	0.8	116	67.2	261	1785	0.2	14.9	5.3	253	21.1	63.7	13.2
n	15	9	5	5	4	8	3	7	7	7	7	7	10

Table 3. Mean chemical composition of the lagoon compared to the background well (PU86, 1.9-3.1 m depths) between July 1, 2008 and January 7, 2010. Mean values are given with standard deviation (S.D.) and number of samples (n).

		$\text{NH}_4^+\text{-N}$ mg/L	$\text{NO}_3^-\text{-N}$ mg/L	$\delta^{15}\text{N-NH}_4^+$ ‰	DON mg/L	TN mg/L
Lagoon	Mean	121	3	44	218	361
	S.D.	98	0.8	13	67	116
	n	10	10	9	5	5
Background Well	Mean	< 0.01	10	NA	< 1	10
	S.D.	0	1	NA	0	1
	n	10	12	NA	6	6

		Cl^- mg/L	EC $\mu\text{S/cm}$	pH	E_h mV	Al^{3+} mg/L	Ca^{2+} mg/L	Fe^{2+} mg/L	K^+ mg/L	Mg^{2+} mg/L	Na^+ mg/L
Lagoon	Mean	700	5500	7.81	38	<0.05	70	16	1120	64	220
	S.D.	250	1800	0.16	86	<0.05	15	5	250	21	64
	n	6	10	7	7	7	10	8	10	10	10
Background Well	Mean	7	600	7.44	84	<0.05	90	<0.02	3	19	6
	S.D.	4	130	0.09	1	<0.05	12	<0.02	2	3	4
	n	7	9	2	2	10	10	10	9	10	9

Table 4. TN concentrations and percent composition as DON, NH₄⁺-N and NO₃⁻-N (vertically averaged within the plume zone, defined by Na⁺ > 30 mg/L, at each well) along the plume centreline: **a)** August 20, 2009 and **b)** November 13, 2009. Pond values are the mean from Aug. 28 2008 to Nov. 13 2009 (n=5-15, from Table 2). Note: Pond values are based on mean values

Location	Distance m	TN mg/L	DON %	NH₄⁺-N %	NO₃⁻-N %
POND	0	361	65	34	1
a) August 20, 2009					
PU122	9	83.0	45	53	3
PU95	15	72.3	57	42	1
PU124	35	65.7	20	24	57
PU92	40	48.4	54	44	2
PU115	60	28.1	53	47	1
PU125	71	19.8	31	14	55
PU96	88	19.8	56	36	7
PU121	101	20.4	48	1	51
Overall Mean			46	33	20
b) November 13, 2009					
PU122	9	110	33	60	7
PU95	15	108	63	35	1
PU124	35	16.0	26	45	28
PU92	40	42.6	28	39	33
PU115	60	92.2	24	61	16
PU125	71	23.0	33	13	54
PU96	88	41.6	44	43	13
PU121	101	23.0	44	25	31
Overall Mean			37	40	23

Table 5. NH_4^+ -N and TN concentrations (vertically averaged within the plume zone, defined by $\text{Na}^+ > 30$ mg/L, at each well) along the plume centreline, compared to expected values normalized to the Na^+ concentration: **a)** August 20, 2009 and **b)** November 13, 2009. Pond values represent the C_0 values (mean value, $n = 15$, from Table 2).

a) August 20, 2009										
Location	Distance m	Na^+ mg/L	Measured		Predicted		Difference		% Remaining	
			NH_4^+ -N	Total N						
mg/L										
POND	0	220	121	361	121	361	0	0	100	100
PU122	9	147	42.0	83.0	80.8	241	-38.8	-158	35	23
PU95	15	148	77.2	72.3	81.5	243	-4.3	-171	64	20
PU124	35	41.3	18.9	65.7	22.7	67.7	-3.8	-2.1	16	18
PU92	40	50.7	31.0	48.4	27.9	83.3	3.1	-34.8	26	13
PU115	60	52.5	31.6	28.1	28.9	86.2	2.7	-58.0	26	8
PU125	71	40.9	9.1	19.8	22.5	67.1	-13.4	-47.3	8	5
PU96	88	47.7	16.3	19.8	26.3	78.3	-10.0	-58.5	13	5
PU121	101	24.0	0.05	20.4	13.2	39.4	-13.2	-19.0	0.04	6

b) November 13, 2009										
POND	0	220	121	361	121	361	0	0	100	100
PU122	9	180	64.1	110	101	301	-36.8	-191	53	31
PU95	15	82.7	20.8	108	45.5	136	-24.6	-28	17	30
PU124	35	37.9	10.0	16.0	20.9	62.2	-10.9	-46	8	4
PU92	40	57.5	9.7	42.6	31.7	94.4	-22.0	-52	8	12
PU115	60	56.4	59.3	92.2	31.0	92.5	28.3	-0.3	49	26
PU125	71	42.5	16.9	23.0	23.4	69.8	-6.5	-47	14	6
PU96	88	51.4	25.7	41.6	28.3	84.3	-2.6	-43	21	12
PU121	101	42.5	16.9	23.0	23.4	69.8	-6.5	-47	14	6

Table 6. Mean Na⁺, NH₄⁺-N, DON and total nitrogen (TN) concentrations measured at distal transect E-E' (88-101 m from the lagoon) compared to the mean lagoon values (n = 5-15). Distal values include plume core wells (Na⁺ > 30 mg/L) at nests PU81, 84, 96 and 121 where available (n = 8-16). Nitrogen values for September and October 2010 provided courtesy of Lucas Carson (unpublished data). The piezometers used in calculations include: July 15, 2009 (PU81, 84, 96, 121; n = 16), August 20, 2009 (PU96, 121; n = 8), November 13, 2009 (PU96, 121; n = 8), Sept. 25, 2010 (PU84, 96, 121; n = 9), October 26, 2010 (PU84, 96, 121; n = 10)

Lagoon (C ₀)	Measured (mg/L)				% Reduction					
	Na ⁺	NH ₄ ⁺ -N	DON	TN	NH ₄ ⁺ -N			TN		
	220	121	218	361	Total	Dilution	Decay	Total	Dilution	Decay
Distal Transect E-E'										
July 15, 2009	33	4.3	-	-	96	85	11	-	-	-
Aug. 20, 2009	36	8.2	10	23	93	84	9	94	84	10
Nov. 13, 2009	41	14	10	25	88	81	7	93	81	12
Sept. 25, 2010	-	15	5.4	27	87	-	-	92	-	-
Oct. 26, 2010	25	9.0	8.3	26	93	89	4	93	89	4
Distal Average	37	10	8.4	25	92	85	8	93	85	9

Table 7. Results from ammonification lab batch experiment 1. Groundwater from each location was left to stir in 160 mL glass bottles with 40 mL of atmospheric headspace for 12 days, and sampled at the indicated days from onset to monitor the evolution of nitrogen species from April 22 – May 10, 2010.

Sample Location	Day	NH ₄ ⁺ -N	NO ₃ ⁻ -N	TKN	DON	TN
		mg/L				
PU125 3.9 m	0	0.3	0.36	44.9	44.6	45.3
	5	3.8	35.1	16.6	12.8	51.7
	12	0.1	35.9	14.1	14.0	50.0
	12	0.1	36.6	12	11.9	48.6
PU121 2.2 m	0	0.1	12.9	3.5	3.4	16.4
	5	0.2	13.6	3	2.8	16.6
	12	0.09	13.6	3	2.9	16.6
	12	0.09	13.7	3.1	3.0	16.8
PU92 1.8 m	0	9.9	1.09	44.9	35	46.0
	5	0.2	11.5	38.5	38.3	50.0
	12	0.2	12.8	32.9	32.7	45.7
	12	0.2	12.6	33.8	33.6	46.4

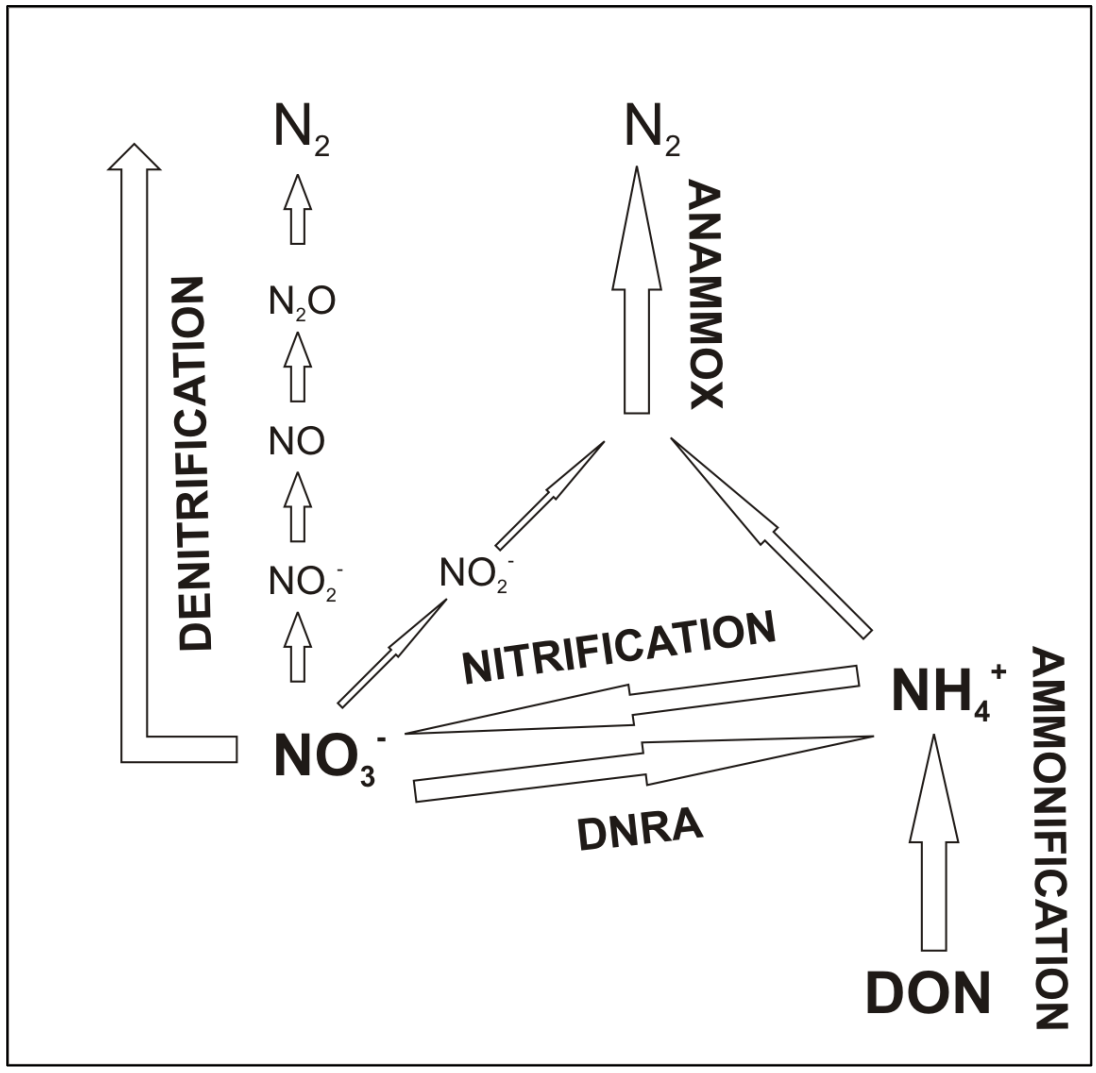


Figure 1. Summary of potential major nitrogen reaction pathways in the Zorra groundwater system. Dissimilatory nitrate reduction to ammonium (DNRA) and nitrification alter the form of dissolved nitrogen from nitrate (NO_3^-) to ammonium (NH_4^+) and vice versa while anammox and denitrification are pathways for the total removal of nitrogen from the dissolved system. Active ammonification represents an additional source of NH_4^+ from organic nitrogen (DON).

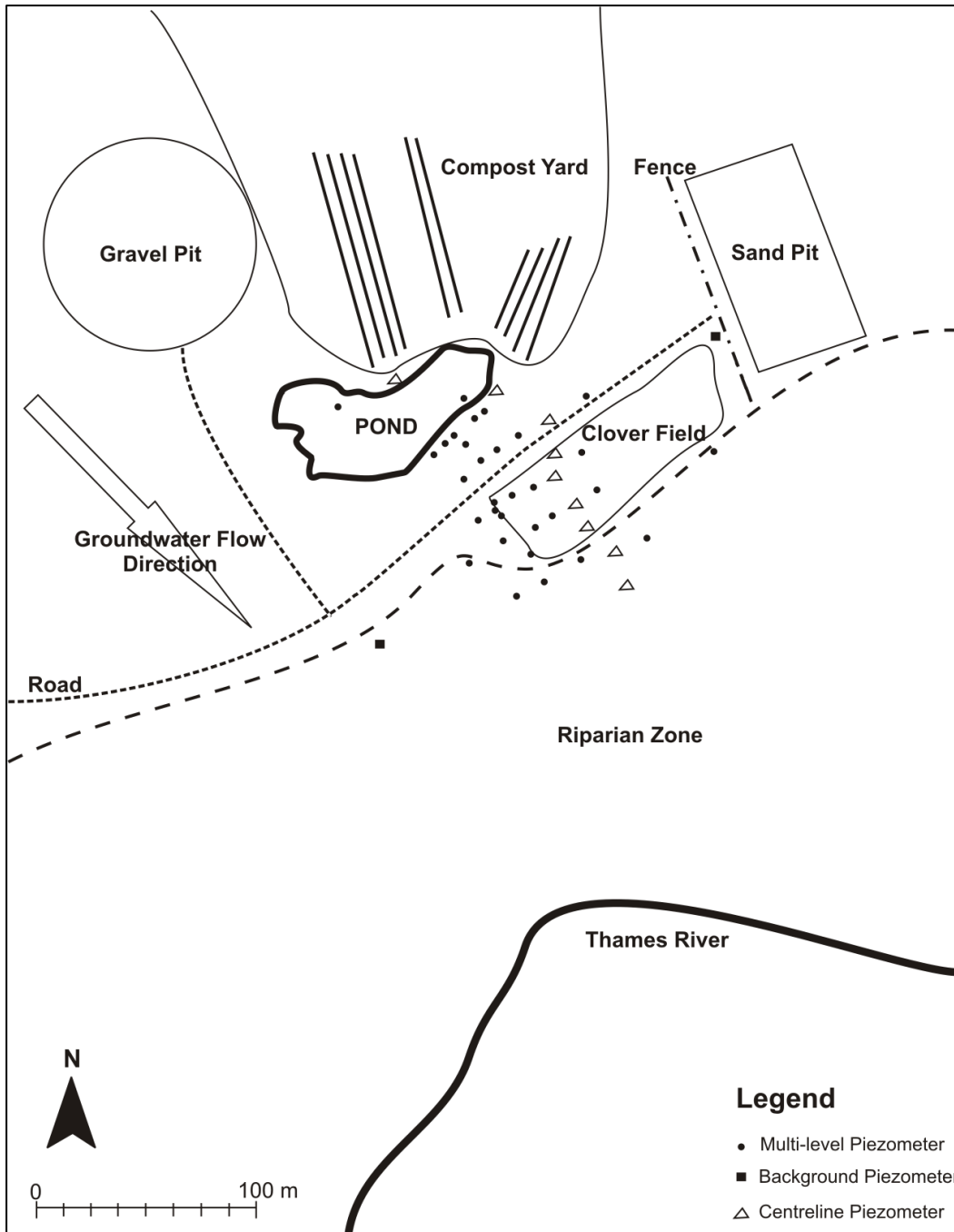


Figure 2. Zorra site monitoring network and local features. The site consists primarily of a manure composting operation and runoff pond ~ 200 m upgradient of the Thames River. The site monitoring network is situated between these features along the groundwater flow path.

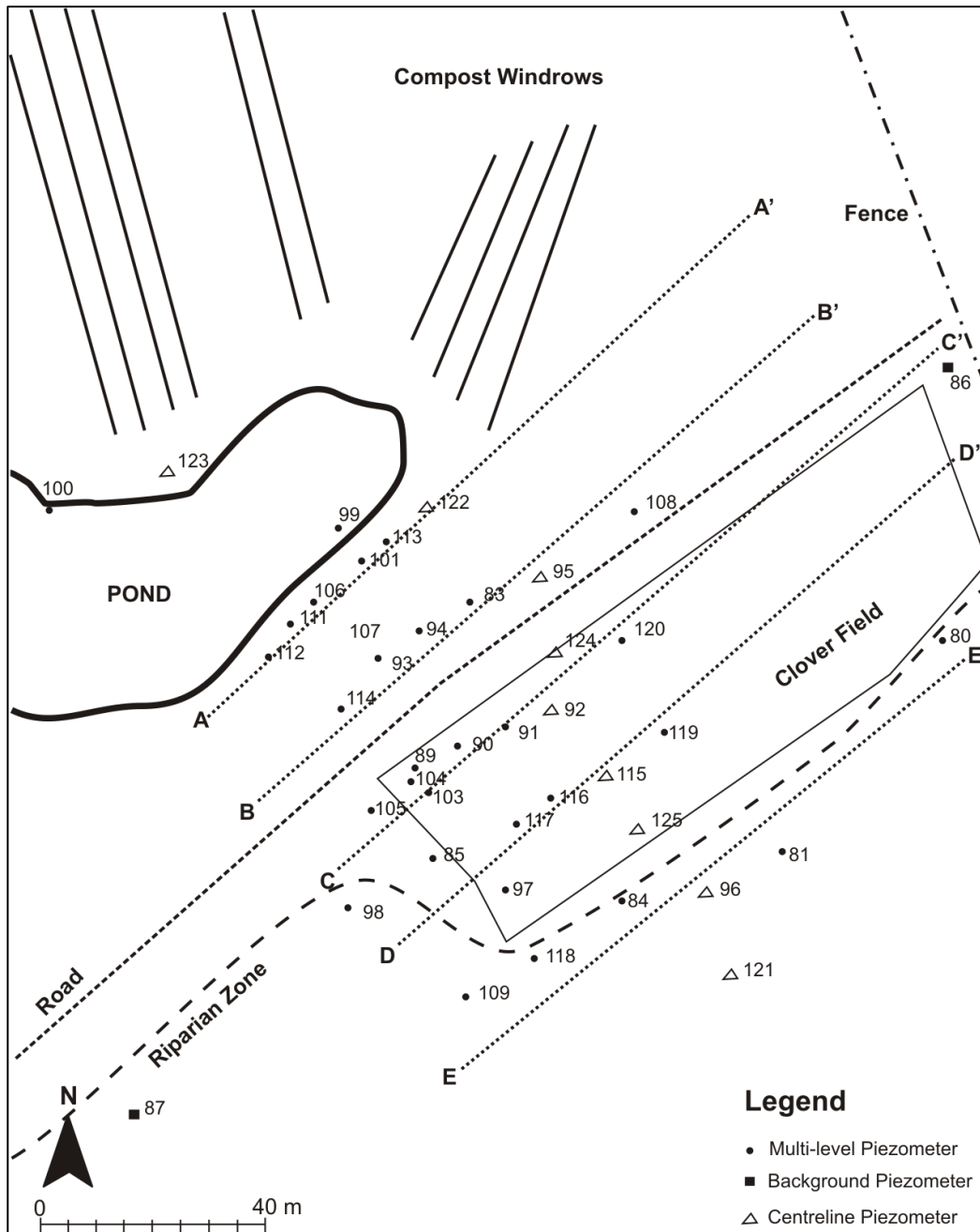


Figure 3. Monitoring well network at the Zorra site and locations of transects A-E.

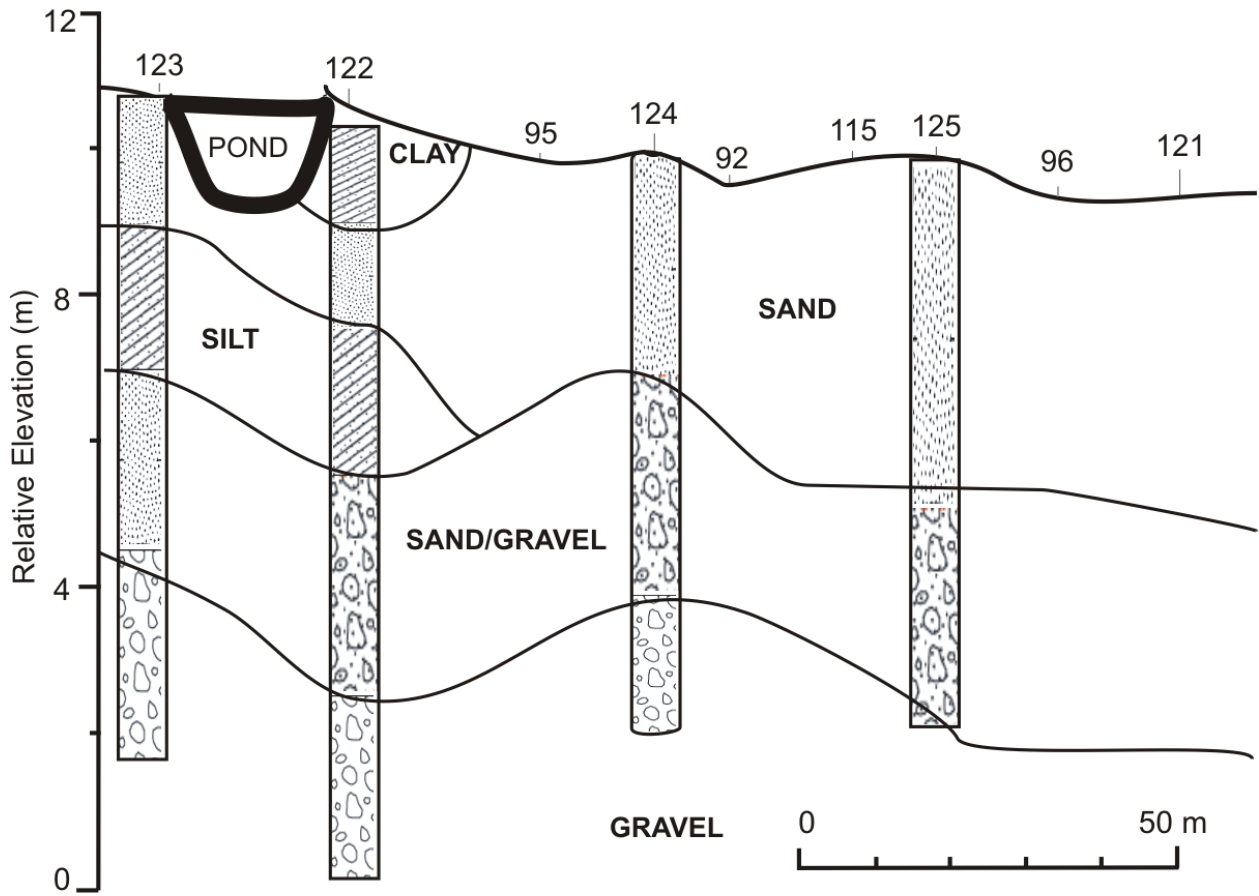


Figure 4. Simplified site geology along the centre line based on continuous core samples taken during piezometer installation (see Appendix B for borehole logs).

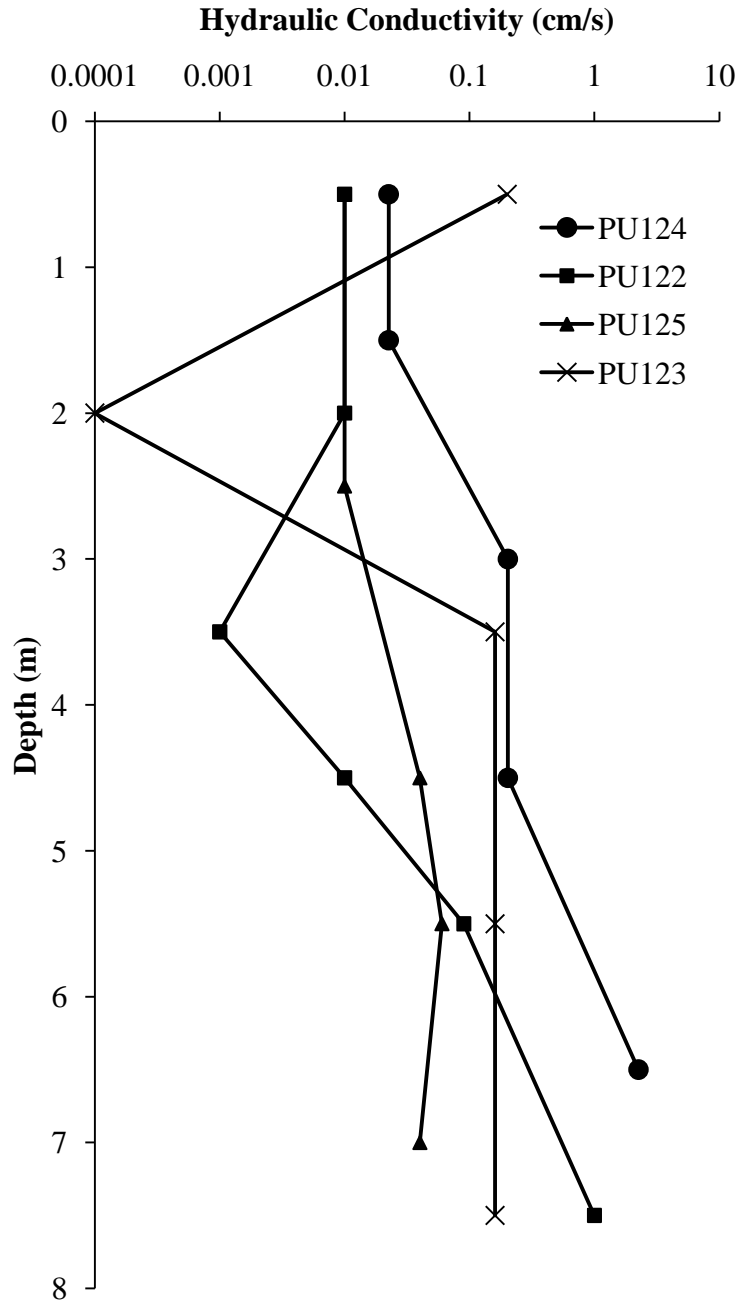


Figure 5. Depth profiles of hydraulic conductivity (K in cm/s) at wells PU122, 123, 124 and 125. K values were determined from grain size analysis of sediment samples taken from continuous coring, using the Hazen equation $K = Cd_{10}^2$, where $C = 1.0$ (for input units of mm and output of cm/s) and d_{10} is the grain size diameter for which 90% of the sediments are coarser; determined graphically (Appendix C).

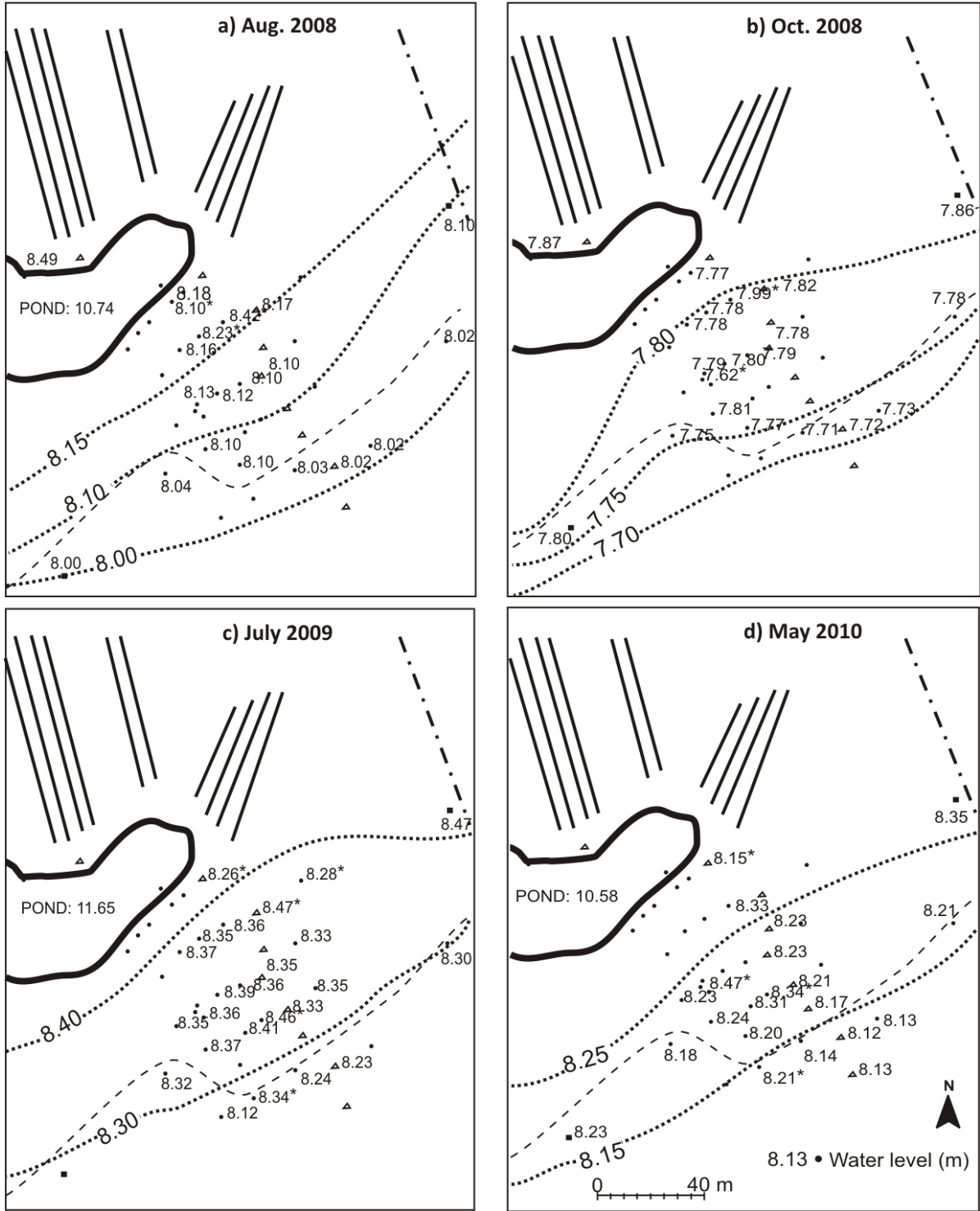


Figure 6. Relative elevation of the water table: **a)** August 28, 2008 **b)** October 20, 2008 **c)** July 7, 2009 **d)** May 26, 2010. Values marked with * indicate questionable measurements.

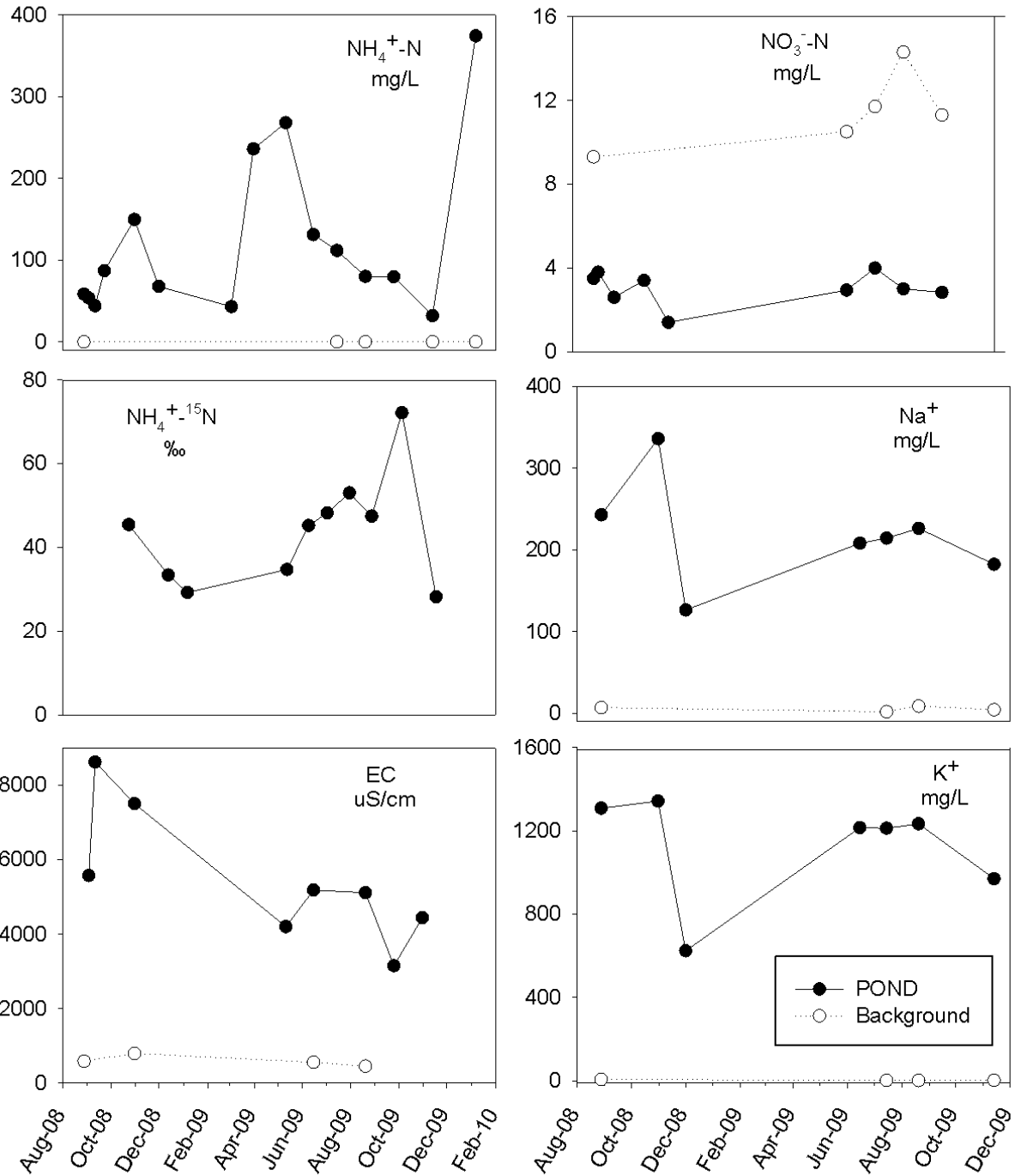


Figure 7. Temporal trends of chemical parameters August 28, 2008 – January 7, 2010 in the pond and in background well PU86. Background values are the vertical average of 2-4 sampling points at 1.9 - 3.1 m depth (PU86).

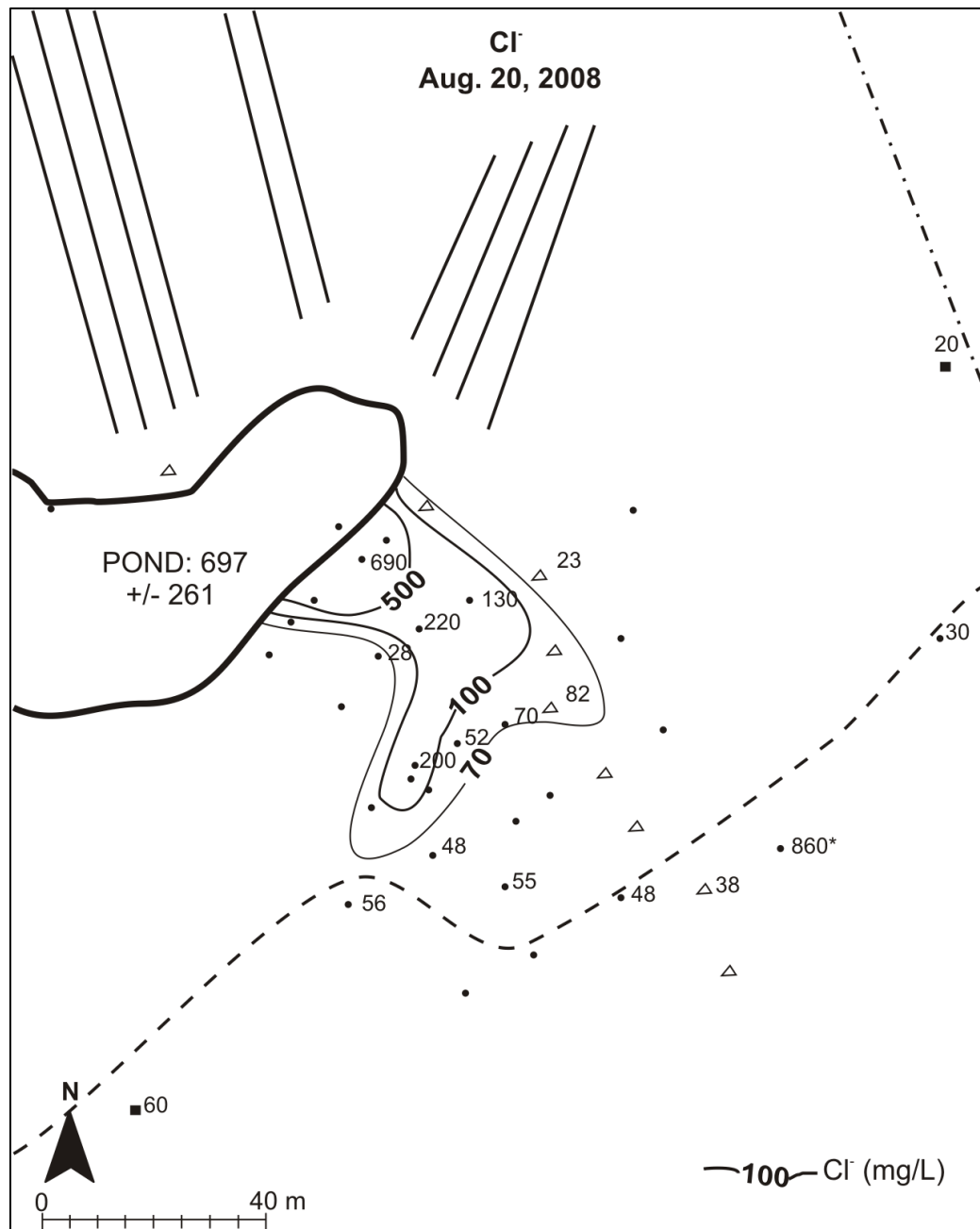


Figure 8. Plan view of Cl⁻, August 28, 2008. Values are vertically averaged over 0-3 m depth (n=2-5). Pond value is the mean and standard deviation measured during Aug. 28-Dec. 1, 2008 (n=4). Value marked with * is questionable (may have been acidified with HCl in the field).

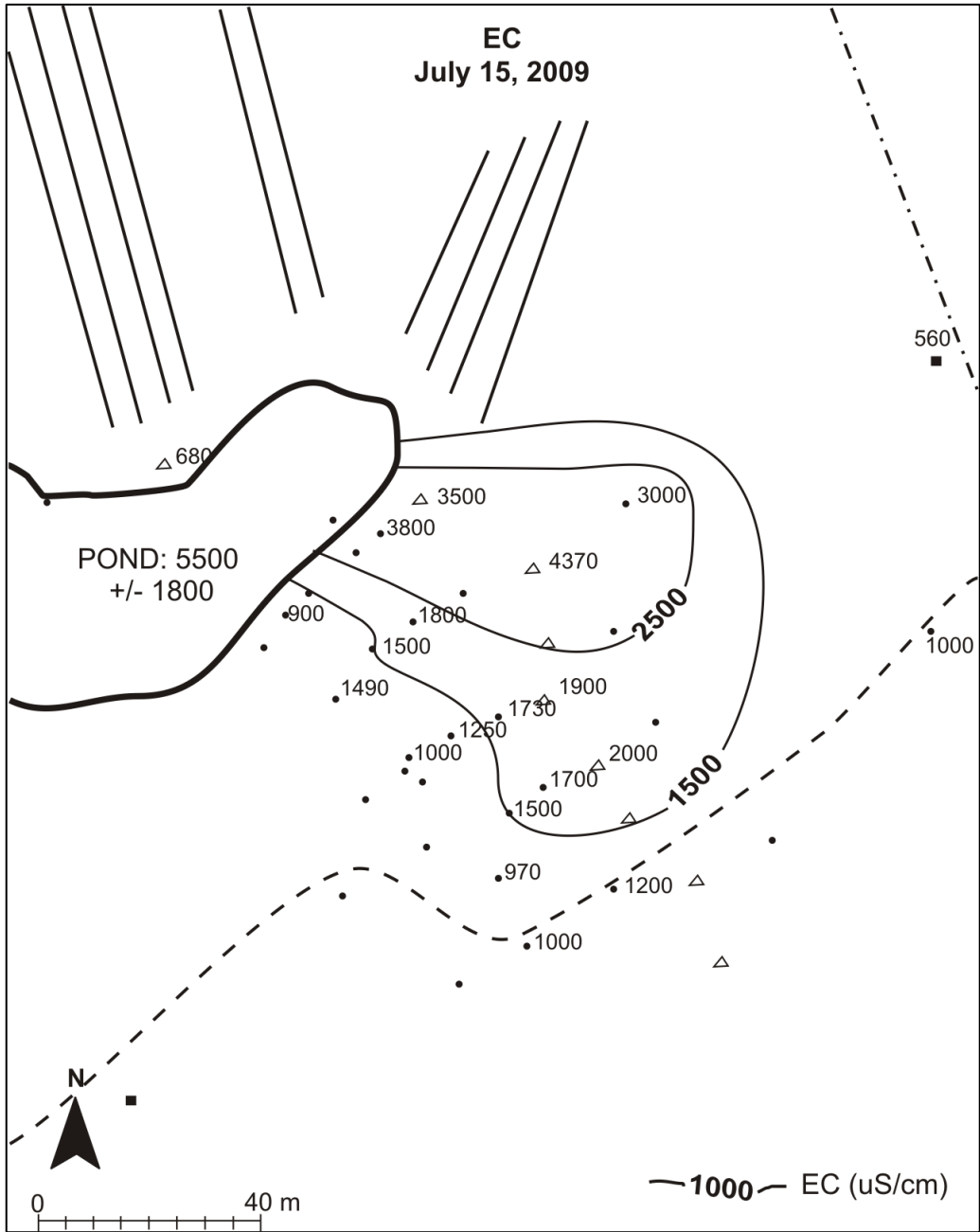


Figure 9. Plan view of electrical conductivity (EC), July 15, 2009. Values are vertically averaged over 0-3 m depth (n=2-5). Pond value is the mean and standard deviation measured during Aug. 28 2008 to Nov. 13 2009 (n=7).

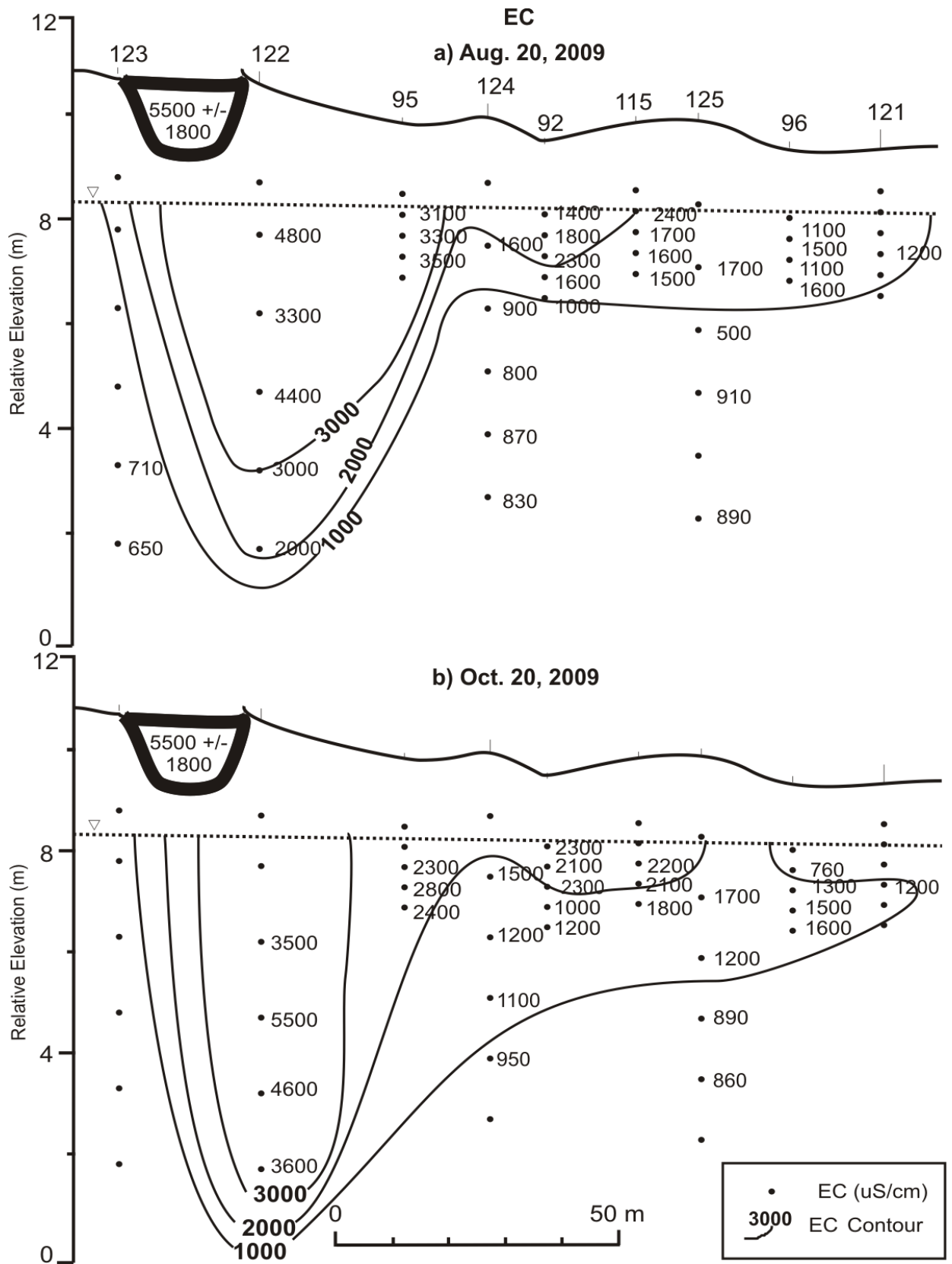


Figure 10. EC distribution along the centre line: **a)** August 20, 2009 and **b)** October 20, 2009. Pond value is the mean and standard deviation measured during Aug. 28, 2008 - Nov. 13, 2009 (n=7). Note the ~10x vertical exaggeration.

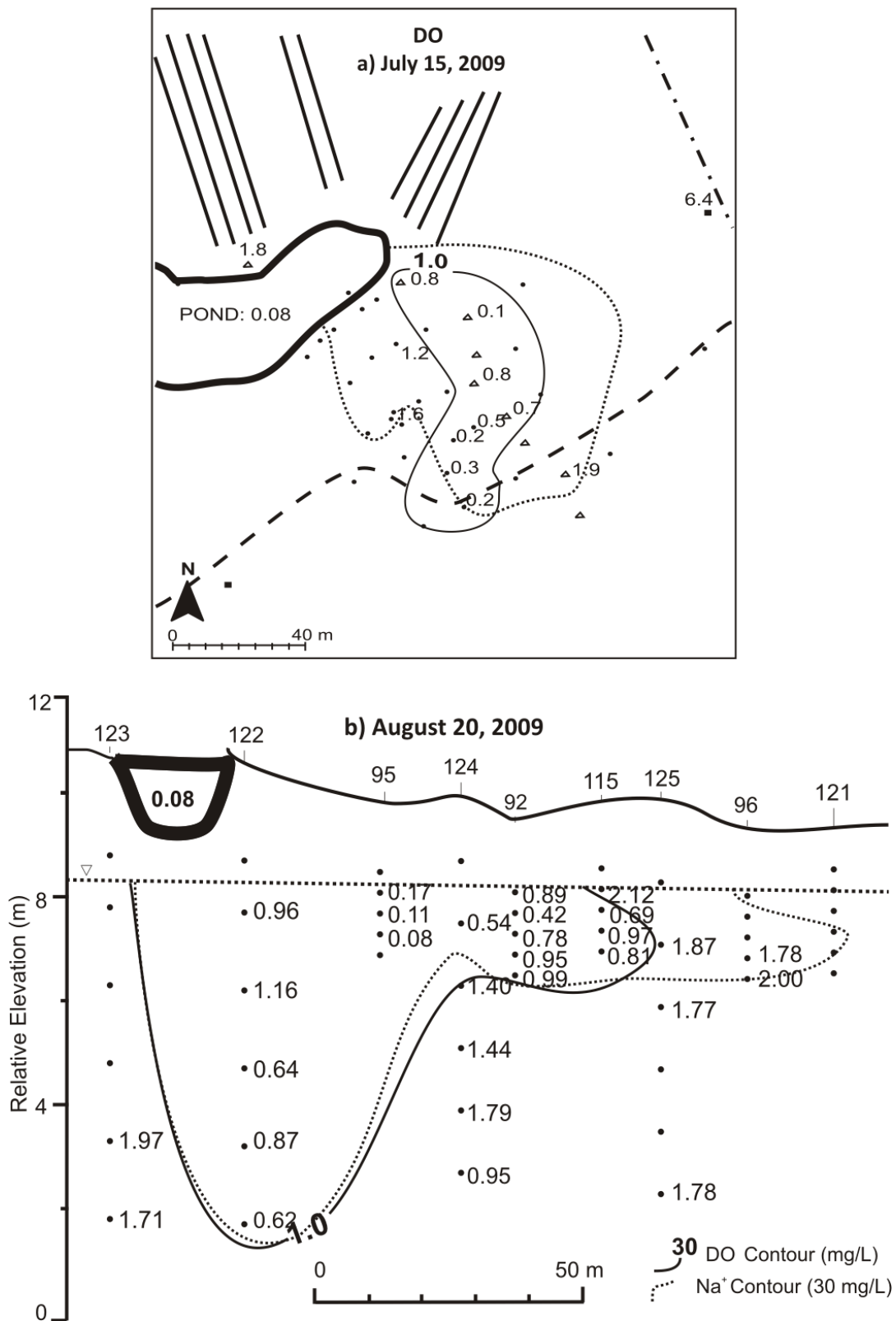


Figure 11. Distribution of dissolved oxygen (DO): **a)** vertically averaged over 0-3 m depth in plan view (July 15, 2009) and **b)** along the centre line (August 20, 2009). Pond value is from August 20, 2009. Note the ~10x vertical exaggeration.

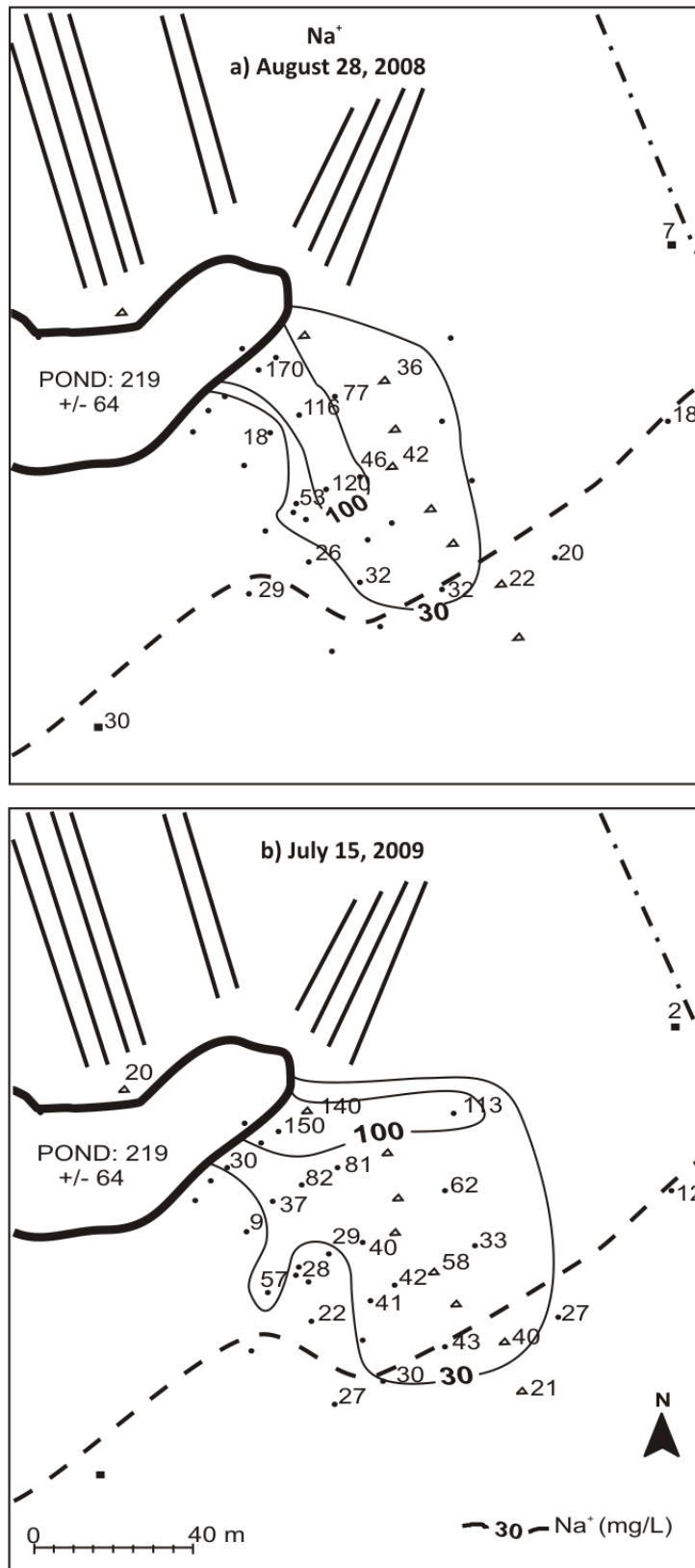


Figure 12. Plan view of Na⁺: **a)** August 28, 2008 and **b)** July 15, 2009. Values are vertically averaged over 0-3 m depth (n=2-5). Pond value is the mean and standard deviation measured during Aug. 28, 2008 to Nov. 13, 2009 (n=7).

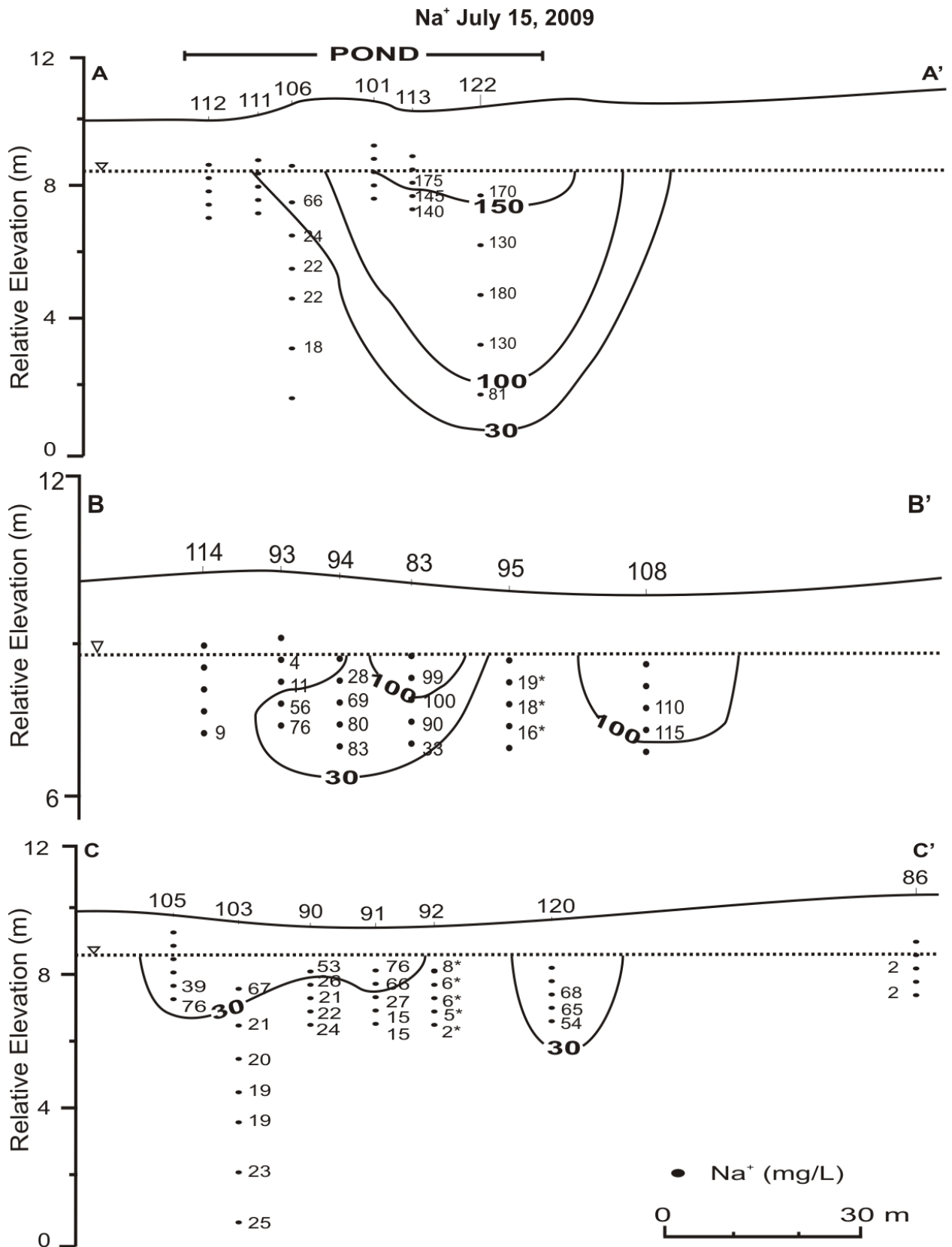


Figure 13. Na⁺ distribution along transverse transects A-E, July 15, 2009. Values marked with * are questionable based on historical Na⁺ values (Appendix C). Note the ~10x vertical exaggeration.

Na⁺ July 15, 2009

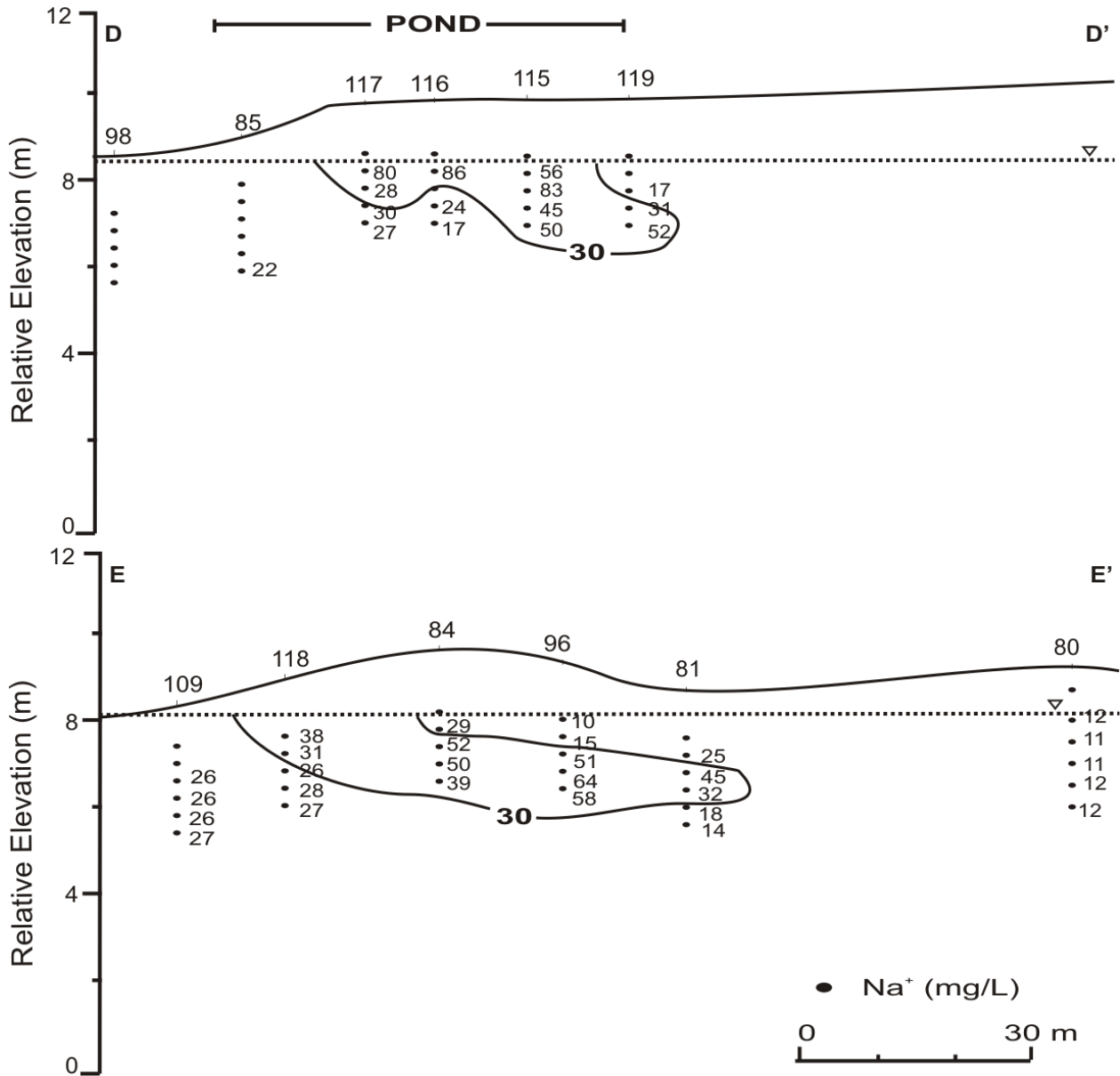


Figure 13. con't

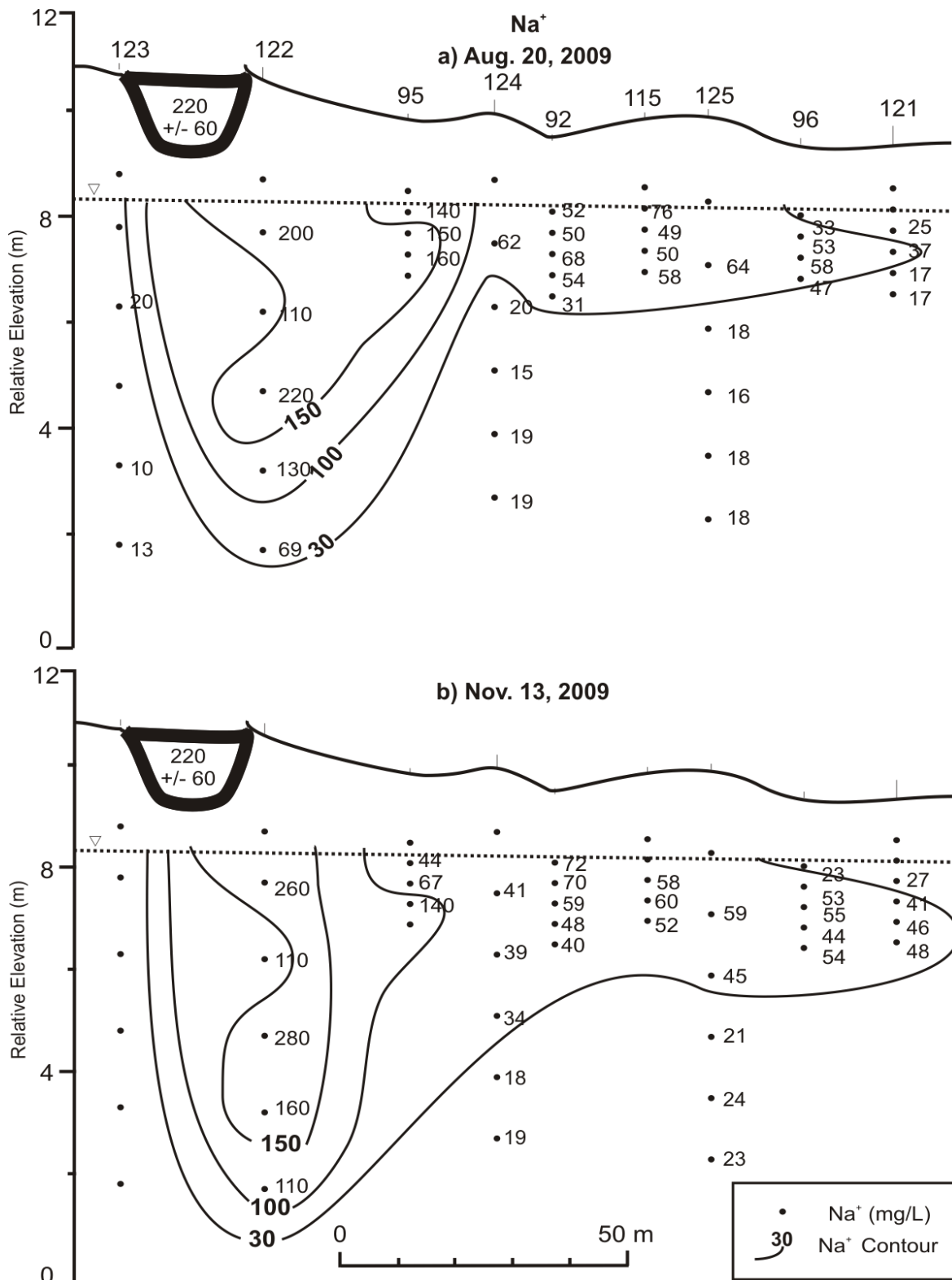


Figure 14. Na⁺ distribution along the centre line: **a)** August 20, 2009 and **b)** November 13, 2009. Pond value is the mean and standard deviation measured during Aug. 28 2008 to Nov. 13 2009 (n=7). Note: Sampling occurred only along the centre line on these dates. Note also the ~10x vertical exaggeration.

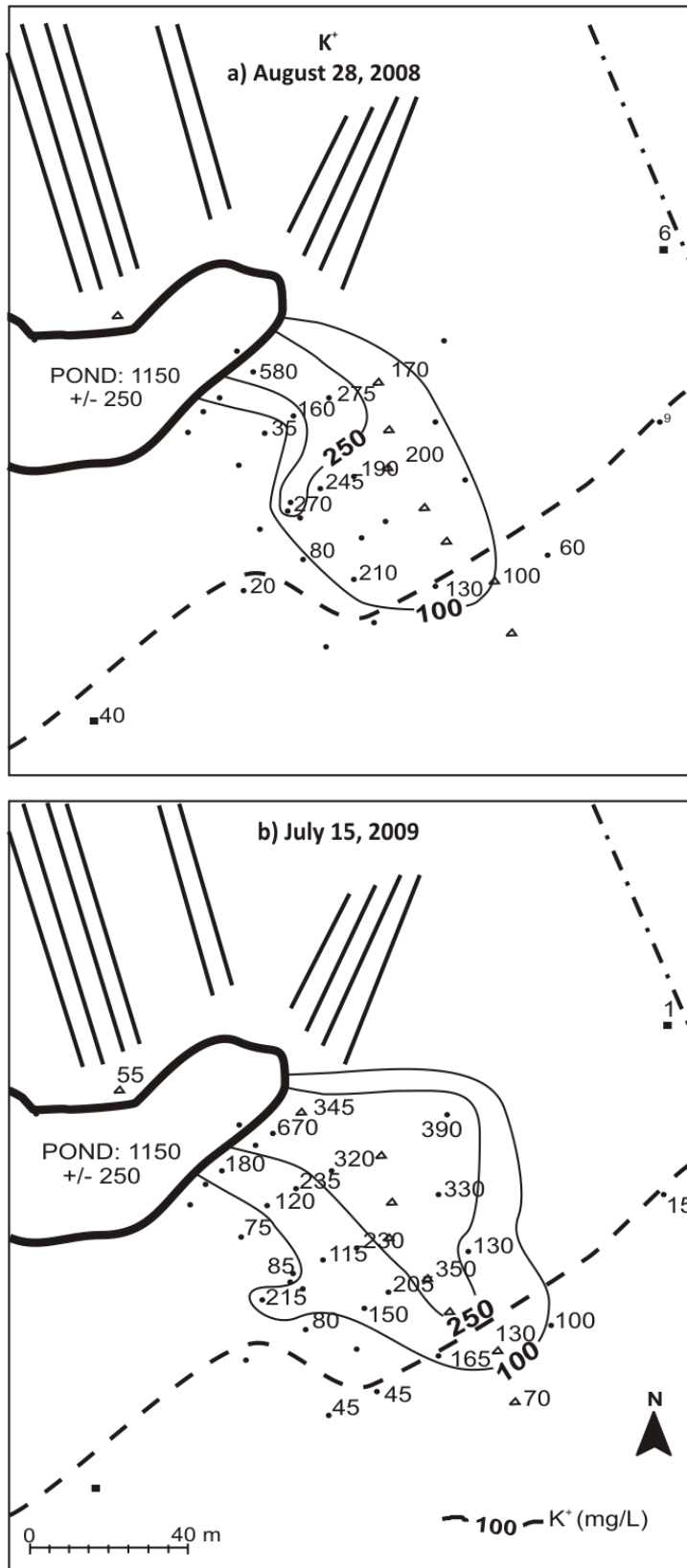


Figure 15. Plan view of K^+ : **a)** August 28, 2008 and **b)** July 15, 2009. Values are vertically averaged over 0-3 m depth ($n=2-5$). Pond value is the mean and standard deviation measured during Aug. 28 2008 to Nov. 13 2009 ($n=7$).

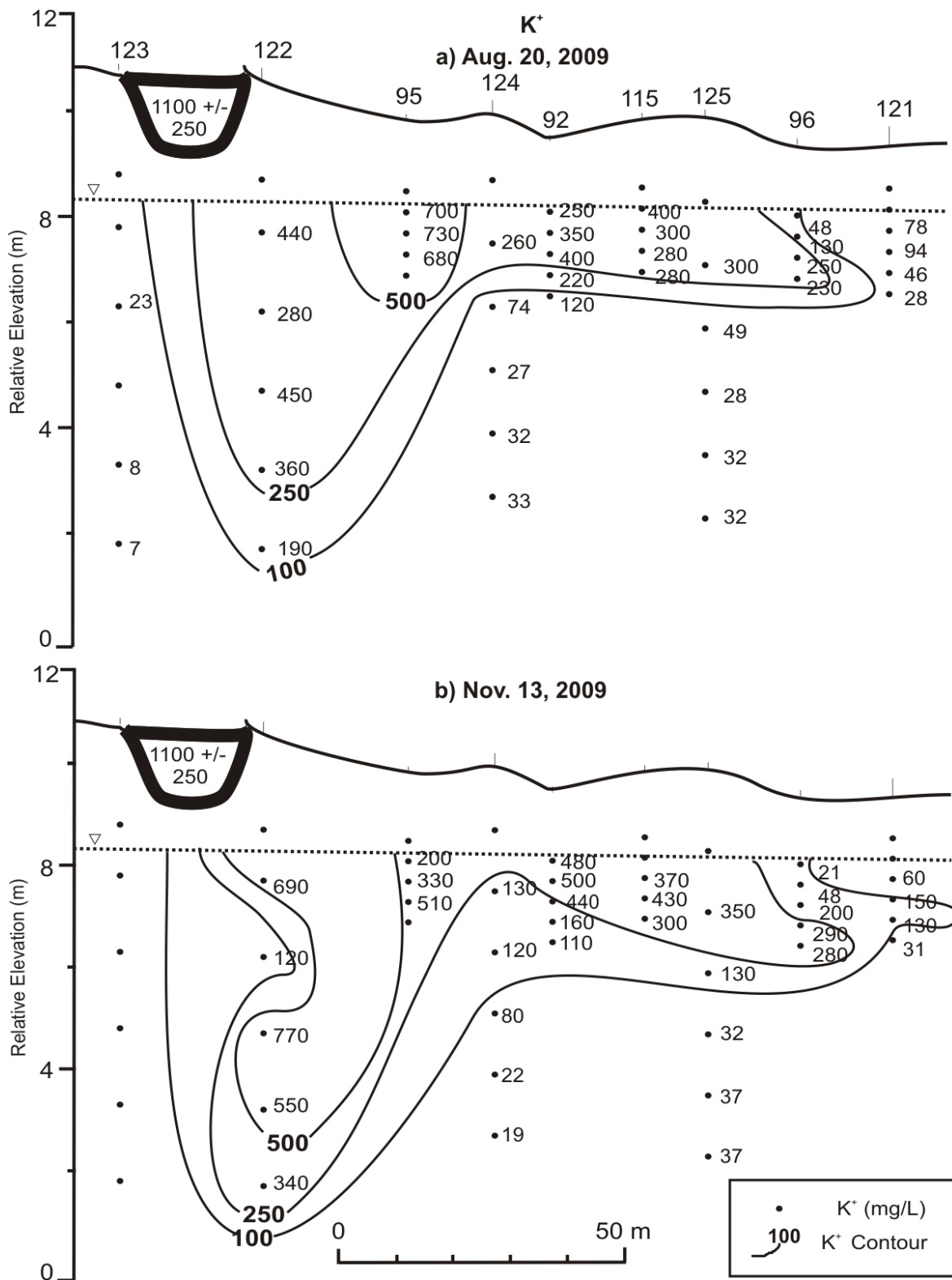


Figure 16. K⁺ distribution along the centre line: **a)** August 20, 2009 and **b)** November 13, 2009. Pond value is the mean and standard deviation measured during Aug. 28 2008 to Nov. 13 2009 (n=7). Note: Sampling occurred only along the centre line on these dates. Note also the ~10x vertical exaggeration.

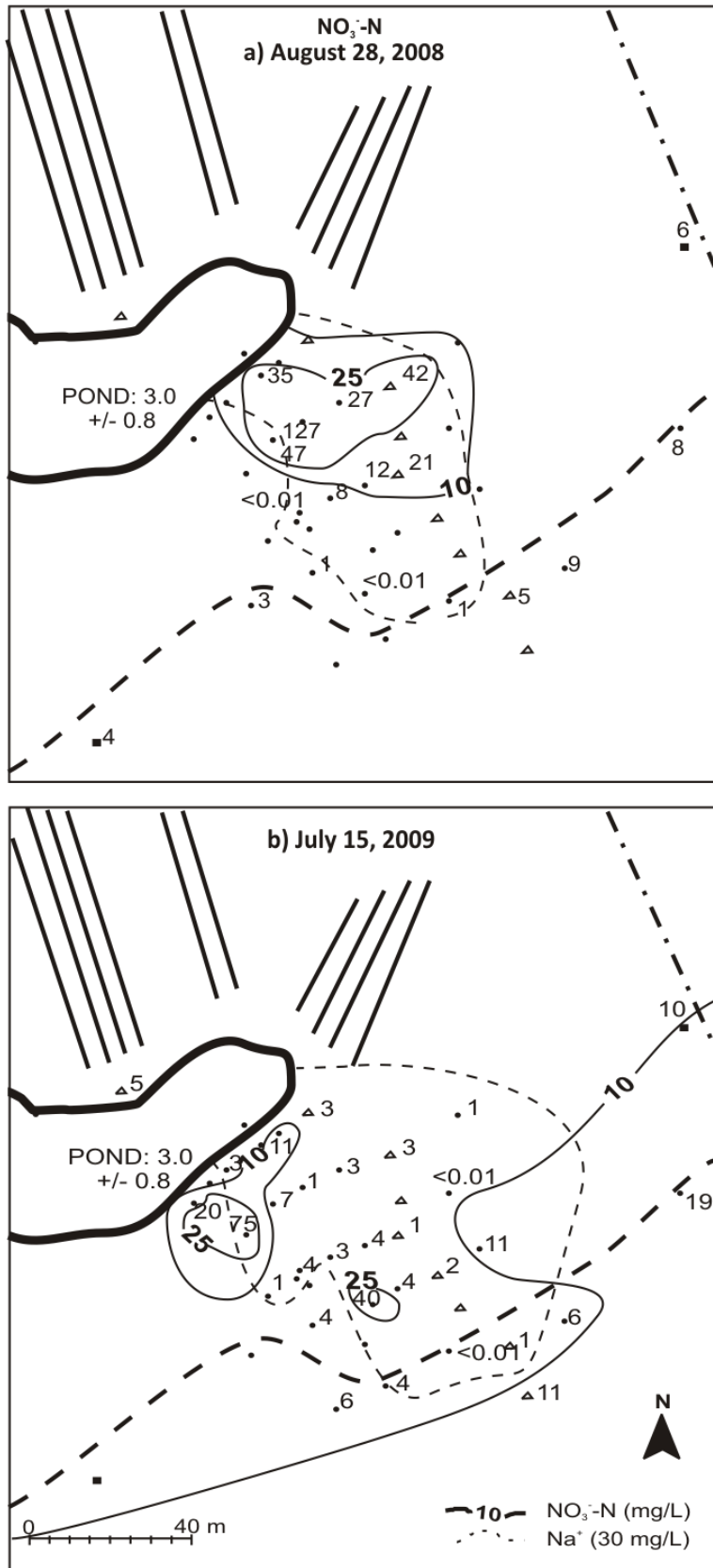


Figure 18. Plan view of NO_3^- -N: **a)** August 28, 2008 and **b)** July 15, 2009. Values are vertically averaged over 0-3 m depth (n=2-5). Pond value is the mean and standard deviation measured during Aug. 28 2008 to Nov. 13 2009 (n=9).

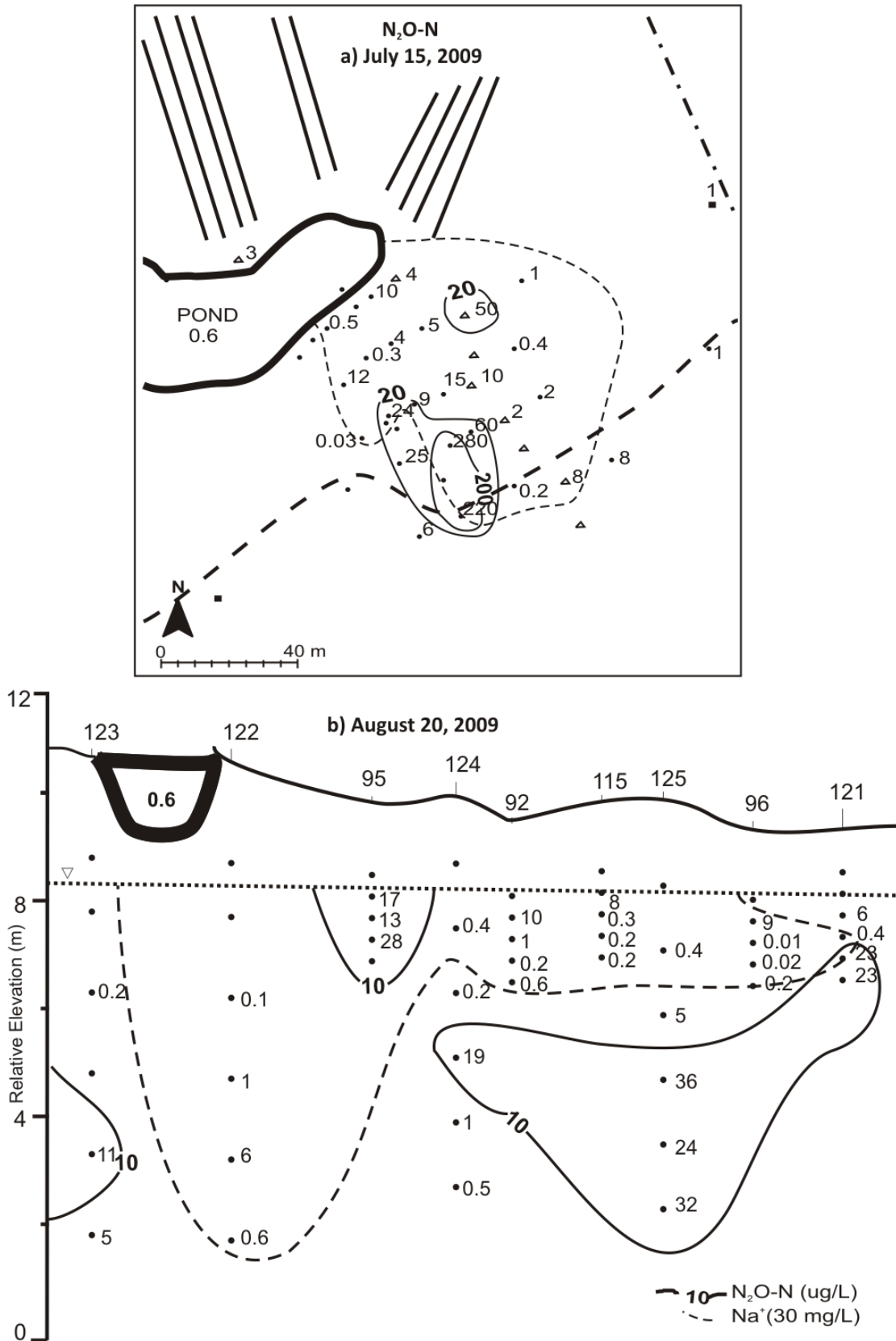


Figure 19. Distribution of dissolved N_2O : **a)** vertically averaged over 0-3 m depth ($n=2-5$) in plan view (July 15, 2009) and **b)** along the centre line (August 20, 2009). Pond value is from August 20, 2009. Note the $\sim 10x$ vertical exaggeration.

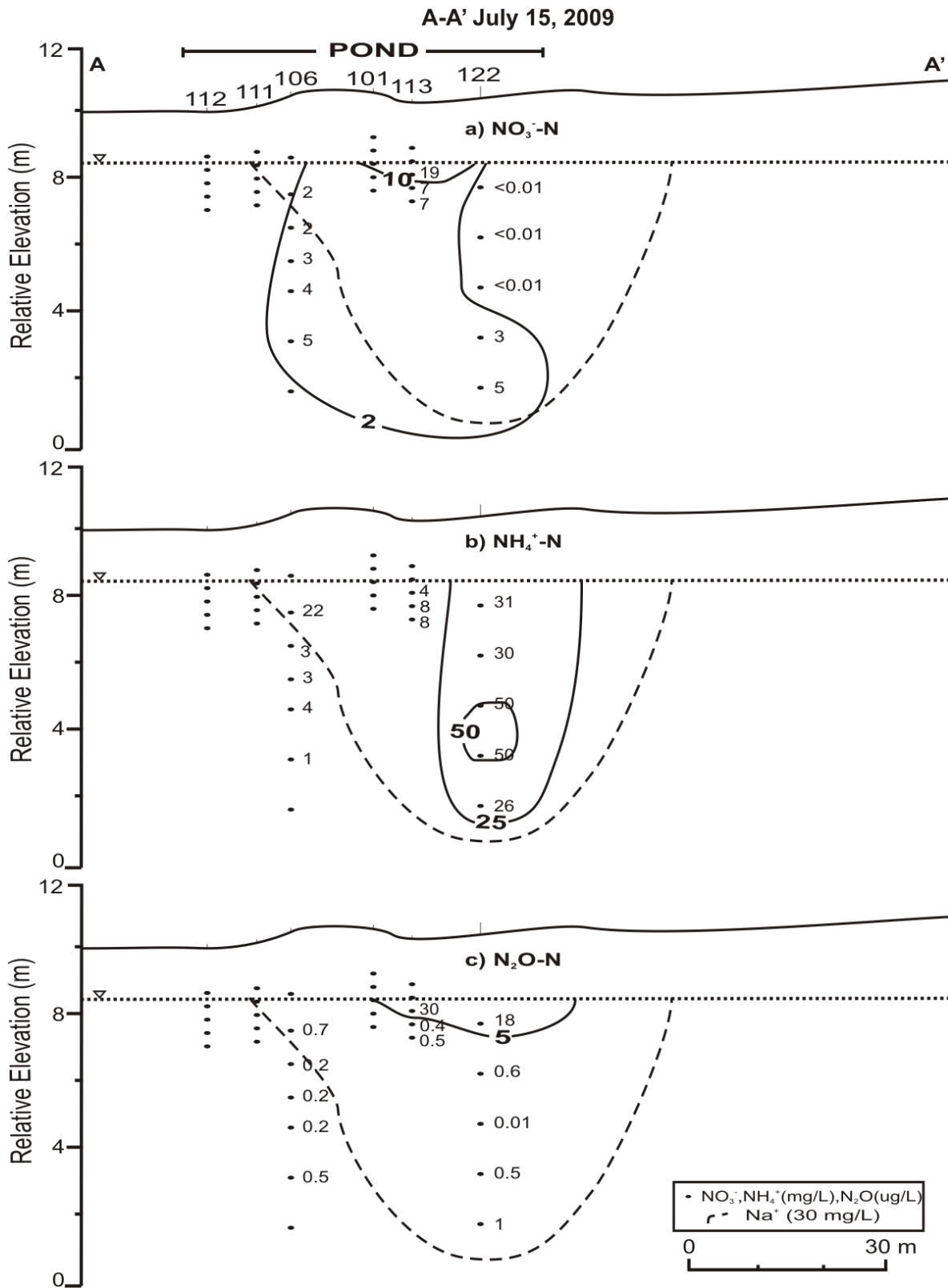


Figure 20. Distribution of nitrogen species: **a) NO_3^-** **b) NH_4^+** **c) N_2O** along transect A, July 15, 2009. Note the ~10x vertical exaggeration.

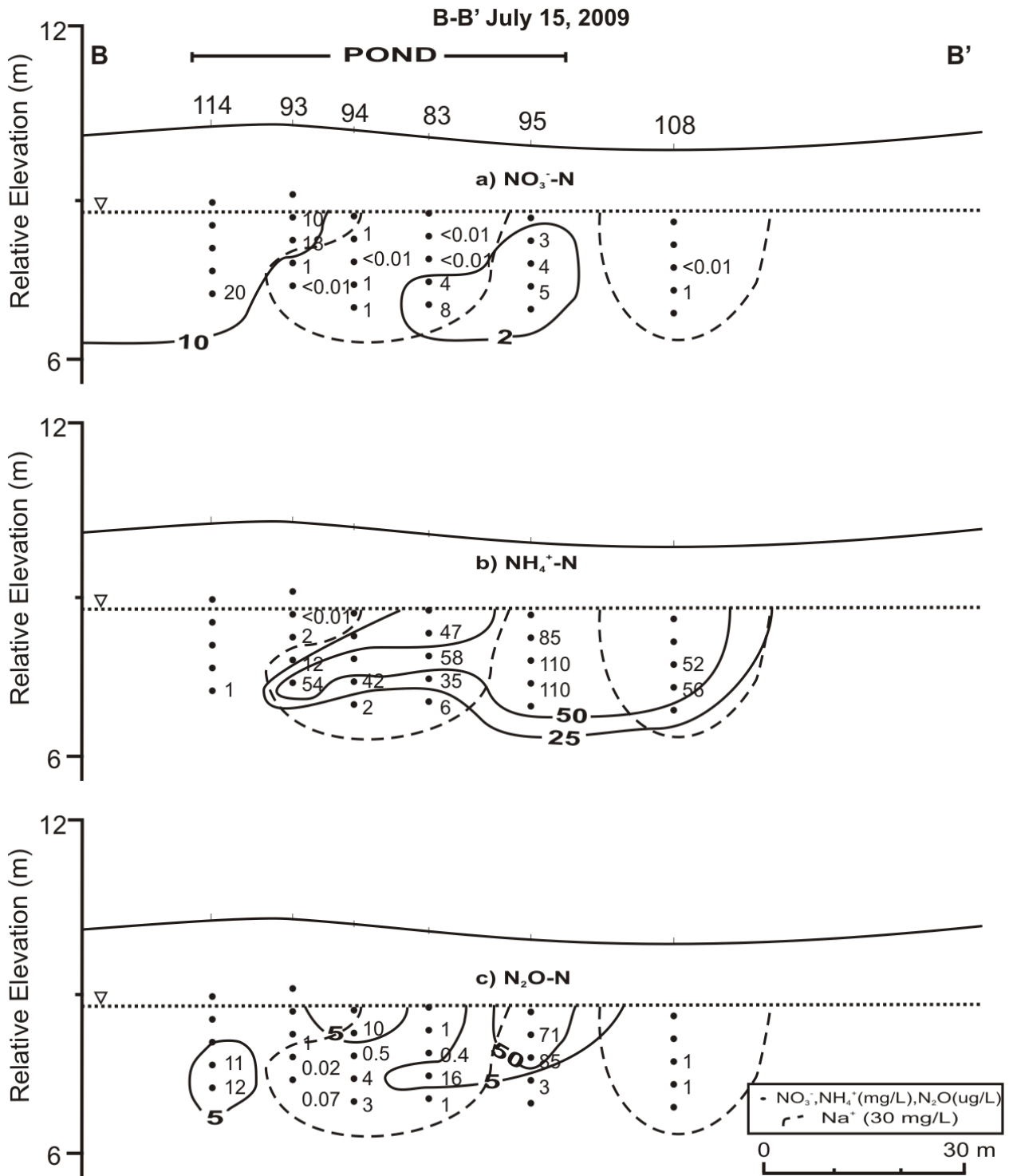


Figure 21. Distribution of nitrogen species: **a)** NO_3^- **b)** NH_4^+ **c)** N_2O along transect B, July 15, 2009.

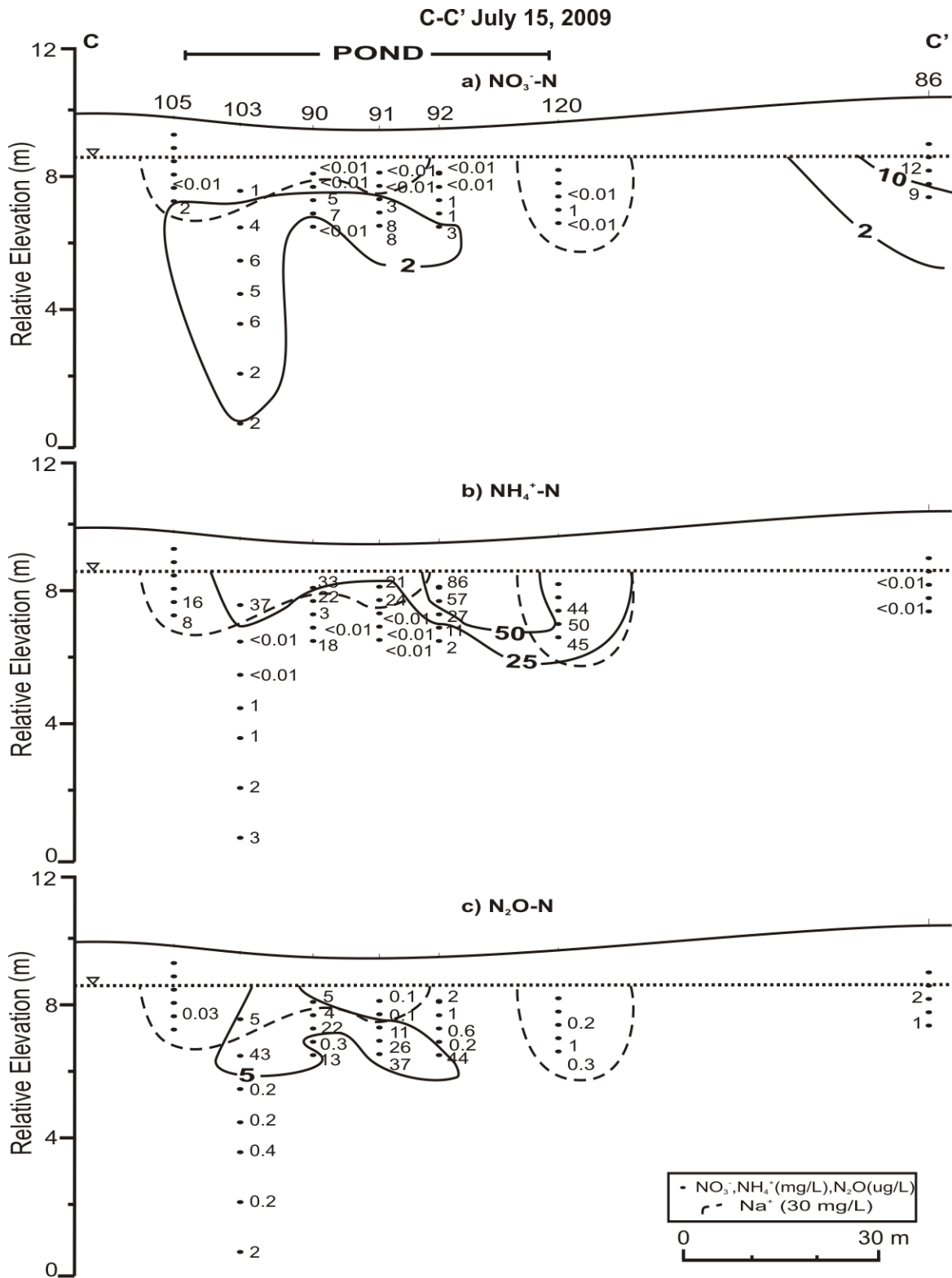


Figure 22. Distribution of nitrogen species: a) NO_3^- b) NH_4^+ c) N_2O along transect C, July 15, 2009.

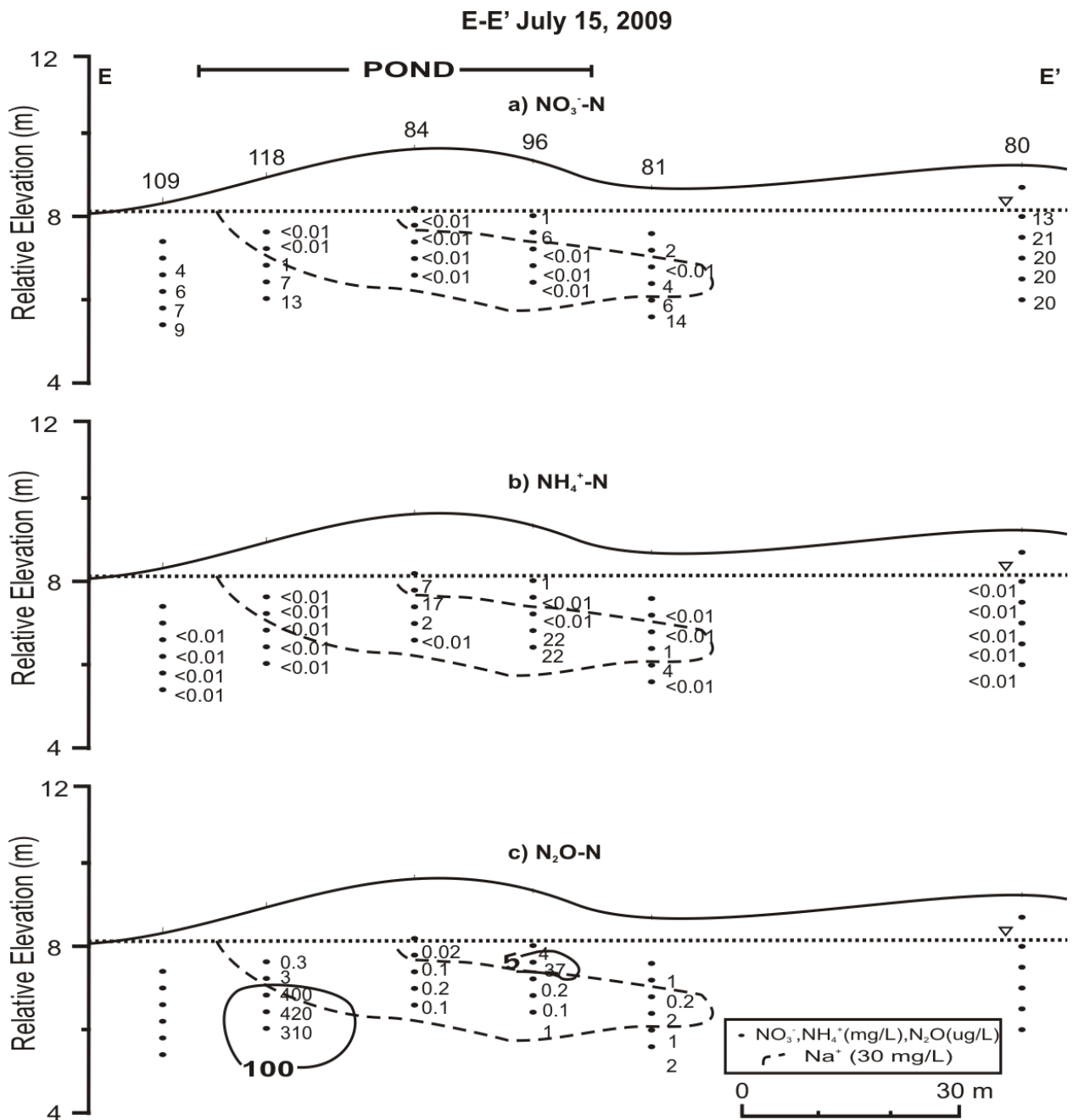


Figure 24. Distribution of nitrogen species: **a)** NO_3^- **b)** NH_4^+ **c)** N_2O along transect E, July 15, 2009.

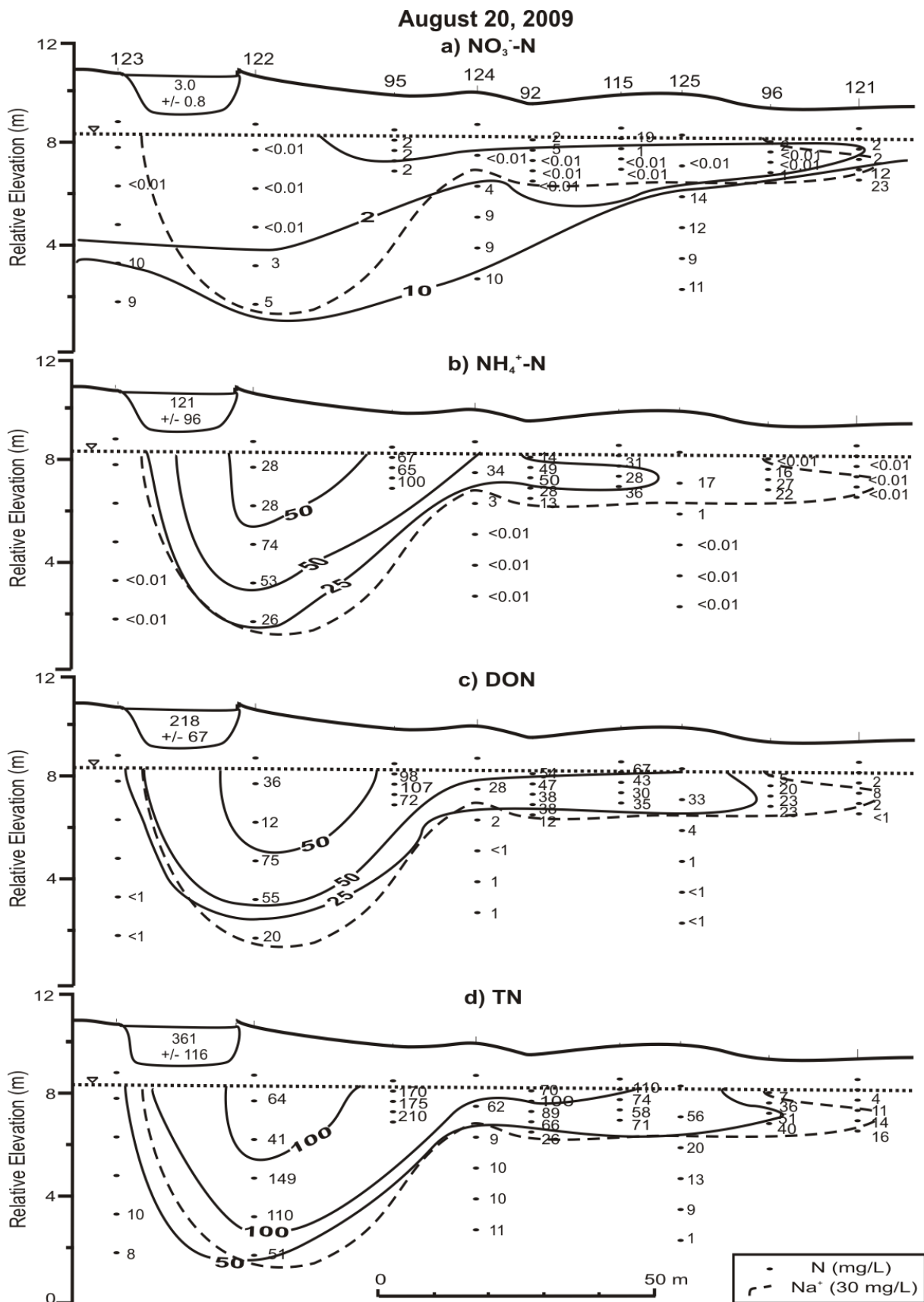


Figure 25. Distribution of nitrogen species: **a)** NO_3^- **b)** NH_4^+ **c)** dissolved organic nitrogen (DON) and **d)** total nitrogen (TN) along the centre line, August 20, 2009. Pond values are the mean and standard deviation from Aug. 28 2008 to Nov. 13 2009 (n=5-15).

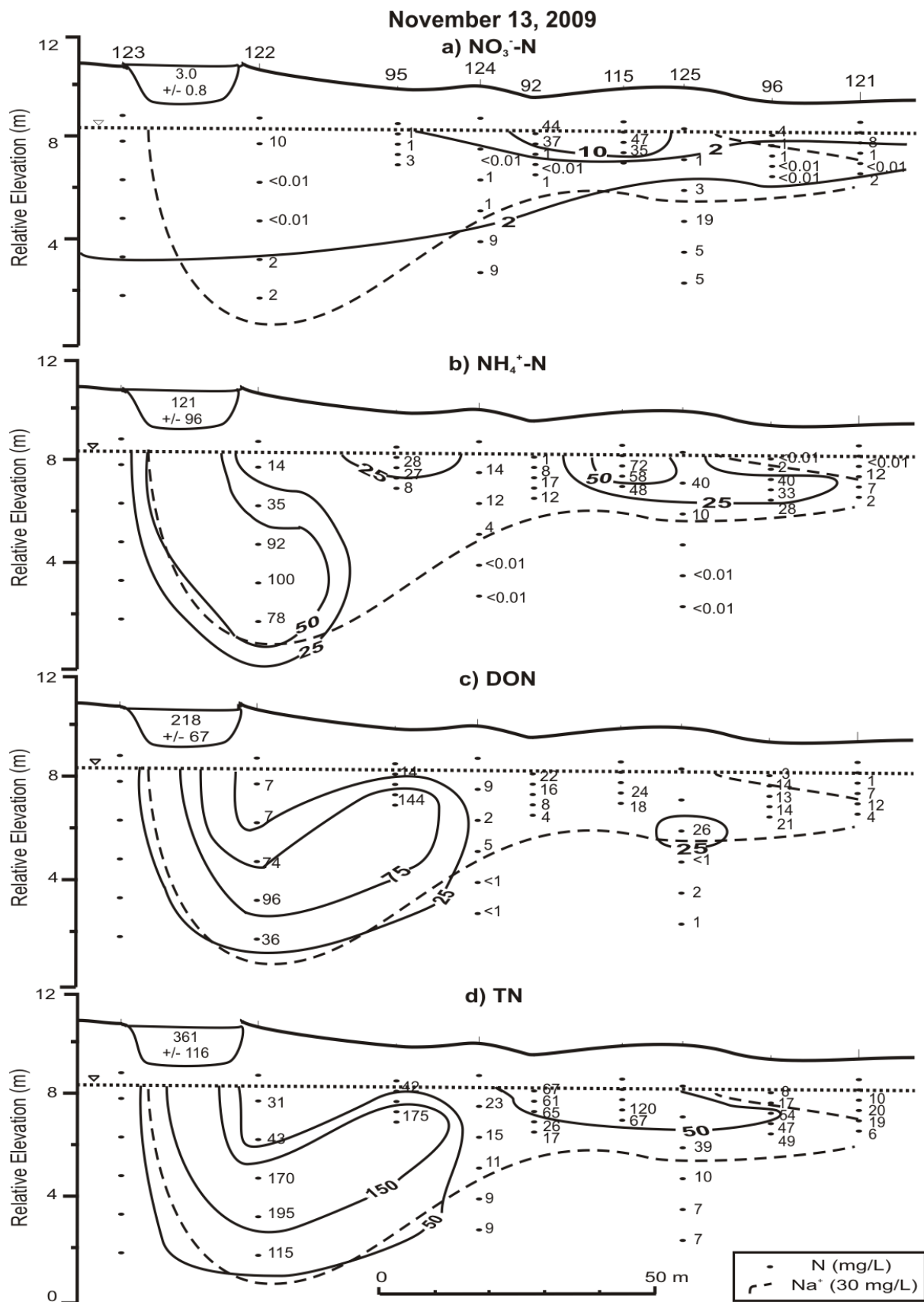


Figure 26. Distribution of nitrogen species: **a)** NO₃⁻ **b)** NH₄⁺ **c)** dissolved organic nitrogen (DON) and **d)** total nitrogen (TN) along the centre line, November 13, 2009. Pond values are the mean and standard deviation from Aug. 28 2008 to Nov. 13 2009 (n=5-15).

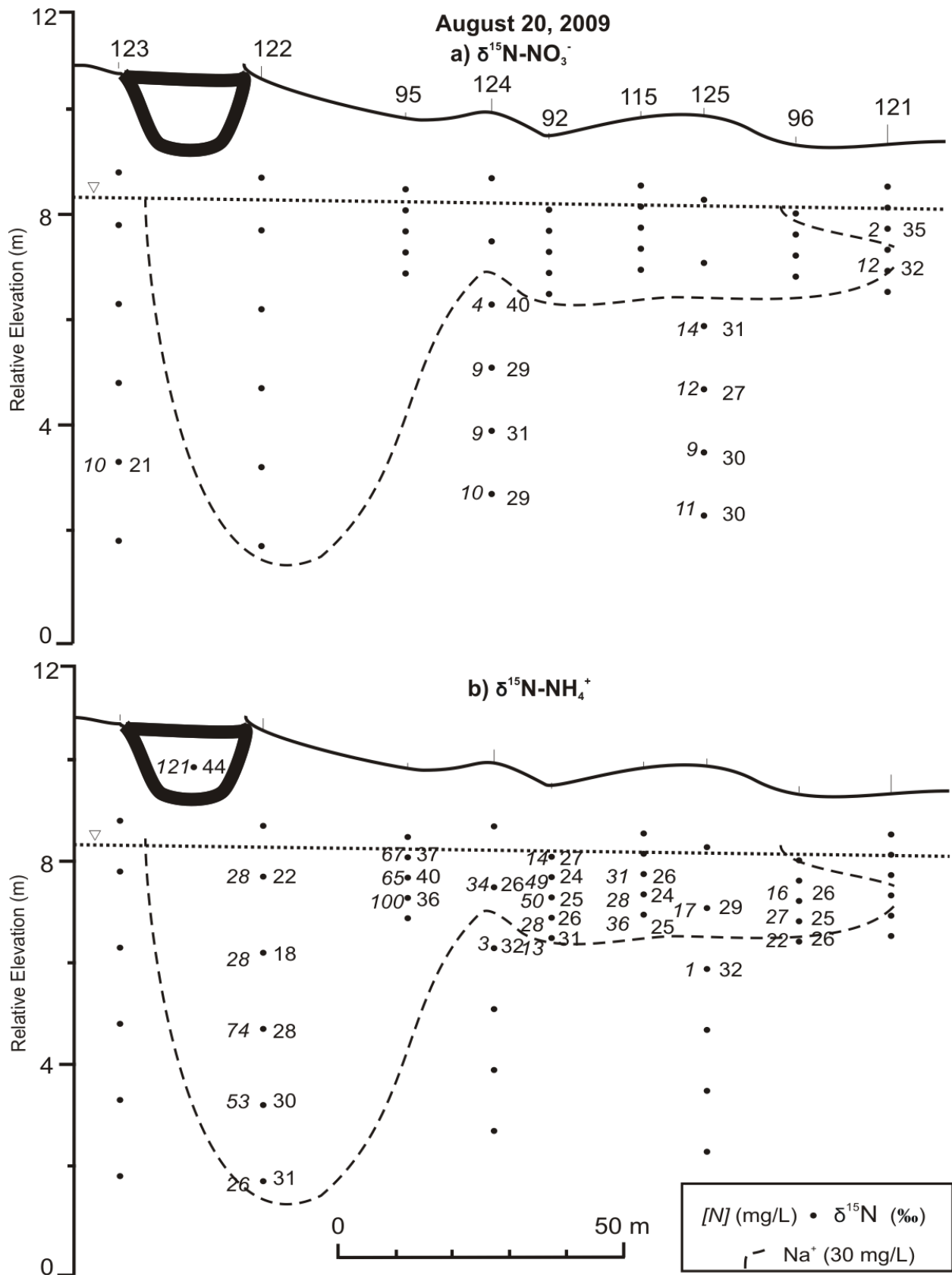


Figure 27. Nitrogen isotopic composition August 20, 2009: a) $\delta^{15}\text{N-NO}_3^-$ and b) $\delta^{15}\text{N-NH}_4^+$. Concentrations of NO_3^- and NH_4^+ , as well as the outline of the plume based on Na^+ are also shown.

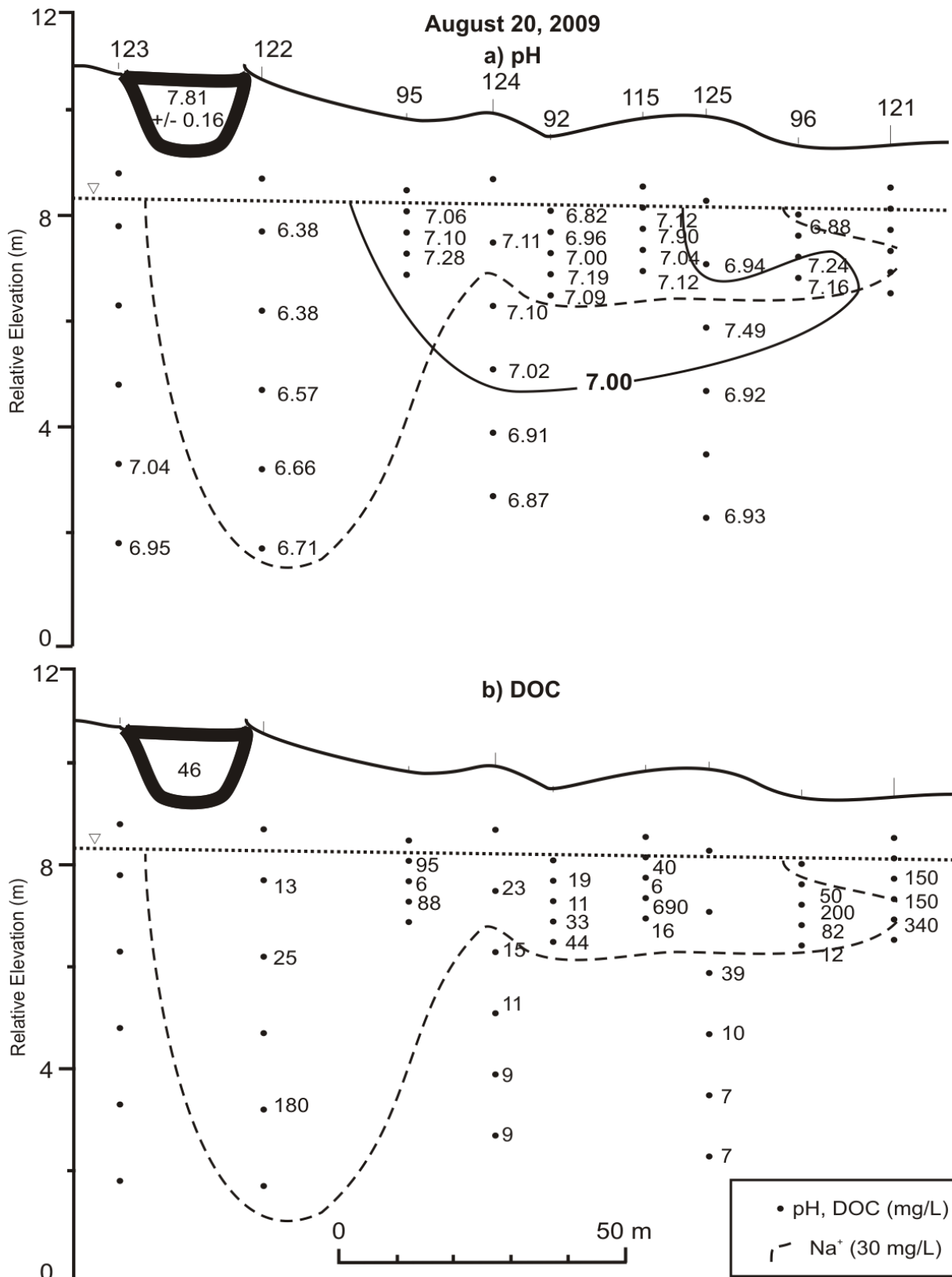


Figure 30. Distribution of **a)** pH and **b)** dissolved organic carbon (DOC) along the centre line, August 20, 2009. Pond concentrations are the mean and standard deviation from Aug. 28, 2008 to Nov. 13, 2009 for pH (n=4) and from August 20, 2009 for DOC.

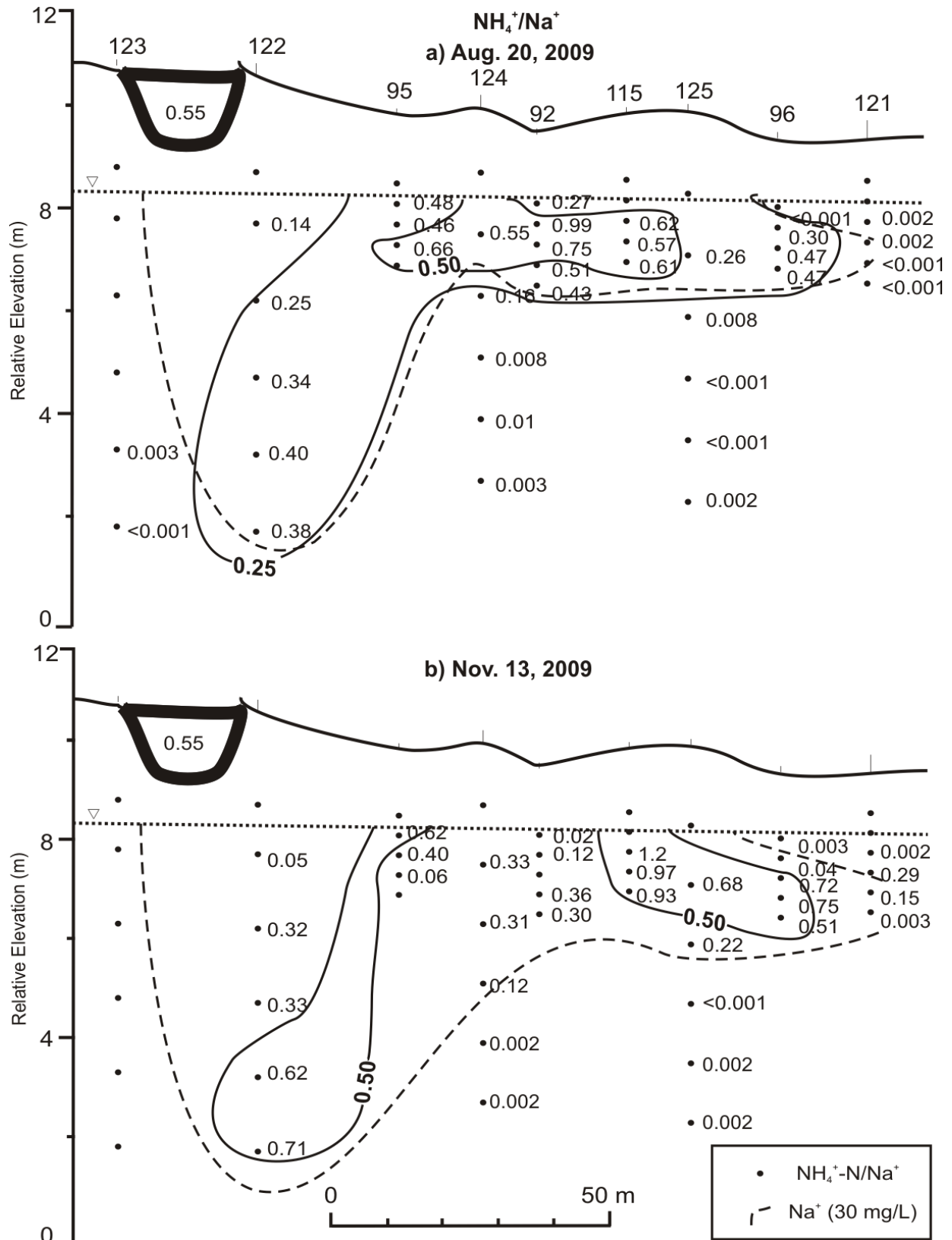


Figure 31. Distribution of the ratio of NH₄⁺-N to the conservative plume tracer Na⁺ along the centre line: **a)** August 20, 2009 and **b)** November 13, 2009. Pond value is the mean value from Aug. 28 2008 to Nov. 13 2009 (n=7-15).

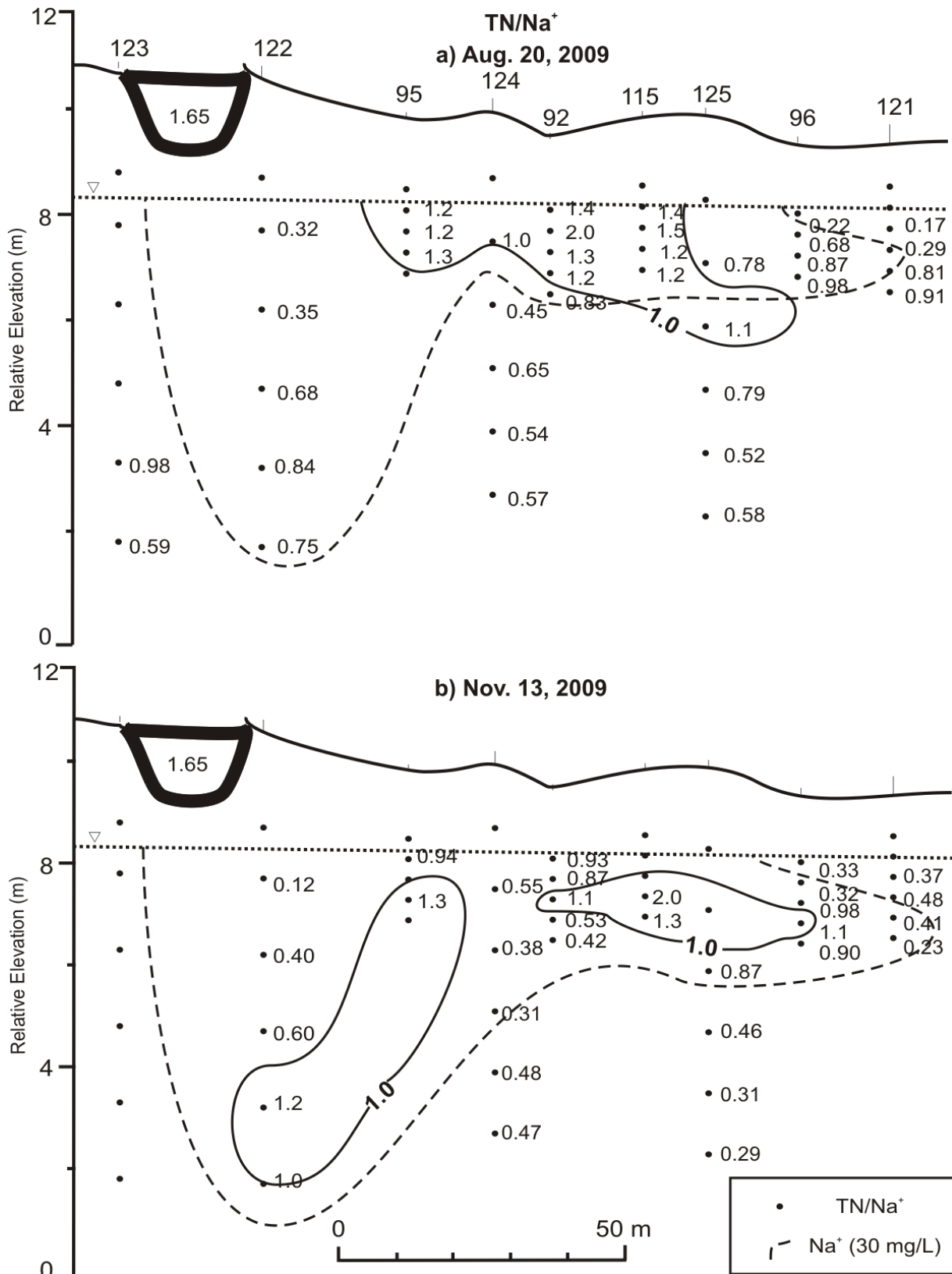
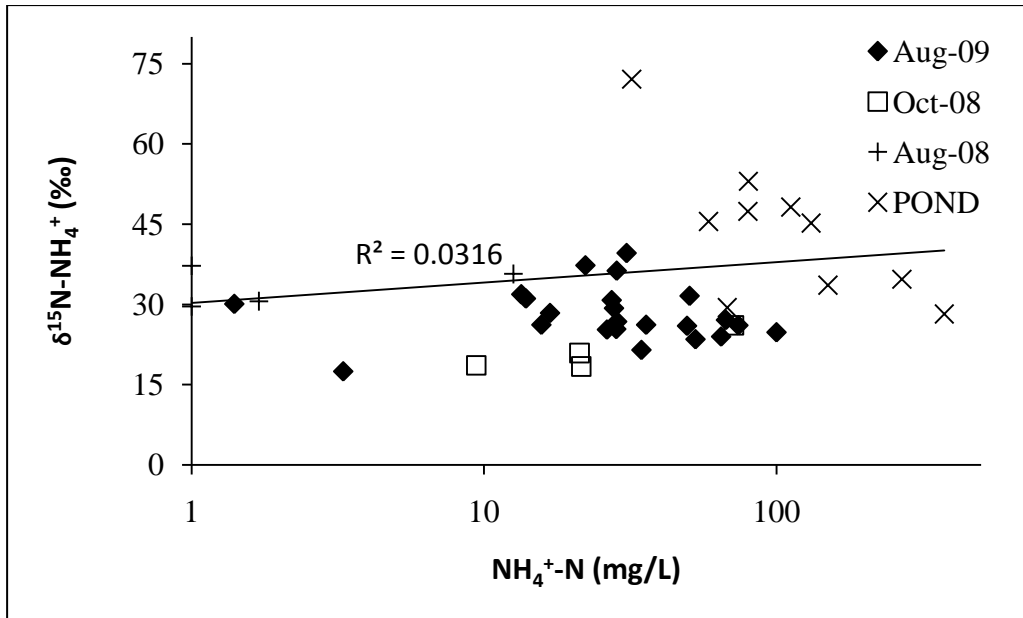


Figure 32. Distribution of the ratio of total nitrogen (TN) to the conservative plume tracer Na⁺ along the centre line: **a)** August 20, 2009 and **b)** November 13, 2009. Pond value is the mean value from Aug. 28 2008 to Nov. 13 2009 (n=5-7).

a) $\text{NH}_4^+\text{-N}$



b) $\text{NO}_3^-\text{-N}$

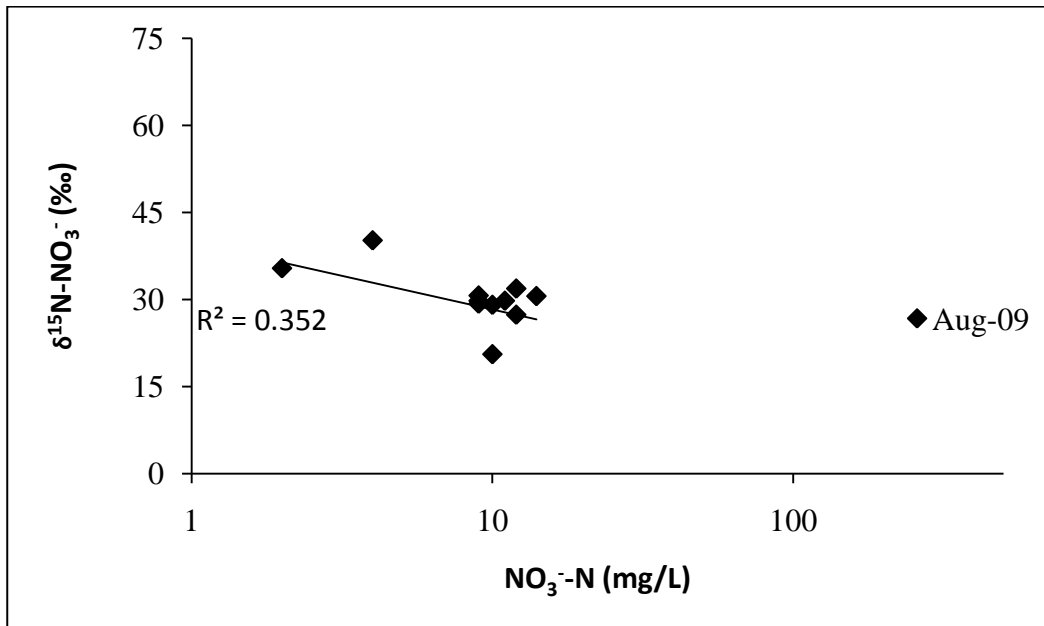


Figure 33. Relationship of $\delta^{15}\text{N}$ isotopic composition to: a) $\text{NH}_4^+\text{-N}$ and b) $\text{NO}_3^-\text{-N}$ concentrations in the plume core (August 2008 to August 2009).

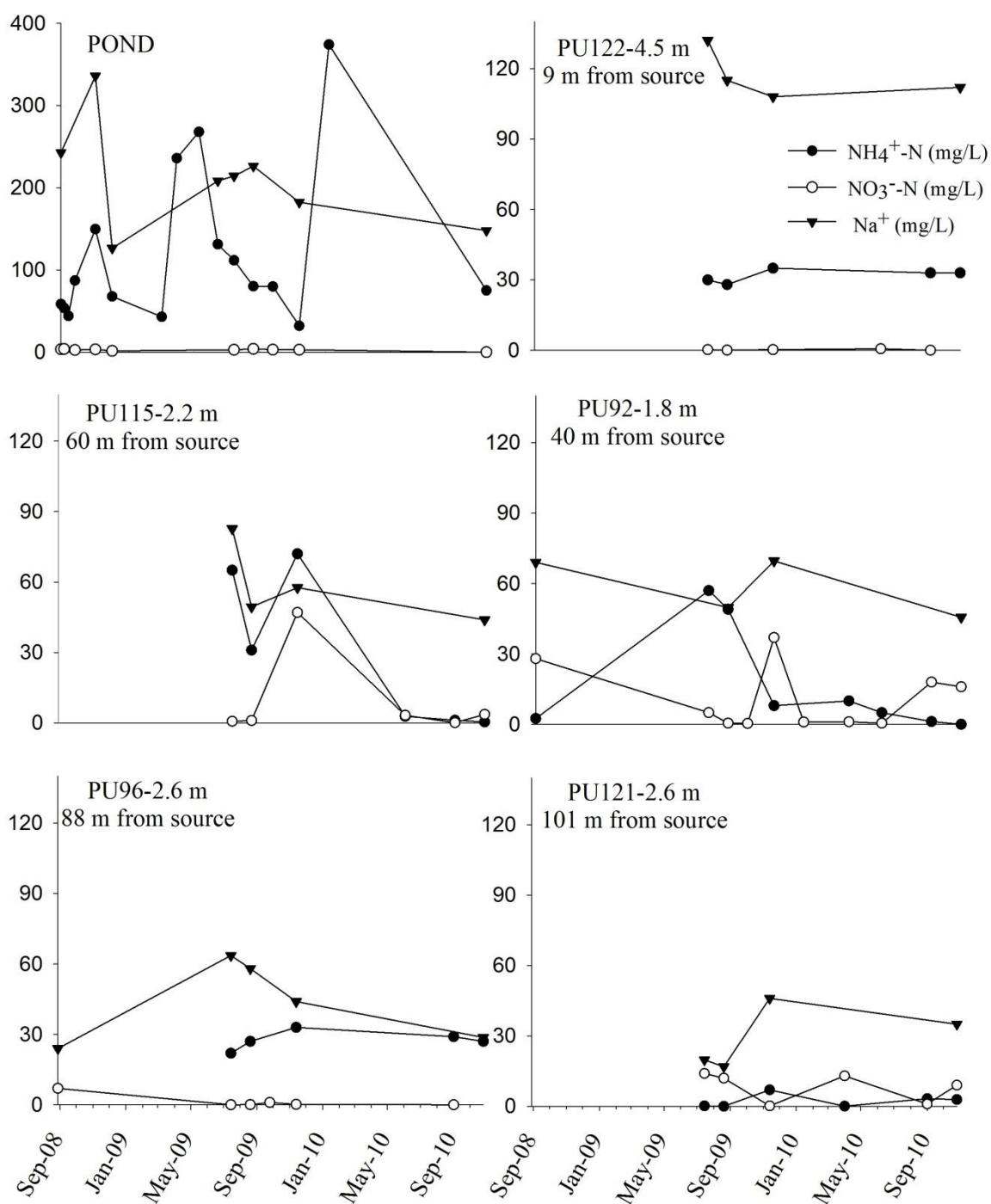


Figure 34. Temporal trends of NO_3^- , NH_4^+ and Na^+ at 5 sampling points (and the Pond) along the centre line. Values taken from August 28, 2008 – October 26, 2010. Values post- June 2010 provided courtesy of Lucas Carson (unpublished data).

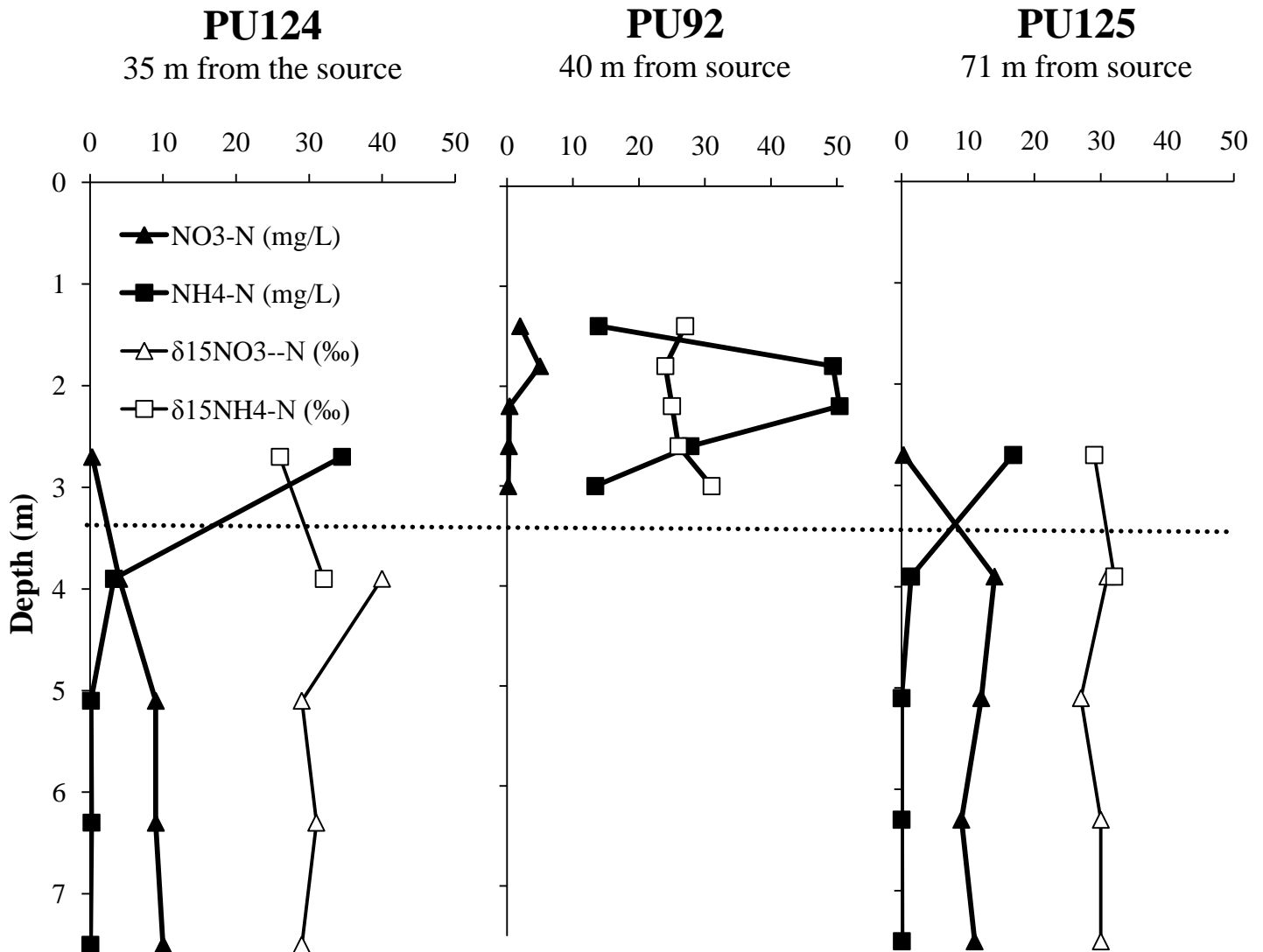


Figure 35. Depth profiles of NO₃⁻-N and NH₄⁺-N concentrations (mg/L) compared to δ¹⁵N (‰) values at wells PU124, PU92 and PU125. All values from August 20, 2009. Dotted line represents the 30 mg/L Na⁺ boundary.

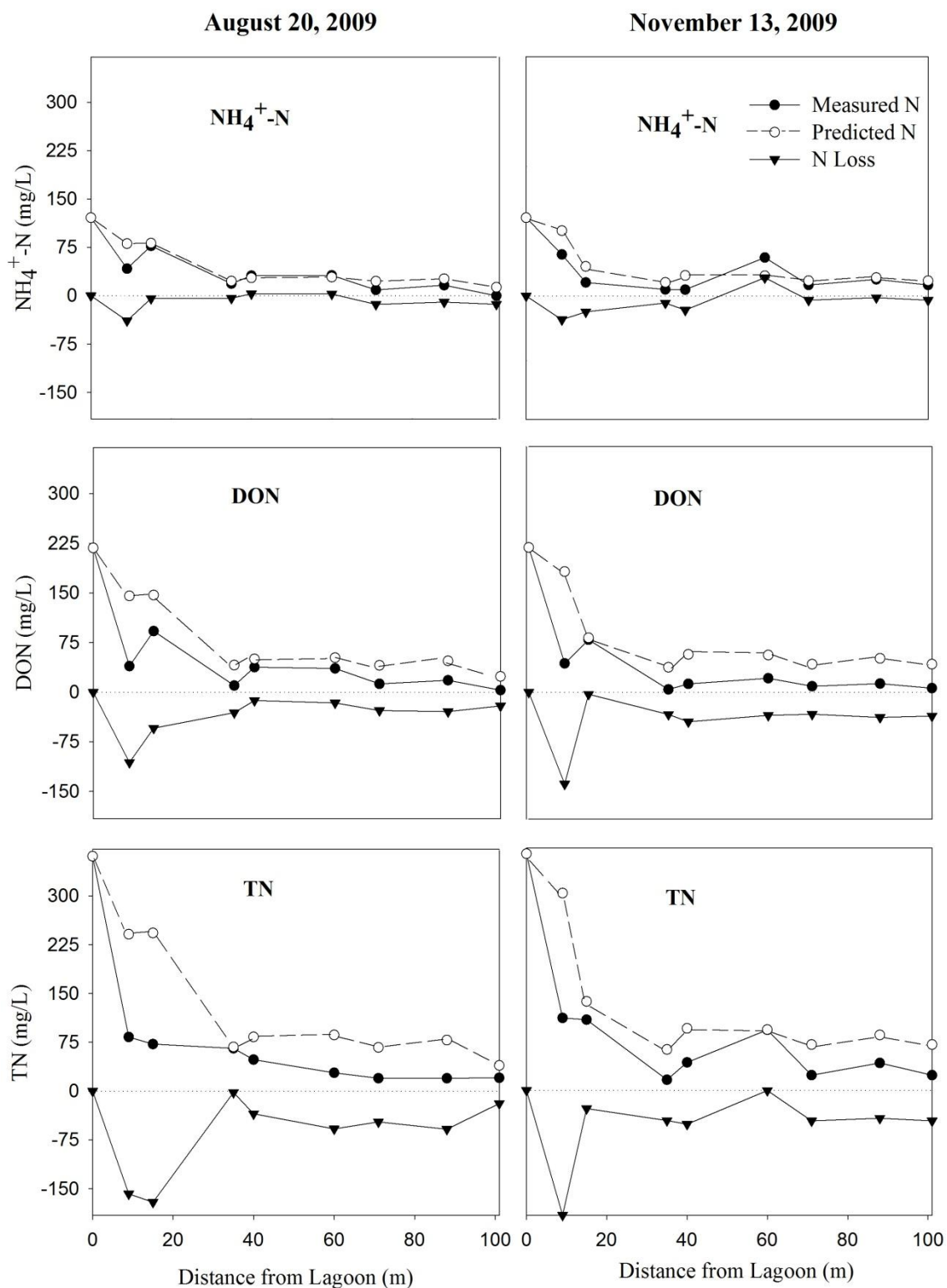


Figure 36: Calculation of predicted $\text{NH}_4^+\text{-N}$, DON and TN compared to measured values for August, 20, 2009 and November 13, 2009 along the plume centreline. Predicted values were calculated based on Na^+ ratios (conservative tracer), while nitrogen loss was calculated as the difference between measured and predicted values. Positive N loss values represent a higher than predicted concentrations. Measured and predicted values are the means within the plume ($n = 2\text{-}5$), defined by $\text{Na}^+ > 30 \text{ mg/L}$.

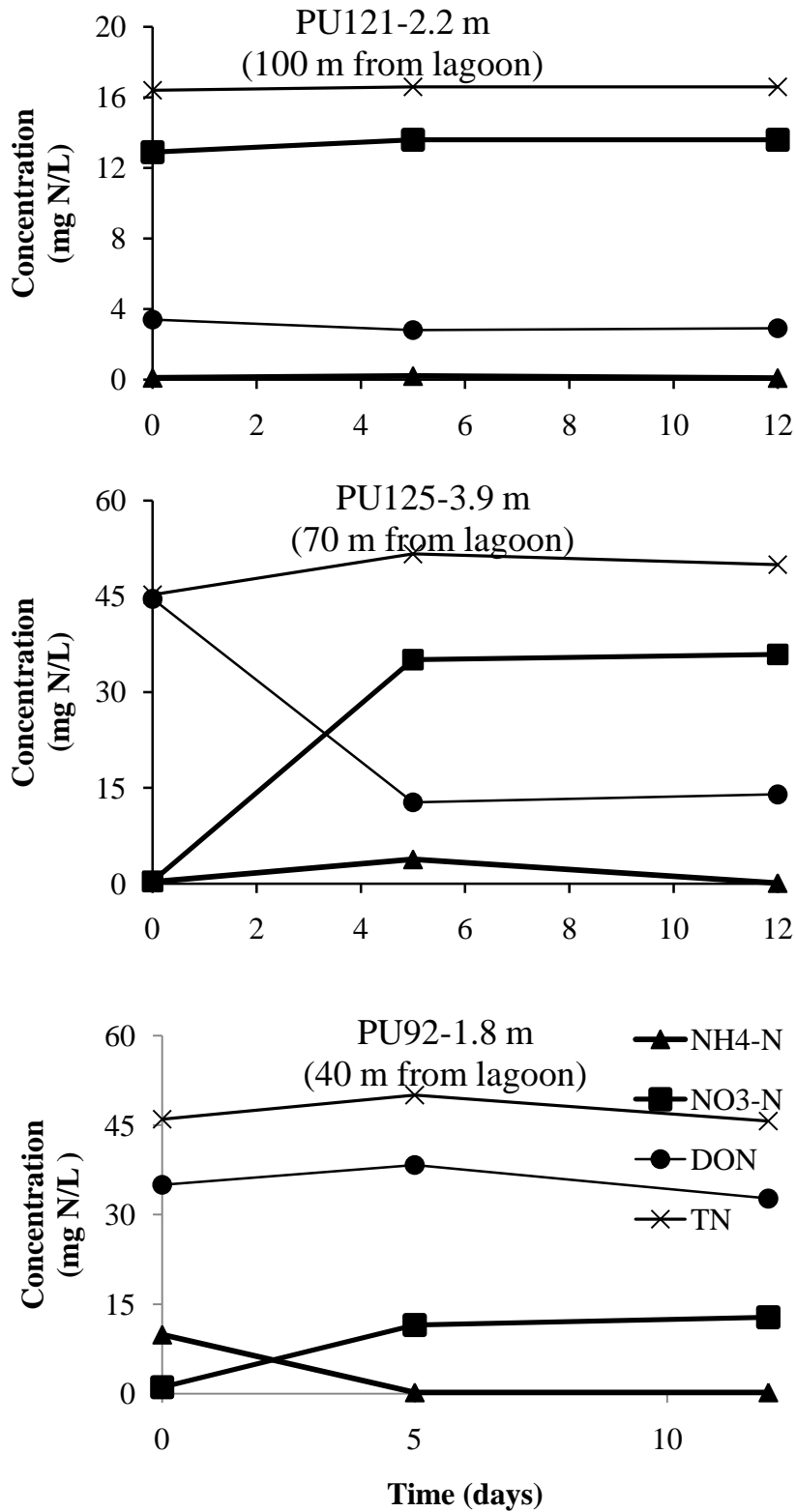


Figure 37. Temporal trends in nitrogen for experiment 1, performed with a 4:1 groundwater from indicated locations to atmospheric headspace mixture, reacting for 12 days.

APPENDIX A

Well construction details and water levels

August 2008 – July 2010

Table A-1. Zorra monitoring network piezometer construction details.

Well Number	Installation Date	Well Type	Stickup m	Relative Elevation of Pipe Top (m)	Installation Method
PU80		1	0.15	9.20	
PU81		1	0.1	8.79	
PU83		1	0	10.06	
PU84		1	0.15	9.69	
PU85		1	0	9.00	
PU86		1	0.25	10.58	
PU87		1	0.15	9.00	
PU89	Aug 22/08	2	0	9.65	Jack Hammer
PU90	Aug 22/08	2	0	9.49	Jack Hammer
PU91	Aug 22/08	2	0	9.52	Jack Hammer
PU92	Aug 22/08	2	0	9.49	Jack Hammer
PU93	Aug 25/08	2	0	10.29	Jack Hammer
PU94	Aug 25/08	2	0	9.91	Jack Hammer
PU95	Aug 25/08	2	0	9.88	Jack Hammer
PU96	Aug 25/08	2	0	9.42	Jack Hammer
PU97	Aug 26/08	2	0.1	9.57	Jack Hammer
PU98	Aug 26/08	2	0.15	8.63	Jack Hammer
PU99	Aug 26/08	2	0.8	10.70	Jack Hammer
PU100	Aug 27/08	2	0.1	10.75	Jack Hammer
PU101	Aug 28/08	2	0	10.60	Jack Hammer
PU103	Oct 20/08	3	0.05	9.57	Enviro-core
PU104	Oct 20/08	4	0.15	9.82	Enviro-core
PU105	Oct 20/08	2	0	10.46	Enviro-core
PU106	Oct 20/08	3	0	10.59	Enviro-core
PU107	Oct 21/08	2	0	-	Enviro-core
PU108	Oct 21/08	2	0	9.88	Enviro-core
PU109	Oct 21/08	2	0	8.40	Enviro-core
PU111	June 11/09	2	0	10.16	Enviro-core
PU112	June 11/09	2	0	10.02	Enviro-core
PU113	June 11/09	2	0	10.28	Enviro-core
PU114	June 11/09	2	0	10.15	Enviro-core
PU115	June 11/09	2	0	9.95	Enviro-core
PU116	June 11/09	2	0	10.00	Enviro-core
PU117	June 11/09	2	0	10.01	Enviro-core
PU118	June 11/09	2	0.05	9.03	Enviro-core
PU119	July 7/09	2	0	9.60	Enviro-core
PU120	July 7/09	2	0	9.95	Enviro-core
PU121	July 7/09	2	0.32	9.53	Enviro-core
PU122	July 7/09	3	0.15	10.70	Enviro-core
PU123	July 7/09	3	0	10.80	Enviro-core
PU124	Aug 19/09	5	0.1	10.19	Enviro-core
PU125	Aug 19/09	5	0	9.78	Enviro-core

Notes:

- Well Type:
- 1) 1.27 cm diameter PVC pipe with 10 cm slotted tip with NYTEX mesh wrap. Monitoring points every 40 cm from 1.2-3.2 m below surface constructed of 0.6 cm diameter polyethylene tubing.
 - 2) 1.27 cm diameter PVC pipe with 10 cm slotted tip with NYTEX mesh wrap. Monitoring points every 40 cm from 1.4-3.0 m below surface constructed of 0.6 cm diameter polyethylene tubing.
 - 3) 1.27 cm diameter PVC pipe with 10 cm slotted tip with NYTEX mesh wrap. Monitoring points every 1 m from 2.0-9.0 m below surface constructed of 0.6 cm diameter polyethylene tubing.
 - 4) 5.1 cm diameter PVC pipe with 1.5 long screened interval installed to a depth of 9 m
 - 5) 1.27 cm diameter PVC pipe with 10 cm slotted tip with NYTEX mesh wrap. Monitoring points every 1.5 m from 1.5-7.5 m below surface constructed of 0.6 cm diameter polyethylene tubing.

Well elevations surveyed initially August 2008 for existing piezometers, resurveyed November 2009 including all additional wells using surveyor's level (± 0.01 m).

Table A-2. Depth to water table from PVC pipetop using water level tape, August 2008 to July 2010.

Well	Depth to Water (m)										
	Aug. 28/08	Oct. 20/08	Apr. 15/09	May 8/09	July 7/09	Sept. 25/09	Oct. 31/09	Nov. 13/09	May 26/10	June 29/10	July 6/10
PU80	1.18	1.42	0.37	-	0.90	-	-	1.10	0.99	1.04	-
PU81	0.77	1.06	-	-	-	-	-	0.74	0.66	-	-
PU83	1.64	2.07	-	-	1.70	-	-	-	1.73	-	-
PU84	1.66	1.98	0.92	-	1.45	-	1.61	1.65	1.55	-	-
PU85	0.90	1.19	0.05	-	0.63	-	-	0.86	0.76	-	-
PU86	2.48	2.72	0.54	1.58	2.11	-	-	-	2.23	2.26	2.43
PU87	1.2	1.40	0.32	0.48	-	-	-	1.07	0.97	0.99	-
PU89	1.52	1.86	-	0.75	-	-	-	-	-	-	-
PU90	1.37	1.69	-	0.38	1.10	-	-	1.36	-	-	-
PU91	1.42	1.73	0.60	0.64	1.16	-	-	-	-	-	-
PU92	1.39	1.71	0.57	0.62	1.14	1.55	1.32	1.39	1.26	1.30	-
PU93	2.13	2.51	1.34	1.38	1.92	-	-	-	-	-	-
PU94	1.68	2.13	0.01	-	1.56	-	-	-	-	-	-
PU95	1.71	2.06	0.88	0.82	1.41	-	2.26	-	-	-	-
PU96	1.40	1.70	0.66	0.72	1.19	1.55	1.34	1.39	1.30	1.33	1.48
PU97	1.47	1.80	0.70	0.76	1.26	-	-	1.48	1.37	-	-
PU98	0.59	0.88	-	-	0.31	-	-	-	0.45	-	-
PU99	2.52	3.00	-	-	-	-	-	-	-	-	-
PU100	2.26	2.88	-	-	-	-	-	-	-	-	-
PU101	2.50	2.83	-	-	-	-	-	-	-	-	-
PU103	-	-	0.63	0.68	1.21	-	1.28	1.45	1.10	-	-
PU104	-	2.20	0.83	0.93	-	-	-	-	-	-	-
PU105	-	-	1.54	0.58	2.11	-	2.30	2.37	2.23	2.27	2.42
PU106	-	-	-	-	-	-	-	-	-	-	-
PU107	-	-	-	-	-	-	-	-	-	-	-
PU108	-	-	1.02	1.06	1.60	-	-	-	-	-	-
PU109	-	-	-	-	0.28	-	-	-	0.47	-	-
PU111	-	-	-	-	2.80	-	-	-	-	-	-
PU112	-	-	-	-	2.98	-	-	-	-	-	-
PU113	-	-	-	-	2.14	-	-	-	-	-	-
PU114	-	-	-	-	2.70	-	-	-	-	-	-
PU115	-	-	-	-	1.62	2.04	1.80	1.87	1.74	1.77	1.94
PU116	-	-	-	-	1.54	-	-	1.93	1.66	-	-
PU117	-	-	-	-	1.60	-	-	1.83	1.70	-	-
PU118	-	-	-	-	0.69	-	-	0.90	0.82	0.85	-
PU119	-	-	-	-	1.25	-	-	1.50	-	-	-
PU120	-	-	-	-	1.62	-	-	-	-	-	-
PU121	-	-	-	-	-	-	1.43	1.48	1.4	1.43	-
PU122	-	-	-	-	2.44	2.86	2.60	-	2.55	2.57	2.75
PU123	-	-	-	-	-	-	3.08	-	-	-	-
PU124	-	-	-	-	-	2.26	2.02	2.08	1.96	1.99	-
PU125	-	-	-	-	1.86	1.62	1.68	1.58	1.61	1.76	-

Table A-3. Hydraulic head measurements, (h = elevation of pipetop – depth to water), August 2008 to July 2010.

Well	h (m)										
	Aug. 28/08	Oct. 20/08	Apr. 15/09	May 8/09	July 7/09	Sept. 25/09	Oct. 31/09	Nov. 13/09	May 26/10	June 29/10	July 6/10
PU80	8.02	7.78	8.83	-	8.30	-	-	8.10	8.21	8.16	-
PU81	8.02	7.73	-	-	-	-	-	8.05	8.13	-	-
PU83	8.42	7.99	-	-	8.36	-	-	-	8.33	-	-
PU84	8.03	7.71	8.77	-	8.24	-	8.08	8.04	8.14	-	-
PU85	8.10	7.81	8.95	-	8.37	-	-	8.14	8.24	-	-
PU86	8.10	7.86	10.04	9.00	8.47	-	-	-	8.35	8.32	8.15
PU87	8.00	7.80	8.88	8.72	-	-	-	8.13	8.23	8.21	-
PU89	8.13	7.79	-	8.90	-	-	-	-	-	-	-
PU90	8.12	7.80	-	9.11	8.39	-	-	8.13	-	-	-
PU91	8.10	7.79	8.92	8.88	8.36	-	-	-	-	-	-
PU92	8.10	7.78	8.92	8.87	8.35	7.94	8.17	8.10	8.23	8.19	-
PU93	8.16	7.78	8.95	8.91	8.37	-	-	-	-	-	-
PU94	8.23	7.78	9.90	-	8.35	-	-	-	-	-	-
PU95	8.17	7.82	9.00	9.06	8.47	-	7.62	-	-	-	-
PU96	8.02	7.72	8.76	8.70	8.23	7.87	8.08	8.03	8.12	8.09	7.94
PU97	8.10	7.77	8.87	8.81	8.31	-	-	8.09	8.20	-	-
PU98	8.04	7.75	-	-	8.32	-	-	-	8.18	-	-
PU99	8.18	7.70	-	-	-	-	-	-	-	-	-
PU100	8.49	7.87	-	-	-	-	-	-	-	-	-
PU101	8.10	7.77	-	-	-	-	-	-	-	-	-
PU103	-	-	8.94	8.89	8.36	-	8.29	8.12	8.47	-	-
PU104	-	7.62	8.99	8.89	-	-	-	-	-	-	-
PU105	-	-	8.92	9.88	8.35	-	8.16	8.09	8.23	8.19	8.04
PU106	-	-	-	-	-	-	-	-	-	-	-
PU107	-	-	-	-	-	-	-	-	-	-	-
PU108	-	-	8.86	8.82	8.28	-	-	-	-	-	-
PU109	-	-	-	-	8.12	-	-	-	7.93	-	-
PU111	-	-	-	-	-	-	-	-	-	-	-
PU112	-	-	-	-	-	-	-	-	-	-	-
PU113	-	-	-	-	8.14	-	-	-	-	-	-
PU114	-	-	-	-	-	-	-	-	-	-	-
PU115	-	-	-	-	8.33	7.91	8.15	8.08	8.21	8.18	8.01
PU116	-	-	-	-	8.46	-	-	8.07	8.34	-	-
PU117	-	-	-	-	8.41	-	-	8.18	8.31	-	-
PU118	-	-	-	-	8.34	-	-	8.13	8.21	8.18	-
PU119	-	-	-	-	8.35	-	-	8.10	-	-	-
PU120	-	-	-	-	8.33	-	-	-	-	-	-
PU121	-	-	-	-	-	-	8.10	8.05	8.13	8.10	-
PU122	-	-	-	-	8.26	7.84	8.10	-	8.15	8.13	7.95
PU123	-	-	-	-	-	-	7.72	-	-	-	-
PU124	-	-	-	-	-	7.93	8.17	8.11	8.23	8.20	-
PU125	-	-	-	-	7.92	8.16	8.10	8.20	8.17	8.02	-

APPENDIX B

Borehole Logs and Grain Size Analyses

Table B-1. Grain size percent passing for boreholes a) PU124, b) PU122, c) PU125, d) PU123, and ten percentile passing value (d_{10}) used to calculated hydraulic conductivity (K) using the Hazen equation, assuming C=1.

a)

PU124		Depth (m)				
		0.5	1.5	3	4.5	6.5
Mesh Size	Mm	% Passing				
5	4	74.57	99.92	92.23	99.99	39.48
8	2.36	67.47	98.01	-	98.09	-
10	2	63.77	-	-	-	-
18	1	55.77	86.92	30.92	56.81	3.72
30	0.6	-	-	19.70	-	1.09
35	0.5	45.00	72.82	-	12.36	-
45	0.355	31.62	44.23	8.12	6.95	0.40
50	0.3	-	-	6.63	-	0.35
60	0.25	18.02	20.83	-	5.22	-
100	0.15	9.22	9.68	3.35	1.11	0.19
140	0.106	5.26	6.42	2.31	0.74	0.13
200	0.075	-	4.10	1.62	0.49	0.11
d_{10}		0.15	0.15	0.45	0.45	1.5
K (cm/s)		0.02	0.02	0.20	0.20	2.25

b)

PU122		Depth (m)						
		0.5	2	3.5	4.5	5.5	6.5	7.5
Mesh Size	mm	% Passing						
5	4	65.19	99.77	99.98	92.63	54.62	28.04	99.24
8	2.36	54.10	-	97.28	-	48.74	-	92.77
18	1	40.00	98.33	96.68	70.81	36.69	10.24	50.97
30	0.6	-	96.24	-	60.86	-	6.34	-
35	0.5	29.28	-	96.16	-	19.84	-	11.18
45	0.355	24.14	79.78	94.03	44.89	12.95	4.10	6.83
50	0.3	-	66.37	-	35.85	-	3.50	-
60	0.25	18.70	-	89.28	-	8.52	-	5.37
100	0.15	12.87	16.22	69.75	13.30	5.78	2.41	4.38
140	0.106	9.43	9.04	51.14	8.30	4.41	1.90	3.29
200	0.075	6.70	6.04	39.55	5.84	3.37	1.39	2.40
d_{10}		0.12	0.11	0.03	0.12	0.3	1	0.4
K (cm/s)		0.01	0.01	0.00	0.01	0.09	1.00	0.16

c)

PU125		Depth (m)				
		0.5	2.5	4.5	5.5	7
Mesh Size	mm	% Passing				
5	4	100	91.23	100	98.86	91.04
8	2.36	-	88.96	-	96.56	-
10	2	-	-	-	-	-
18	1	99.01	84.54	98.98	85.19	80.95
30	0.6	95.21	-	95.07	-	73.93
35	0.5	-	70.93	-	63.26	-
45	0.355	67.90	48.21	64.85	39.25	41.27
50	0.3	54.11	-	45.96	-	25.84
60	0.25	-	20.76	-	11.28	-
100	0.15	19.49	2.22	3.21	1.03	1.20
140	0.106	11.80	0.92	1.71	0.29	0.29
200	0.075	7.37	0.58	1.09	0.19	0.13
d ₁₀		0.1	0.2	0.2	0.25	0.2
K (cm/s)		0.01	0.04	0.04	0.063	0.04

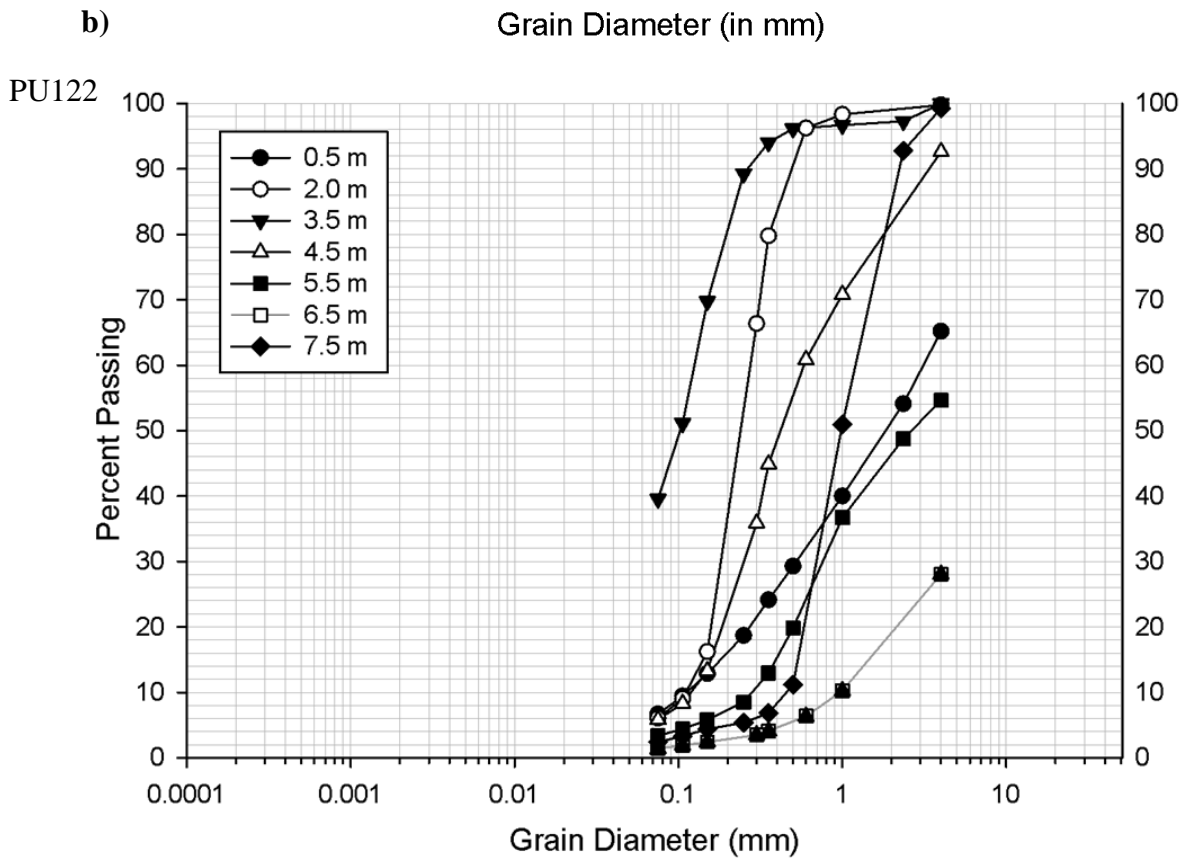
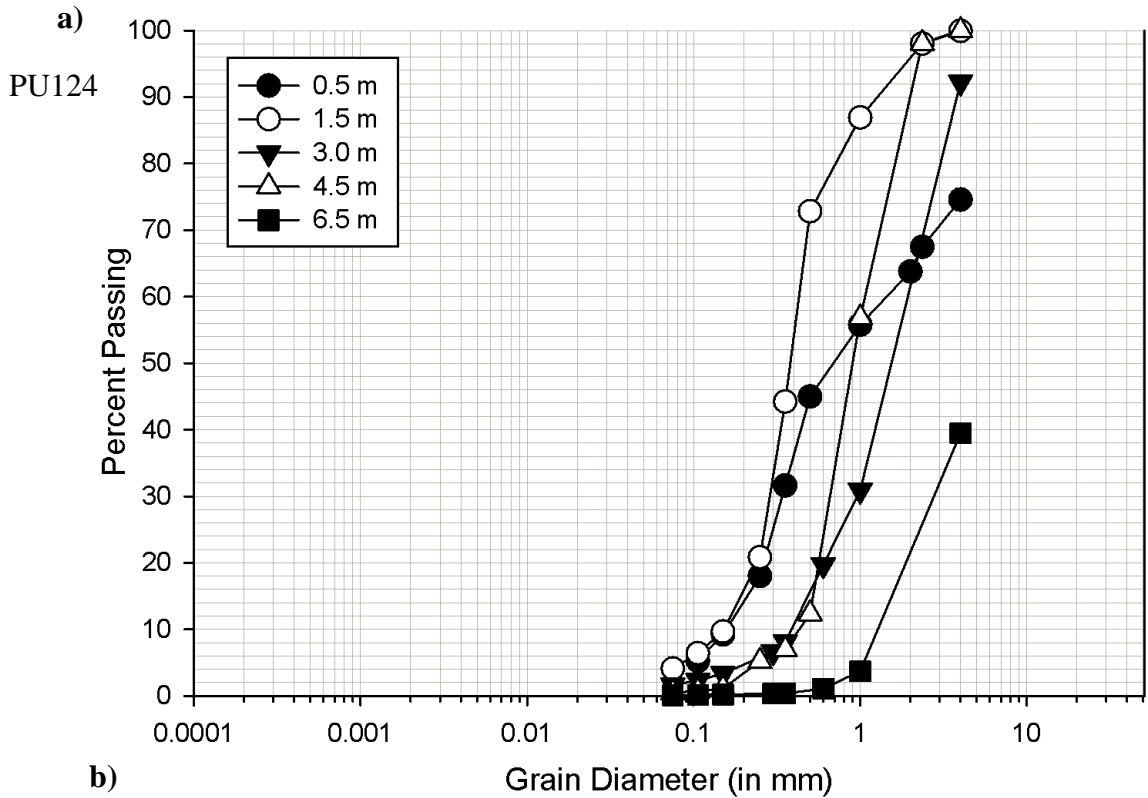
d)

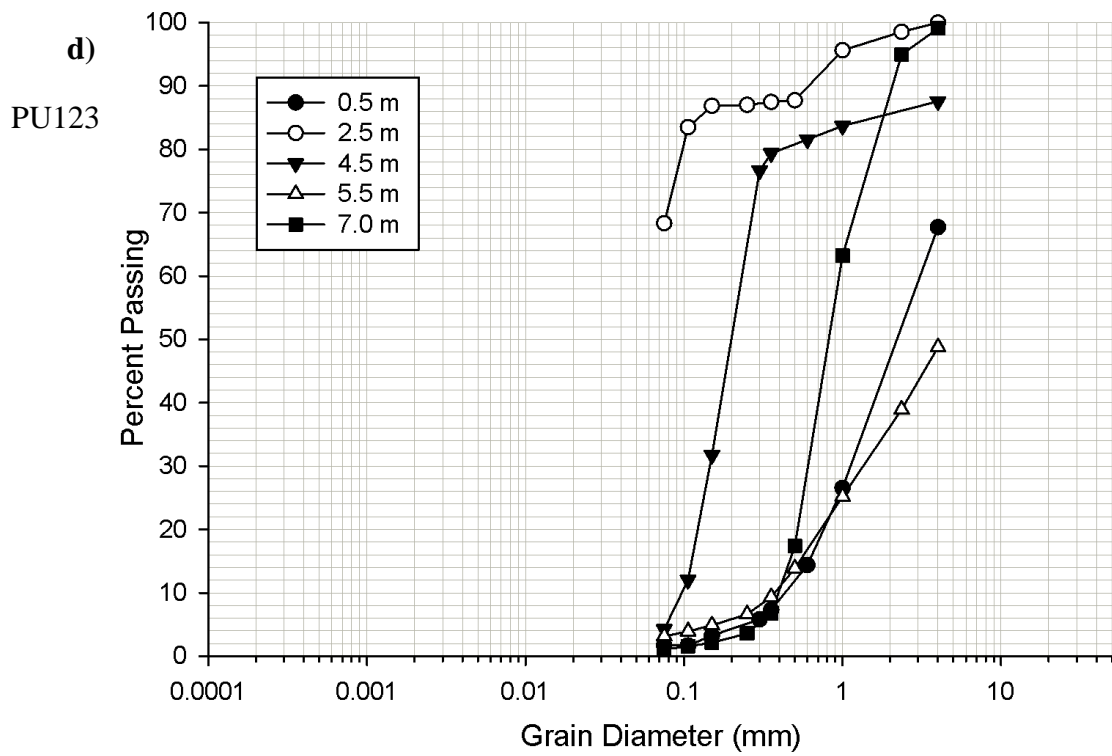
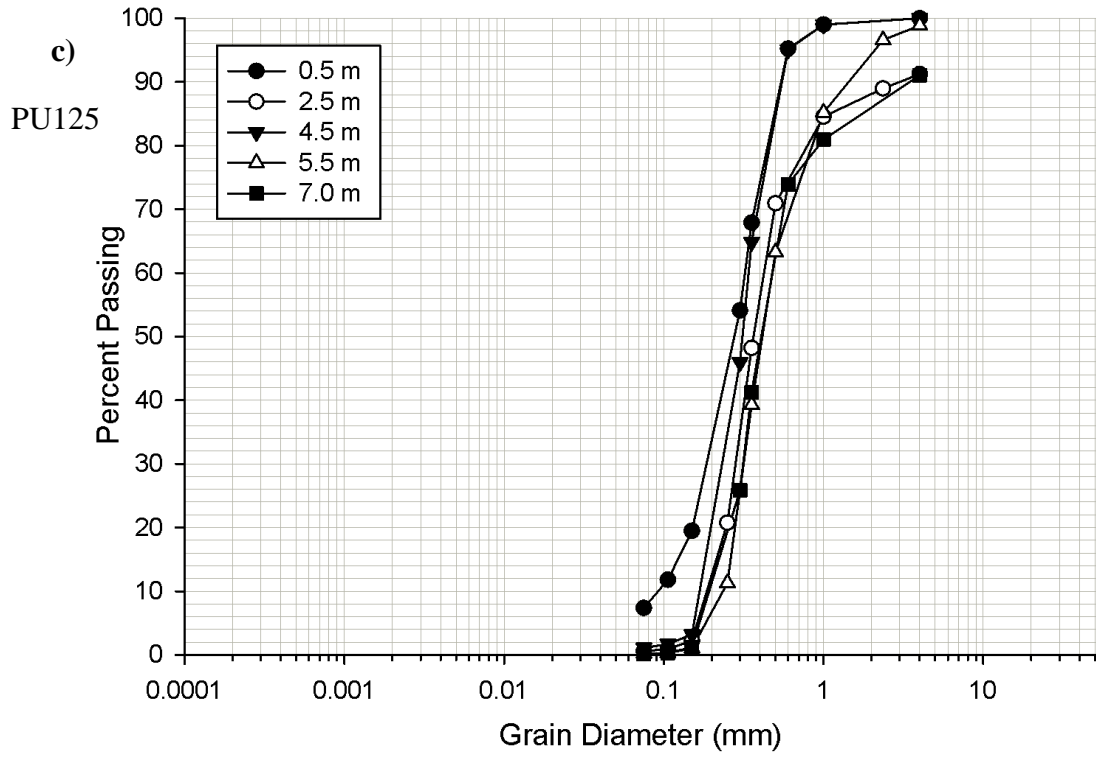
PU123		Depth (m)				
		0.5	2	3.5	5.5	7.5
Mesh Size	mm	% Passing				
Size 5	4	67.70	100	87.56	48.76	99.07
Size 8	2.36	-	98.53	-	38.92	94.93
Size 10	2	-	-	-	-	-
Size 18	1	26.53	95.61	83.68	25.20	63.21
Size 30	0.6	14.39	-	81.54	-	-
Size 35	0.5	-	87.72	-	13.86	17.37
Size 45	0.355	7.29	87.45	79.37	9.34	6.73
Size 50	0.3	5.81	-	76.64	-	-
Size 60	0.25	-	87.00	-	6.62	3.59
Size 100	0.15	3.25	86.86	31.76	4.86	2.13
Size 140	0.106	1.67	83.47	12.04	3.91	1.55
Size 200	0.075	1.67	68.33	4.23	3.14	1.06
d ₁₀		0.45	0.01	0.4	0.4	0.4
K (cm/s)		0.2025	0.0001	0.16	0.16	0.16

Table B-2. Depth to water measurements (m) during pumping test at PU104, October 30, 2008 at proximal wells. Note a pumping rate of 110 L/min, well diameter of 0.051 m and screen length of 1.52 m.

Well	Time (min)						
	T0	1	3	7	12	20	23
PU97-3.0	1.59				1.6		
PU85-3.0	0.99				1		
PU89-3.0	1.65		1.7		1.7		1.7
PU104 (PW)	2.00	2.00	2	2	2		2
PU90-3.0	1.49			1.50		1.50	
PU91-3.0	1.53			1.5		1.5	
PU107-3.0	1.64			1.6	1.6		
PU93-3.0	2.31			2.3		2.3	
PU94-3.0	1.93			1.9		1.9	
PU83-3.0	2.07			2.1		2.1	
PU106-9	2.62			2.6			
PU103-3.0, 9.0	1.58	1.6				1.6	

Figure B-1. Grain size curves for core samples from boreholes a) PU124 b) PU122 c) PU125 and d) PU123





BOREHOLE LOG			PROJECT			SHEET NO.	HOLE NO.
SITE LOCATION			COORDINATES		LOGGED BY	1 OF 1	
DATE START			FINISH	DRILLER	DRILL EQUIPMENT	BORING DIA.	TOTAL DEPTH
MONITOR WELL INSTALLED			SCREEN INTERVAL		WEATHER CONDITIONS		PIPE TOP ELEV.
PIEZO & WELL DIAGRAM (S)	MAIN COMPONENT SUMMARY	DEPTH (m)	GRAPHIC LOG	U.S.C.S.	DESCRIPTION AND CLASSIFICATION Colour, size range, MAIN COMPONENT, minor component (s), moisture content, structure, angularity, odour, and geologic unit (if known).	LAB SAMPLING	
						FIELD ID	DEPTH RANGE (m)
	SAND	1	SP	SP	dark organic topsoil with roots to 0.25m reddish-brown homogeneous medium grain SAND with few pebbles		
		2				0-2.0m	
	pebbly SAND	3	SP	SP	fine to medium grained SAND with pebbles (up to 1cm). Inclusion of pebbles increases with depth, pebbles mostly rounded		
		4				2.0-4.5m	
	sandy GRAVEL	5	GP	GP	sandy GRAVEL, increasing in size with depth, well graded. sand fine to coarse (grading with depth)		
		6				4.5-6.5m	
	SAND & GRAVEL	7	SP	SP	medium to coarse grain SAND and medium sized GRAVEL (~3cm), very heterogeneous		
		8				6.5-8.0m	
	GRAVEL	9	GP	GP	loose, large GRAVEL, ~2-5cm mostly angular, variable shape, size, etc.		
		10				8.0-9.0m	
					END of BOREHOLE		

NOTES: MISSING CORE; 3.5-4.0m
7.1-7.3m

OCT. 20, 2008

Figure B-2. Borehole log for PU103.

BOREHOLE LOG				PROJECT		SHEET NO. 1 OF 1	HOLE NO.		
SITE LOCATION			COORDINATES		LOGGED BY	CHECKED BY			
DATE START	FINISH	DRILLER		DRILL EQUIPMENT	BORING DIA.	TOTAL DEPTH	PIPE TOP ELEV.		
MONITOR WELL INSTALLED		SCREEN INTERVAL		WEATHER CONDITIONS		SAMPLE TYPE (S)			
PIEZO & WELL DIAGRAM (S)	MAIN COMPONENT SUMMARY	DEPTH (m)	GRAPHIC LOG	U.S.C.S.	DESCRIPTION AND CLASSIFICATION Colour, size range, MAIN COMPONENT, minor component (s), moisture content, structure, angularity, odour, and geologic unit (if known).		LAB SAMPLE		
							FIELD ID	DEPTH RANGE (m)	
	SAND	1		SP	Dark brown topsoil consisting of SAND with some pebbles, mostly thin, small and angular. Some roots and organics			0-1.0m	
	silty SAND	2		SM	very fine SAND and silt, trace clays, brown to dark brown in colour			1.0-1.8m	
	pebbly SAND	3		SP	medium to coarse light coloured SAND with small to medium sized pebbles, trace fines heterogeneous with some darker coloured patches, relatively compact			1.8-4.4m	
		4			pebbles increasing in size with depth, becoming less compact				
	sandy GRAVEL	5			heterogeneous GRAVEL with coarse sand. Traces of silt, Large gravel (>5cm) sometimes angular, sometimes rounded,			4.4-7.2	
		6		GP	Poorly graded, some pebbles as well				
		7			very large GRAVEL pieces, packed very loosely, mostly consisting of >5cm chunks and angular				
		GRAVEL	8		GP				7.2-9.0
			9						
			10			END OF BOREHOLE			

NOTES: MISSING CORE: 7.5-8.5 m
3.0-3.3 m
5.5-5.9 m
Oct. 20, 2008

Figure B-3. Borehole log for PU106.

BOREHOLE LOG			PROJECT			SHEET NO. 1 OF 1	HOLE NO.	
SITE LOCATION			COORDINATES		LOGGED BY	CHECKED BY		
DATE START	FINISH	DRILLER	DRILL EQUIPMENT		BORING DIA.	TOTAL DEPTH	PIPE TOP ELEV.	
MONITOR WELL INSTALLED		SCREEN INTERVAL		WEATHER CONDITIONS		SAMPLE TYPE (S)		
PIEZO & WELL DIAGRAM (S)	MAIN COMPONENT SUMMARY	DEPTH (m)	GRAPHIC LOG	USCS	DESCRIPTION AND CLASSIFICATION Colour, size range, MAIN COMPONENT, minor component (s), moisture content, structure, angularity, odour, and geologic unit (if known).	LAB SAMPLE FIELD ID	DEPTH RANGE (m)	
	PU122							
		silty CLAY	1		CL	dense silty CLAY w fine sand, organic until ~0.5m some pebbles (heterogeneous), mostly dark brown to black, some red, strong 'manure-like' odor		0-1.0m
		sandy GRAVEL			GP	loosely packed gravel & coarse sand		1.0-1.6m
		silty CLAY	2		CL	dark dense silty CLAY, some pebbles		1.6-2.2m
		clayey SILT	3		ML	homogeneous, soft, loosely packed clayey SILT, grey to brown in colour, some fine sand Becomes moist 3.5-4.0m.		2.2-3.5m
		pebbly SAND	4		SP	pebbly fine SAND, with some large rocks particularly 4.5-5.0m heterogeneous small-medium rounded pebbles light brown-grey sand		3.5-6.1m
		GRAVEL	7		GP	medium-coarse, very heterogeneous GRAVEL, >3cm in many cases, many colours, shapes, sizes. Angular and rounded pieces.		
			8					
			9					
			10			END OF BOREHOLE		

NOTES: MISSING CORE: 1.10-1.50m 8.6-9.0m
2.6-3.0m
4.3-4.5m
5.5-6.0
7.2-7.5
JULY 7/09

Figure B-4. Borehole log for PU122.

BOREHOLE LOG			PROJECT			SHEET NO. 1 OF 1	HOLE NO.
SITE LOCATION			COORDINATES		LOGGED BY	CHECKED BY	
DATE START	FINISH	DRILLER		DRILL EQUIPMENT	BORING DIA.	TOTAL DEPTH	PIPE TOP ELEV.
MONITOR WELL INSTALLED		SCREEN INTERVAL		WEATHER CONDITIONS		SAMPLE TYPE (S)	
PIEZO & WELL DIAGRAM (S)	MAIN COMPONENT SUMMARY	DEPTH (m)	GRAPHIC LOG	U.S.C.S.	DESCRIPTION AND CLASSIFICATION Colour, size range, MAIN COMPONENT, minor component (s), moisture content, structure, angularity, odour, and geologic unit (if known).	LAB SAMPLE	
						FIELD ID	DEPTH RANGE (m)
	pebbly SAND	0	SP	Coarse SAND with many pebbles, SAND is mostly light brown, pebbles are angular	0-0.75m		
	silty SAND	1	SM	silty SAND, light brown and fine grained, becoming increasingly fine grained and dense with depth	0.75-2.0m		
	silty CLAY	2	CL	soft, homogenous dark silty CLAY	2.0-3.0m		
	SILT	3	ML	homogeneous brown compacted SILT, saturated throughout	3.0-5.0m		
	pebbly SAND	4	SP	medium sized pebbles loosely arranged through medium-coarse grained SAND			
	GRAVEL	5	GP	Heterogeneous pebbles and GRAVEL some medium grained sand loosely packed, saturated, largest rocks angular, smaller pebbles more rounded			
		6					
		7					
		8					
		9					
					END OF BOREHOLE		

NOTES: MISSING CORES 1.2-1.5 m
4.4-4.5 m
6.6-7.5 m
8.7-9.0 m

JULY 7/09

Figure B-5. Borehole log for PU123.

BOREHOLE LOG			PROJECT			SHEET NO. 1 OF 1	HOLE NO.		
SITE LOCATION			COORDINATES		LOGGED BY	CHECKED BY			
DATE START	FINISH	DRILLER	DRILL EQUIPMENT		BORING DIA.	TOTAL DEPTH	PIPE TOP ELEV.		
MONITOR WELL INSTALLED		SCREEN INTERVAL		WEATHER CONDITIONS		SAMPLE TYPE (S)			
PIEZO & WELL DIAGRAM (S)	MAIN COMPONENT SUMMARY	DEPTH (m)	GRAPHIC LOG	U.S.C.S.	DESCRIPTION AND CLASSIFICATION Colour, size range, MAIN COMPONENT, minor component (s), moisture content, structure, angularity, odour, and geologic unit (if known).		LAB SAMPLE		
							FIELD ID	DEPTH RANGE (m)	
	silty SAND	1		SM	silty, fine to medium grain SAND, darker & more heterogeneous near surface, lighter coloured past 0.9m. Some pebbles. 0-0.9m				
	SAND	2		SP	coarse light brown SAND with small pebbles throughout. 0.9-2.3m				
	SAND & GRAVEL	3		SP	very heterogeneous SAND and GRAVEL three alternating sequences of sand → pebbles → gravel with depth. Gravel typically angular, trace fines 2.3-6.9m				
	SAND & GRAVEL	4		SP					
	SAND & GRAVEL	5		SP					
	SAND & GRAVEL	6		SP					
	sandy GRAVEL	7		GP	heterogeneous GRAVEL, more rounded than above. some coarse SAND, gravel mostly > 2 cm, few small pebbles, VERY coarse 6.9-7.5m				
			8			END OF BOREHOLE			
			9						
			10						
NOTES: MISSING CORE 1.2-1.5m 2.6-3.0m 3.7-4.5m 6.9-7.5m Well screen set in sloughed material and backfilled with bentonite. Installation of PVC piezometer using Enviro-Core drill w continuous coring Aug. 19, 2009									

Figure B-6. Borehole log for PU124.

BOREHOLE LOG				PROJECT		SHEET NO. 1 OF 1	HOLE NO.	
SITE LOCATION			COORDINATES		LOGGED BY	CHECKED BY		
DATE START	FINISH	DRILLER		DRILL EQUIPMENT	BORING DIA.	TOTAL DEPTH	PIPE TOP ELEV.	
MONITOR WELL INSTALLED		SCREEN INTERVAL		WEATHER CONDITIONS		SAMPLE TYPE (S)		
PIEZO & WELL DIAGRAM (S)	MAIN COMPONENT SUMMARY	DEPTH (m)	GRAPHIC LOG	U.S.C.S.	DESCRIPTION AND CLASSIFICATION Colour, size range, MAIN COMPONENT, minor component (s), moisture content, structure, angularity, odour, and geologic unit (if known).		LAB SAMPLE	
							FIELD ID	DEPTH RANGE (m)
	silty SAND	0	[Diagonal hatching]	SM	dark and reddish medium silty SAND with organics (topsoil)	0-0.7m		
		1						
	SAND	2	[Dotted pattern]	SP	uniform and homogeneous medium grained SAND, loosely packed with few pebbles and few fines. Mostly light brown in colour, sometimes reddish	0.7-3.6m		
		3						
		4						
	sandy GRAVEL	5	[Large circles]	GP	medium to large sandy GRAVEL. Heterogeneous throughout, with predominant size increasing with depth, largest below 7.0m before missing core	3.6-7.5m		
		6						
		7						
		8						
			9			END of BOREHOLE		
		10						

NOTES: MISSING CORE; 0.4-1.5m
2.5-3.0m
5.4-6.0m
7.2-7.5m

AUG. 19, 2009

Figure B-7. Borehole log for PU125.

APPENDIX C

Zorra Site Geochemistry

July 2008 – November 2009

Table C-1. Geochemistry of existing wells, July 1, 2008.

Well	Depth m	Cl ⁻ mg/L	Al ³⁺ mg/L	Ca ²⁺ mg/L	Fe ²⁺ mg/L	K ⁺ mg/L	Mg ²⁺ mg/L	Na ⁺ mg/L	NO ₃ ⁻ -N mg/L	NH ₄ ⁺ - N mg/L	EC μS/cm
PU80	1.2	40	<0.01	93.1	0.0	9.3		23.6	0.4	0.2	666
PU80	1.7	41	<0.015	84.3	0.0	13.2	27.5	25.5	1.7	0.0	689
PU80	2.2	41	<0.011	90.1	0.0	13.4	25.7	23.8	2.5	0.0	683
PU80	2.7	14	<0.01	100	0.0	7.8	24.5	11.6	14.4	0.5	813
PU80	3.2	15	<0.005	60.4	0.0	3.8	35.8	6.7	18.6	0.0	871
PU81	1.2	721	<0.01	79.6	0.0	56.0		18.9	1.6	0.3	721
PU81	1.6	699	<0.011	93.7	0.0	35.5	22.1	18.1	2.1	0.1	699
PU81	2	720	<0.01	93.9	0.0	52.7	23.9	15.3	1.4	0.0	720
PU81	2.4	918	<0.006	68.8	0.0	81.6	25.5	8.1	9.4	1.1	918
PU81	2.8	1000	<0.007	97.6	0.0	79.1	23.9	24.8	24.8	0.6	1003
PU81	3.2	1100	<0.008	128	0.0	56.4	29.8	35.1	12.7	0.5	1097
PU83	1.9		<0.013	183	0.0	321	46.6	94.2	0.0	2.3	2490
PU83	2.3		<0.007	141	0.0	168	42.4	75.5	0.8	1.0	1980
PU83	2.7		<0.015	200	0.0	50.6	48.9	46.8	31.8	0.3	1594
PU83	3.1		<0.02	164	0.0	16.3	44.8	31.4	26.7	0.0	1127
PU84	1.5	12	<0.006	123	0.0	26.3	26.3	7.5	26.4	0.8	877
PU84	1.9	49	<0.008	124	0.0	47.7	33.1	26.9	14.3	0.5	1020
PU84	2.3		<0.005	123	0.0	124	32.6	37.2	9.5	0.9	1245
PU84	2.7		<0.008	83.1	0.0	195	26.6	40.1	0.0	0.1	1357
PU84	3.1		<0.009	122	0.0	205	30.5	48.8	37.3	0.3	1539
PU85	1.5		<0.111	81.5	11.4	167	13.3	28.4	88.0	52.8	1270
PU85	1.9		<0.057	123	8.1	112	38.1	31.7	23.5	12.0	1341
PU85	2.3	57	<0.005	95.3	1.1	67.0	32.5	23.9	0.0	2.2	1064
PU85	2.7	57	<0.012	126	0.0	46.8	34.4	26.4	1.2	0.0	1037
PU85	3.1	55	<0.008	122	0.3	40.7	32.8	26.8	3.2	0.2	971
PU86	1.9	6	<0.009	83.3	0.0	8.6	20.5	5.9	8.0	0.0	549
PU86	2.3	10	<0.009	78.7	0.0	4.1	20.9	6.1	10.9	0.0	585
PU86	3.1	15	<0.015	99.8	0.0		19.4	9.3	9.1	0.0	625
PU87	1.5	51	<0.007	98.4	0.0	18.2	39.8	26.9	4.1	9.1	626
PU87	1.9	51	<0.006	97.6	<0.003	18.2	39.6	26.3	4.2	11.7	601
PU87	2.3	54	<0.007	98.4	0.0	19.0	35.1	27.0	5.4	3.4	548
PU87	2.7	75	<0.009	110	0.0	66.5	33.8	35.9	2.5	0.1	554
PU87	3.1	69	<0.013	118	0.0	67.8	33.0	36.4	1.8	0.4	580

Table C-2. Geochemistry of enhanced monitoring network, August 28, 2008.

Well	Depth m	Cl ⁻ (mg/L)	Al ³⁺ (mg/L)	Ca ²⁺ (mg/L)	Fe ²⁺ (mg/L)	K ⁺ (mg/L)	Mg ²⁺ (mg/L)	Na ⁺ (mg/L)	NO ₃ ⁻ -N (mg/L)	NH ₄ ⁺ -N (mg/L)	EC μS/cm
PU83	1.9	154	<0.158	128	2.1	533	42.6	103	18.9	12.6	1570
PU83	2.3	189	<0.158	195	0.4	397	48.9	107	36.0	7.1	1740
PU83	2.7	115	<0.008	188	0.0	137	47.1	62.2	31.0	0.7	1100
PU83	3.1	64	<0.008	132	0.0	35.5	40.6	33.9	22.0	0.1	700
PU84	1.5	43.9	<0.005	129	0.0	28.6	25.0	6.3	0.1	0.0	1499
PU84	1.9	45.9	<0.005	113	0.0	66.3	32.6	27.1	< 0.1	1.0	1679
PU84	2.3	49.6	<0.005	106	0.0	172	29.1	36.6	0.8	1.7	2280
PU84	2.7	52.4	<0.006	99.0	0.0	245	27.0	45.3	1.8	1.0	2630
PU84	3.1	50.1	<0.005	127	0.0	158	36.0	46.8	0.8	0.0	2530
PU85	1.5	44	<0.005	79.8	1.0	162	19.8	28.2	0.1	34.1	2450
PU85	1.9	46	<0.05	96.8	5.6	101	26.5	25.6	<0.1	19.0	2010
PU85	2.3	50	<0.005	117	3.9	56.1	32.3	25.2	0.8	1.2	1745
PU85	2.7	52	<0.005	114	0.0	46.0	31.8	25.2	1.8	0.0	1658
PU85	3.1	50	<0.006	116	0.1	44.2	32.0	25.9	0.8	0.0	1608
PU86	2.3	4.6							10.3		
PU86	3.1	4.9							8.4		
PU89	1.4	228									
PU89	1.8	228	<0.012	86.5	4.2	165	22.7	36.8	0.1	21.0	1190
PU89	2.2	222	<0.011	91.4	15.3	197	17.0	39.4	0.3	24.0	1280
PU89	2.6	112	<0.023	90.3	16.6	362	14.2	67.7	0.1	25.0	1770
PU89	3		<0.135	104	15.4	352	19.9	68.6	0.0	28.0	1920
PU90	1.4	81	<0.013	122	1.1	264	35.2	59.3	6.2	10.5	1690
PU90	1.8	48	<0.018	129	0.0	48.9	35.8	29.8	9.2	0.2	960
PU90	2.2	44	<0.09	1229	0.3	418	333	241	9.8	0.0	980
PU90	2.6	45	<0.11	1236	0.1	457	349	262	9.5		940
PU90	3	44	<0.008	121	0.0	36.8	34.6	25.7	7.6	0.2	900
PU91	1.4	128	<0.206	152	4.7	597	48.0	115	16.0	0.7	2630
PU91	1.8	100	<0.011	134	0.7	166	37.8	45.0	16.0	<0.02	720
PU91	2.4	43	<0.007	121	0.1	137	34.2	24.2	10.0	0.0	510
PU91	2.6	40	<0.012	123	0.0	31.5	34.4	23.0	9.3		470
PU91	3	41	<0.006	113	0.6	28.4	32.8	21.0	9.4	0.4	460
PU92	1.4	153	<0.108	97.6	1.7	507	29.9	74.5	51.2	0.7	1650
PU92	1.8	150	<0.176	96.5	1.2	389	25.3	69.0	28.0	2.5	1335
PU92	2.2	43.1	<0.009	137	0.1	47.6	39.0	28.9	7.5	0.1	670
PU92	2.6	30.5	<0.01	119	0.0	29.3	34.1	19.0	8.8	0.1	565
PU92	3	31.6	<0.008	117	0.0	19.0	32.0	16.5	11.8		530
PU93	2.2	25.8	<0.01	140	0.0	33.5	40.0	17.5	45.0		830
PU93	2.6	27.5	<0.008	162	0.0	36.6	44.3	18.4	42.0		710
PU93	3	29.8	<0.008	189	0.0		45.0	18.5	55.0		780
PU94	2.2	174	<0.008	234	0.0	210	68.9	106	112		1690
PU94	2.6	263	<0.007	290	0.0	105	89.5	126	142		1670

Table C-2. con't

Well	Depth m	Cl ⁻ (mg/L)	Al ³⁺ (mg/L)	Ca ²⁺ (mg/L)	Fe ²⁺ (mg/L)	K ⁺ (mg/L)	Mg ²⁺ (mg/L)	Na ⁺ (mg/L)	NO ₃ ⁻ -N (mg/L)	NH ₄ ⁺ -N (mg/L)	EC μS/cm
PU95	1.8	6.3	<0.007	90.3	0.0	41.8	35.6	9.2	32.0		480
PU95	2.2	15.5	<0.075	1028	0.2	501	402	105	49.0		555
PU95	2.6	35	<0.008	126	0.0	66.6	47.4	14.9	44.0		670
PU95	3	37	<0.011	139	0.0	63.4	50.9	17.0	43.0		710
PU96	1.4	14.3	<0.005	96.3	0.0	18.0	22.8	13.0	0.8		1257
PU96	1.8	44	<0.009	119	0.0	46.2	40.1	20.9	1.4		1736
PU96	2.2	48	<0.008	90.2	0.0	136	33.8	29.8	2.9		2050
PU96	2.6	46	<0.006	86.5	0.0	166	29.5	24.1	7.1		2130
PU96	3	41	<0.005	94.9	0.1	157	28.2	24.5	13.7		2070
PU97	1.8	58	<0.011	79.6	0.4	143	35.7	44.0	<0.1	17.7	2250
PU97	2.2	55	<0.064	47.3	0.4	226	13.2	28.1	0.0	18.6	2200
PU97	2.6	54	<0.054	41.3	0.3	227	11.7	27.7	0.0	21.2	2090
PU97	3	54	<0.068	60.8	0.3	251	159	26.4	0.0	7.6	2180
PU98	1.8	52	<0.057	144	0.0	22.2	40.3	28.6	1.1		750
PU98	2.2	59	<0.059	147	<0.002	23.6	40.2	29.5	3.1		737
PU98	2.6	56	<0.005	120	<0.002	25.2	35.5	28.6	3.5		726
PU98	3	59	<0.005	119	<0.002	23.7	35.2	28.8	4.6		683
PU100	2.2	700	<1.016	133	44.5	1314	55.6	302	3.0	267	5380
PU100	2.6	830	3.6	280	120	1194	49.7	278	6.2	260	4620
PU100	3	775	<1.025	234	128	1271	38.4	256	6.8	336	4620
PU101	2.2	692	<1.31	206	13.3	921	184	246	35.0	87.0	4180
PU101	3		<0.007	176	0.0	229	55.4	88.2			1558

Table C-3. Geochemistry of proposed centre line wells, October 31, 2008

Well	Depth m	Cl ⁻ mg/L	SO ₄ ²⁻ -S mg/L	PO ₄ ³⁻ -P mg/L	F ⁻ mg/L	Al ³⁺ mg/L	Ca ²⁺ mg/L	Fe ²⁺ mg/L	K ⁺ mg/L	Mg ²⁺ mg/L	Na ⁺ mg/L	NO ₃ ⁻ -N mg/L	NH ₄ ⁺ -N mg/L	EC μS/cm
PU81	1.2	1246												1250
PU81	1.6	1574												1570
PU81	2	1260		22.8										1260
PU81	2.4	965		220										960
PU81	2.8	991		1340										990
PU81	3.2	403												400
PU94	2.6	255	144									183	0.3	5020
PU94	3	264	147									180	0.3	5090
PU97	1.8	60	13.700	0.100								0.1	21.5	1690
PU97	2.2	61	12.500	0.000	0.000							0.1	9.4	1650
PU97	2.6	61	11.400	0.100	0.100							0.1		1750
PU97	3	62	6.800	0.300	0.100							0.2	21.2	1970
PU103	2	37.1	89.0	0.03	0.004	<0.05	84.6	2.4	330	22.8	60.7	40.0	173	3470
PU103	3.1	70.2	15.7	0.26	0.003	<0.05	122	2.0	54.5	35.6	35.0	3.2	2.5	1520
PU103	4.1	72.9	17.3		0.006	<0.05	129	0.0	42.4	36.9	34.4	5.9	1.3	1510
PU103	5.1	74.2	15.4		0.004	<0.05	127	0.0	42.1	36.2	34.5	4.0	1.5	1490
PU103	6	78.5	12.1		0.004	<0.05	120	0.0	44.2	34.5	33.0	2.6	3.4	1390
PU103	7.5	92.7	9.7		0.004	<0.05	127	0.1	75.6	36.0	41.4	0.2	8.3	1700
PU103	9	108	10.7	0.002	0.1	<0.05	116	1.2	91.0	39.8	59.9	0.3	12.3	1750
PU105	2.8	20.7	32.8			<0.05	138	0.0	146	45.1	20.9	18.6	40.6	
PU105	3.2	80.6	22.6			<0.05	145	0.1	50.5	47.9	43.4	7.2	12.2	
PU106	3	129	36.3	0.7	0.187	<0.05	173	0.1	40.4	48.8	49.2	4.6	1.6	1950
PU106	4	69.9	16.1	0.3	0.005	<0.05	131	0.2	36.8	36.4	34.2	1.6	1.4	1400
PU106	5	65.7	10.9			<0.05	111	0.0	33.2	32.8	28.0	2.6	1.5	1340
PU106	6	70.4	11.2	0.3	0.007	<0.05	114	<0.002	32.7	32.7	28.7	2.5	1.6	1360
PU106	7.5	69.9	10.7		0.007	<0.05	115	0.0	29.2	34.5	30.6	2.3	1.3	1370
PU106	9	76.9	10.7	0.1	0.004	<0.05	121	0.1	38.7	34.1	30.0	3.1	2.7	1440
PU107	1.9	35.8	18.4	0.4	0.003	<0.05	116	1.5	120	51.6	42.1	0.0	24.4	
PU107	2.3	128	63.7	0.9	0.1	<0.05	109	0.3	175	36.1	69.5	0.2	71.4	
PU107	2.7			0	0.1	<0.05	120	3.3	268	47.8	87.5			
PU107	3	206	106			<0.05	143	3.4	285	47.1	102	0.4	87.6	
PU108	2.2	12.0	19.4			<0.05	123	<0.002	50.7	21.2	10.4	2.5	0.1	

Table C.3. con't

Well	Depth m	Cl⁻ mg/L	SO₄²⁻-S mg/L	PO₄³⁻-P mg/L	F⁻ mg/L	Al³⁺ mg/L	Ca²⁺ mg/L	Fe²⁺ mg/L	K⁺ mg/L	Mg²⁺ mg/L	Na⁺ mg/L	NO₃⁻-N mg/L	NH₄⁺-N mg/L	EC μS/cm
PU108	2.6	12.5	21.7			<0.05	133	0.0	53.9	21.5	10.7	3.0	0.1	
PU109	1.8	54.5	22.2	0.3		<0.05	129	0.1	62.3	37.2	33.9	1.1	1.2	1590
PU109	2.2	54.4	18.8		0.004	<0.05	129	0.0	46.0	38.0	29.3	2.5	0.7	1580
PU109	2.6	56.3	19.7		0.0001	<0.05	127	0.0	59.3	36.8	29.4	2.8	0.8	1600
PU109	3	60.4	15.4	0.3	0.004	<0.05	129	<0.002	38.5	35.5	29.2	3.8	0.1	1490

Table C-4. Geochemistry of full monitoring network, July 15, 2009

Well	Depth m	Cl ⁻ mg/L	DOC mg/L	Al ³⁺ mg/L	Ca ²⁺ mg/L	Fe ²⁺ mg/L	K ⁺ mg/L	Mg ²⁺ mg/L	Na ⁺ mg/L	NO ₃ ⁻ -N mg/L	NO ₂ ⁻ -N mg/L	NH ₄ ⁺ -N mg/L	N ₂ O-N μg/L	EC μS/cm
PU80	1.2	21.3		<0.005	115	0.1	18.8	32.2	11.9	12.8	0.3	0.2		
PU80	1.7	30.5		<0.005	142	0.2	16.7	40.3	11.2	21.0		0.3		
PU80	2.2	22.6		<0.005	129	<0.002	11.6	35.2	11.4	20.0		0.2		
PU80	2.7	29.7		<0.005	124	0.1	15.5	33.2	12.0	19.5		0.1		
PU80	3.2	29.6		<0.005	123	0.2	15.9	33.5	12.1	19.8		0.0		
PU81	1.6	64.5	37.6	<0.005	117	0.0	54.8	35.9	25.0	1.8		0.0	1.0	
PU81	2			<0.005	126	0.1	89.2	38.0	44.8	<0.007		0.0	0.2	
PU81	2.4			<0.005	86.8	0.0	142	26.1	32.1	4.4		0.9	1.9	
PU81	2.8	86.2	33.2	<0.005	89.3	0.0	156	25.3	18.2	6.3		4.3	0.9	
PU81	3.2	54.6		<0.005	112	0.0	63.9	30.9	14.4	13.5		0.1	2.2	
PU83	1.9		221	<0.005	82.1	9.9	477	42.1	99.2	0.4		47.2	0.8	
PU83	2.3		201	<0.005	75.8	7.3	418	36.5	100	0.4		58.1	0.4	
PU83	2.7			<0.005	130	6.4	302	44.5	89.9	3.5		34.7	16.2	
PU83	3.1	61.0	35.0	<0.005	116	1.8	80.0	31.1	33.1	8.1		5.9	0.9	
PU84	1.9	67.9	40.4	<0.005	99.7	0.0	107	29.3	29.2	0.0		6.9	0.0	1112
PU84	2.3	131		<0.005	93.3	0.1	228	26.1	52.3	0.2		16.8	0.1	1561
PU84	2.7		73.9	<0.005	147	0.0	207	40.8	49.7	0.0		1.8	0.2	1509
PU84	3.1			<0.005	127	0.1	118	37.8	39.3	0.2		0.1	0.1	
PU85	3.1	40.5		<0.005	95.8	1.4	38.2	26.3	22.5	4.1	0.4	1.3	25.0	
PU86	2.3	3.9		<0.005	77.2	0.1	1.4	16.7	1.9	11.9		0.0	1.8	
PU86	3.1	3.6		<0.005	76.6	0.1	1.3	14.2	2.3	9.1		0.0	1.3	
PU90	1.4			<0.005	75.9	9.2	248	27.0	52.6	0.3		33.3	5.3	1880
PU90	1.8		24.9	<0.005	54.4	3.3	136	21.6	25.7	0.4		22.5	3.9	1140
PU90	2.2	45.2		<0.005	95.5	0.0	44.9	26.5	21.2	4.8	1.0	2.7	22.3	
PU90	2.6	46.5		<0.005	92.3	0.0	50.4	27.2	21.5	6.8		0.3	0.3	820
PU90	3	42.3		<0.005	68.1	2.2	104	25.8	24.1	0.5	0.4	18.2	13.0	1150
PU91	1.4			<0.005	84.5	5.9	492	31.2	75.6	0.4		20.9	0.1	2980
PU91	1.8			<0.005	77.7	1.1	463	36.1	66.3	0.3		23.7	0.1	2750
PU91	2.4		52.5	<0.005	94.5	0.2	136	26.9	27.0	2.7		0.0	11.1	1180
PU91	2.6	32.9		<0.005	98.9	0.0	31.4	27.1	15.4	7.9	0.9	0.1	25.7	870

Table C-4. Con't

Well	Depth m	Cl ⁻ mg/L	DOC mg/L	Al ³⁺ mg/L	Ca ²⁺ mg/L	Fe ²⁺ mg/L	K ⁺ mg/L	Mg ²⁺ mg/L	Na ⁺ mg/L	NO ₃ ⁻ -N mg/L	NO ₂ ⁻ -N mg/L	NH ₄ ⁺ -N mg/L	N ₂ O-N μg/L	EC μS/cm
PU91	3	32.5		<0.005	99.6	0.0	28.8	26.8	15.4	8.2		0.0	36.6	860
PU92	1.4			<0.05	8.3	1.0	55.7	4.1	8.1	0.5	0.5	85.9	1.8	2970
PU92	1.8		305	<0.05	8.7	1.7	43.6	3.0	6.3	0.5		57.1	0.8	2340
PU92	2.2		335	<0.05	9.2	1.0	33.8	2.7	5.7	0.7		26.8	0.6	2030
PU92	2.6			<0.05	10.6	0.5	18.2	2.8	4.6	0.6		10.9	0.2	1240
PU92	3		49.1	<0.05	11.5	0.1	6.8	3.1	2.2	3.4		1.5	44.3	900
PU93	1.8	7.2		<0.005	129	0.1	24.2	19.2	4.5	9.7		0.0		871
PU93	2.2	9.4		1.2	104	1.2	35.0	26.1	10.7	18.0		1.6	0.8	868
PU93	2.6	126	85.7	<0.005	148	0.2	94.8	39.7	55.6	0.8		11.6	0.0	1752
PU93	3	81.1	25.2	<0.005	128	3.3	321	34.1	76.3	0.4		53.9	0.0	2370
PU94	1.8		69	0.1	71.7	5.4	237	18.1	28.4	0.8			9.5	1450
PU94	2.2		101	<0.005	95.9	3.6	284	29.7	68.7	0.4			0.5	2200
PU94	2.6			<0.005	119	1.5	233	41.9	80.4	1.2		42.2	3.9	2050
PU94	3	199	38.2	<0.005	119	5.2	235	47.8	83.3	0.7		2.1	3.0	2270
PU95	1.8			<0.05	12.9	4.4	90.0	3.8	18.7	3.4		85.1	70.8	4900
PU95	2.2		1841	<0.05	14.1	4.0	89.5	3.5	18.5	3.6		108	84.7	4840
PU95	2.6		1387	<0.05	14.8	4.8	70.4	2.6	16.4	3.1		106	3.0	3840
PU96	1.4	10.6		<0.005	95.8	1.4	10.0	19.6	9.8	1.0		1.0	4.0	
PU96	1.8	27.6		<0.005	104	0.4	26.2	31.5	15.4	6.0		0.0	36.7	
PU96	2.2			<0.002	144	0.3	64.7	49.0	50.6	0.2		0.4	0.2	
PU96	2.6		144	1.5	141	2.5	202	48.6	63.6	0.0		21.5	0.1	
PU96	3			0.7	99.6	2.0	234	34.0	58.0	0.1		21.8	1.1	
PU103	2		292	<0.005	109	29.9	327	22.0	66.9	0.7		37.0	5.0	1980
PU103	3.1	39.1		<0.005	101	0.0	38.1	29.2	21.0	3.5	0.7	0.0	42.6	870
PU103	4.1	41.9		<0.005	98.3	0.1	35.3	29.1	20.0	5.7		0.5	0.2	830
PU103	5.1	34.5		<0.005	98.1	0.0	33.0	29.1	19.2	4.7		0.6	0.2	820
PU103	6	36.0		<0.005	98.5	0.1	33.0	28.9	18.9	5.6		0.7	0.4	820
PU103	7.5			<0.005	87.6	0.1	55.1	29.5	22.6	2.5		2.2	0.2	890
PU103	9			<0.005	85.8	0.8	72.2	29.4	25.4	2.1		2.7	1.7	950
PU105	2.8		88.0	<0.005	104	0.3	164	35.8	39.1	0.5		15.8	0.03	
PU105	3.2			<0.005	118	0.6	265	43.2	75.6	1.8		8.3		

Table C-4. con;t

Well	Depth m	Cl ⁻ mg/L	DOC mg/L	Al ³⁺ mg/L	Ca ²⁺ mg/L	Fe ²⁺ mg/L	K ⁺ mg/L	Mg ²⁺ mg/L	Na ⁺ mg/L	NO ₃ ⁻ -N mg/L	NO ₂ ⁻ -N mg/L	NH ₄ ⁺ -N mg/L	N ₂ O-N μg/L	EC μS/cm
PU106	3			<0.005	114	1.1	177	45.7	65.8	2.1		22.3	0.7	
PU106	4	47.0		<0.005	91.8	0.2	52.9	31.0	24.5	2.0		2.6	0.2	
PU106	5	38.0		<0.005	87.7	0.1	47.5	28.9	21.8	2.7		2.7	0.2	
PU106	6	47.9		<0.005	77.7	0.1	49.4	29.4	21.8	4.0		3.9	0.2	
PU106	7.5	39.8		<0.005	83.7	0.1	30.4	28.6	17.8	5.3		0.7	0.5	
PU108	2.2		238	<0.005	124	16.3	382	34.5	110	0.5		51.5	0.9	3030
PU108	2.6		316	<0.005	91.2	15.5	394	34.0	115	0.6		55.5	1.3	3200
PU109	1.8	55.3		<0.005	79.1	0.0	47.0	36.5	25.5	4.0		0.3		
PU109	2.2	66.6		<0.005	102	0.0	42.1	33.7	25.8	6.2		0.0		
PU109	2.6	56.6		<0.005	117	0.0	42.2	35.5	25.8	6.7		0.0		
PU109	3	57.6		<0.005	74.4	0.2	44.0	34.1	27.2	8.8		0.2		
PU113	2.2		210	<0.005	106	0.3	723	46.3	175	19.2		3.6	29.9	4190
PU113	2.6		203	<0.005	102	1.5	645	37.7	145	7.1		8.0	0.4	3670
PU113	3		204	<0.005	94.8	1.6	640	34.8	138	6.6		8.3	0.5	3670
PU114	2.6												11.3	1431
PU114	3	8.9		<0.005	144	0.2	74.3	49.8	9.1	19.9	0.1	1.2	12.0	1548
PU115	1.8		144	<0.005	54.1	3.4	315	23.1	56.0	7.9		53.8	7.0	2200
PU115	2.2		321	<0.005	68.8	15.6	474	37.8	82.7	0.7		65.1	0.7	1951
PU115	2.6			<0.005	50.8	2.1	310	21.8	44.8	0.3		31.9	0.2	2410
PU115	3		156	<0.005	65.7	2.6	303	23.6	50.4	0.4		29.7	0.2	1545
PU116	1.8		201	<0.005	80.6	7.4	451	31.6	85.4	0.3		85.3	0.8	2830
PU116	2.2		144							4.0		10.4	0.3	1649
PU116	2.6		50.2	<0.005	79.5	0.2	124	27.4	24.5	5.3		0.0	36.1	1142
PU116	3	30.0	126	<0.005	99.8	0.1	45.4	28.7	16.7	6.1	0.6	0.6	215	1084
PU117	1.8		84.3	<0.005	193	0.0	210	50.1	80.5	154		50.2	495	2690
PU117	2.2	48.3	31.4	<0.005	50.4	1.5	209	18.0	27.9	0.5		16.1	2.1	1641
PU117	2.6		36.7	<0.005	101	0.1	118	28.1	30.2	4.2		3.8	304	901
PU117	3			<0.005	98.3	0.1	62.6	30.8	27.2	3.2		0.9	330	899
PU118	1.4	81.3	31.3	<0.005	127	0.5	46.5	41.6	37.8	0.0		0.1	0.3	981
PU118	1.8	68.0	31.8	<0.005	108	0.6	46.3	38.2	31.1	0.0		0.1	2.8	1172
PU118	2.2	49.3		<0.005	107	0.1	42.4	34.5	26.3	1.0	0.7	0.0	395	994

Table C-4. Con't

Well	Depth m	Cl ⁻ mg/L	DOC mg/L	Al ³⁺ mg/L	Ca ²⁺ mg/L	Fe ²⁺ mg/L	K ⁺ mg/L	Mg ²⁺ mg/L	Na ⁺ mg/L	NO ₃ ⁻ -N mg/L	NO ₂ ⁻ -N mg/L	NH ₄ ⁺ -N mg/L	N ₂ O-N μg/L	EC μS/cm
PU118	2.6	65.2		<0.005	101	0.0	43.5	37.0	27.6	7.1	1.5	0.0	421	1002
PU118	3	74.6		<0.005	130	0.1	43.4	38.5	26.6	13.3	1.2	0.0	307	1087
PU119	2.2	44.4	43.9	<0.005	49.3	1.7	124	45.3	16.9	6.1	0.7	5.5	1.7	
PU119	2.6	56.1		<0.005	124	0.0	112	43.0	31.3	28.2	1.2	3.6	5.3	
PU119	3		41.3	<0.005	112	1.5	150	54.6	52.1	0.3		18.5	0.1	
PU120	2.2		183	<0.005	96.0	4.9	364	31.8	67.9	0.4		43.8	0.2	
PU120	2.6		324	<0.005	70.4	4.0	363	22.7	65.1	0.7		50.4	0.9	
PU120	3		179	<0.005	73.4	2.5	271	21.1	54.0	0.4		44.8	0.3	
PU121	1.8			<0.005	179	0.7	61.6	86.4	20.0	2.4		0.2		
PU121	2.2	53.0		<0.005	122	1.0	123	45.2	23.3	11.0		0.8		
PU121	2.6	47.2		0.1	137	1.4	62.6	46.2	19.8	14.2	0.5	0.2		
PU121	3	48.0		<0.005	127	0.5	23.9	41.0	20.7	16.3		0.0		
PU122	3			<0.005	406	35.9	435	120	169	0.4		30.8	17.7	
PU122	4.5		127	<0.005	374	6.9	279	117	132	0.3		29.8	0.6	
PU122	6		346	<0.005	297	7.3	452	124	180	0.5		50.0	0.0	
PU122	7.5		169	<0.005	208	1.4	362	88.5	129	4.6		49.7	0.5	
PU122	9		89.3	<0.005	180	0.2	193	66.7	81.3	7.9		25.8	1.4	
PU123	3											1.4		
PU123	4.5	45.9		4.7	131	4.6	16.0	53.5	13.3	0.0		19.1	3.4	
PU123	6			1.9	126	6.5	141	43.2	36.8	8.4		0.6	3.4	
PU123	7.5	21.7		<0.005	113	<0.002	10.9	30.2	11.3	7.6				

Table C-5. Geochemistry of centreline wells, August 20, 2009.

Well	Depth m	Al ³⁺ mg/L	Ca ²⁺ mg/L	Fe ²⁺ mg/L	K ⁺ mg/L	Mg ²⁺ mg/L	Na ⁺ mg/L	NO ₃ ⁻ -N mg/L	NH ₄ ⁺ -N mg/L	N ₂ O-N µg/L	EC µS/cm
PU86	2.3	<0.05	90.1	<0.002	1.0	18.2	16.2	12.5	0.0	1.9	470
PU86	3.1	<0.05	78.0	<0.002	0.9	14.7	1.7	10.8	0.0	1.6	440
PU92	1.4	<0.05	117	9.0	246	37.3	51.5	2.0	13.9		1360
PU92	1.8	<0.05	52.8	13.7	348	16.7	49.8	5.0	49.4	9.9	1830
PU92	2.2	<0.05	87.0	7.7	399	28.4	67.5	0.4	50.4	1.1	2270
PU92	2.6	<0.05	96.7	6.0	221	27.1	54.1	0.3	27.8	0.2	1560
PU92	3	<0.05	91.9	1.5	122	25.6	30.9	0.2	13.4	0.6	1030
PU95	1.8	<0.05	85.8	30.1	697	31.1	139	2.0	67.1	17.2	3080
PU95	2.2	<0.05	87.8	25.8	735	33.1	148	2.0	64.6	13.1	3270
PU95	2.6	<0.05	134	44.9	685	33.4	157	2.0	99.9	27.7	3540
PU96	1.8	<0.05	126	0.0	47.9	40.6	33.1	2.0	0.0	8.6	1080
PU96	2.2	<0.05	108	0.1	133	34.0	52.6	0.1	15.7	0.0	1500
PU96	2.6	<0.05	82.6	1.0	252	26.8	58.2	0.1	27.3	0.0	1130
PU96	3	<0.05	76.3	0.8	227	22.1	47.1	0.7	22.2	0.2	1580
PU115	1.8	<0.05	111	3.1	395	29.0	75.9	19.0		7.5	2430
PU115	2.2	<0.05	61.5	5.7	302	26.6	49.4	1.0	30.7	0.3	1740
PU115	2.6	<0.05	91.2	1.5	278	26.8	49.9	0.2	28.4	0.2	1600
PU115	3	<0.05	67.2	2.5	282	22.0	58.3	0.3	35.8	0.2	1490
PU121	1.8	<0.05	127	1.0	78.5	37.8	25.3	2.0	0.1	5.6	
PU121	2.2	<0.05	113	0.0	93.7	34.1	36.9	2.0	0.1	0.4	
PU121	2.6	<0.05	119	<0.002	46.1	33.2	16.9	12.0	0.0	22.9	
PU121	3	<0.05	123	<0.002	27.5	34.3	17.0	23.0	0.0	22.9	
PU122	3	<0.05	238	22.2	469	89.7	201	0.1	28.3		4770
PU122	4.5	<0.05	235	40.8	192	73.6	115	0.1	28.5	0.1	3310
PU122	6	<0.05	283	60.9	611	132	218	0.2	74.0	1.1	4400
PU122	7.5	<0.05	202	6.5	390	84.5	132	3.0	52.8	6.1	2950
PU122	9	<0.05	140	0.7	178	49.4	68.5	5.0	26.3	0.6	2030
PU123	4.5	<0.05	126	1.6	23.3	53.4	20.0	0.0		0.2	
PU123	7.5	<0.05	91.9	<0.002	7.7	27.7	10.4	10.0	0.0	10.8	710
PU123	9	<0.05	86.9	<0.002	7.4	25.5	12.9	9.0	0.0	4.6	650
PU124	2.7	<0.05	99.5	11.1	258	35.5	62.3	0.3	34.5	0.5	1640
PU124	3.9	<0.05	86.1	0.1	74.4	26.3	20.3	4.0	3.3	0.2	900
PU124	5.1	<0.05	95.6	0.0	26.9	29.0	14.8	9.0	0.1	18.6	800
PU124	6.3	<0.05	112	0.0	31.6	30.5	18.9	9.0	0.2	1.1	870
PU124	7.5	<0.05	93.1	0.0	33.2	30.8	18.9	10.0	0.1	0.5	830
PU125	2.7	<0.05	122	3.4	294	36.2	64.3	0.3	16.8	0.4	1700
PU125	3.9	<0.05	103	0.2	48.7	30.6	17.5	14.0	1.4	4.7	500
PU125	5.1	<0.05	81.5	<0.002	27.7	28.3	16.4	12.0	0.0	36.5	910
PU125	6.3	<0.05	102	<0.002	32.5	27.1	17.6	9.0	0.0	24.1	
PU125	7.5	<0.05	103	0.0	31.5	28.2	18.3	11.0	0.0	32.4	890

Table C-6. Geochemistry of centreline wells, November 13, 2009.

Well	Depth m	Al ³⁺ mg/L	Ca ²⁺ mg/L	Fe ²⁺ mg/L	K ⁺ mg/L	Mg ²⁺ mg/L	Na ⁺ mg/L	NO ₃ ⁻ -N mg/L	NH ₄ ⁺ -N mg/L	EC μS/cm
PU86	2.3	<0.05	94.5	<0.02	2.1	21.3	4.7	11.6	0.0	
PU86	2.7	<0.05	97.5	<0.02	2.1	20.0	4.4	10.9	0.0	
PU86	3.1	<0.05	111	<0.02	1.9	21.3	4.4	11.5	0.1	
PU92	1.4	<0.05	122	0.4	475	40.4	72.2	43.7	1.3	2340
PU92	1.8	<0.05	87.0	0.8	496	40.8	69.6	36.5	8.1	2100
PU92	2.2	<0.05	72.5	2.9	436	23.7	59.4	1.4		2310
PU92	2.6	<0.05	171	3.7	165	51.2	48.3	0.3	17.4	1010
PU92	3	<0.05	162	0.4	113	45.3	40.1	1.1	12.0	1230
PU95	1.8	<0.05	55.2	5.8	212	22.9	44.0	0.5	27.5	2290
PU95	2.2	0.1	155	17.0	335	48.7	66.7	0.7	26.8	2810
PU95	2.6	<0.05	181	34.8	509	55.8	137	2.9	8.2	2450
PU96	1.4	<0.05	125	0.5	20.9	33.1	23.0	4.4	0.1	760
PU96	1.8	<0.05	190	<0.02	48.0	59.7	52.7	0.5	2.1	1300
PU96	2.2	<0.05	93.6	<0.02	204	32.6	55.0	1.1	39.7	1530
PU96	2.6	<0.05	67.3	1.3	291	23.6	44.0	0.2	33.2	1640
PU96	3	<0.05	81.6	0.9	280	23.3	53.8	0.4	27.7	
PU115	2.2	<0.05	50.7	0.9	373	19.8	57.6	47.0	71.9	2190
PU115	2.6	<0.05	43.8	0.8	434	11.8	60.0	35.4	58.2	2110
PU115	3	<0.05	88.6	0.7	305	35.8	51.6	1.0	47.9	1860
PU121	1.8	<0.05	133	0.1	60.5	43.5	26.8	8.3	0.1	
PU121	2.2	<0.05	112	<0.02	150	37.5	41.3	0.5	12.0	1220
PU121	2.6	<0.05	129	0.0	130	42.2	46.0	0.2	6.9	
PU121	3	<0.05	171	<0.02	31.2	48.5	27.6	2.4	0.1	
PU122	3	<0.05	275	8.5	688	93.3	258	9.8	14.2	
PU122	4.5	<0.05	446	49.3	124	103	108	0.3	35.0	3470
PU122	6	<0.05	368	22.5	775	183	276	0.3	92.0	5470
PU122	7.5	<0.05	187	16.5	553	86.5	164	1.8	101	4600
PU122	9	<0.05	169	2.6	345	69.1	111	1.9	78.4	3570
PU124	2.7	<0.05	109	4.0	133	39.7	41.2	0.2	13.8	1520
PU124	3.9	<0.05	105	1.0	124	33.4	38.6	0.6	11.9	1190
PU124	5.1	<0.05	126	0.0	80.0	38.6	34.0	1.1	4.2	1140
PU124	6.3	<0.05	125	0.0	22.1	38.4	18.3	8.7	0.0	950
PU124	7.5	<0.05	138	0.0	19.0	40.3	19.2	9.3	0.0	
PU125	2.7	<0.05	88.6	1.7	347	25.6	59.2	0.5	40.5	1710
PU125	3.9	<0.05	144	1.7	128	39.0	44.6	2.8	10.0	1240
PU125	5.1	<0.05	134	0.4	32.1	36.4	20.9	10.2		890
PU125	6.3	<0.05	135	<0.02	36.9	38.5	23.7	5.7	0.1	860
PU125	7.5	<0.05	139	0.1	36.9	39.0	22.9	5.7	0.1	

Table C-7. Field measurements of dissolved oxygen (DO), reduction potential (E_h), pH and temperature (°C) October 31, 2008 - October 19, 2009.

Well	Depth (m)	DO (mg/L)		Eh (mV)		pH		Temp. (°C)		
		July 3/09	Aug. 21/09	Oct 31/08	Aug. 21/09	Oct 31/08	Aug. 21/09	Aug. 21/09	Sept. 25/09	Oct. 19/09
PU84	1.1	0.48								
PU84	1.5	0.21								
PU84	1.9	0.18								
PU84	2.3	0.17								
PU84	2.7	0.24								
PU86	2.3	5.63			83		7.50	16.2		
PU86	2.7									
PU86	3.1	7.26			85		7.37	16.7		
PU92	1.4		0.89		-35		6.82	21.4	16.9	12.9
PU92	1.8		0.42		-29		6.96	18.5	15.8	13.5
PU92	2.2		0.78		-40		7.00	17.7	15.4	13.8
PU92	2.6		0.95		-45		7.19	18.1	15	13.8
PU92	3		0.99		-7		7.09	19.5	14.8	13.9
PU94	2.2	1.5		28		6.84				
PU94	2.6	1		50		6.77				
PU94	3	1		93		6.88				
PU95	1.8		0.17		-103		7.06	21.2		
PU95	2.2		0.11		-115		7.10	20.3	16.7	14.6
PU95	2.6		0.08		-118		7.28	19.1	16.7	14.5
PU95	3								16.7	14
PU96	1.4								15.4	12.2
PU96	1.8						6.88		13.8	12.5
PU96	2.2							15.6	13.6	12.6
PU96	2.6		1.78		94		7.24	16.7	13.2	12.5
PU96	3		2		92		7.16	17.4		
PU97	1.4	0.13								
PU97	1.8	0.18		-18		7.28				
PU97	2.2	0.29		-57		7.12				
PU97	2.6	0.75		-50		7.14				
PU97	3	0.2		-66		7.14				
PU103	2			-135		7.24				
PU103	3.1	1.62		-98		7.22				
PU103	4.1	0.17		-41		7.11				
PU103	5.1	0.17		2		7.13				
PU103	6	0.19		-4		7.13				
PU103	7.5	0.21		4		7.13				
PU103	9			-15		7.83				
PU106	3			-3		6.86				
PU106	4			-7		7.06				
PU106	5			-1		7.08				
PU106	6			9		7.10				
PU106	7.5			-90		7.13				
PU106	9			-54		7.09				

Table C-7. con't

Well	Depth (m)	DO (mg/L)		Eh (mV)		pH		Temp. (°C)		
		July 3/09	Aug. 21/09	Oct 31/08	Aug. 21/09	Oct 31/08	Aug. 21/09	Aug. 21/09	Sept. 25/09	Oct. 19/09
PU109	1.8			-21		7.06				
PU109	2.2			4		7.01				
PU109	2.6			11		7.03				
PU109	3			7		7.05				
PU115	1.8	0.43	2.12		38		7.12	17.2		
PU115	2.2		0.69		-72		7.90	16.6	14.8	13.3
PU115	2.6	5.94	0.97		8		7.04	16.1	14	13.5
PU115	3	0.21	0.81		16		7.12	18.5	14	13.5
PU116	1	0.25								
PU116	1.4	7.67								
PU116	1.8	4.3								
PU116	2.2	0.25								
PU116	2.6	2								
PU116	3	0.25								
PU117	1.4									
PU117	1.8	0.14								
PU117	2.2	0.19								
PU117	2.6	0.17								
PU117	3	0.35								
PU118	1.4	0.23								
PU118	1.8									
PU118	2.2	0.2								
PU118	2.6	0.13								
PU118	3	0.16								
PU121	2.2								12.8	11.6
PU122	3		0.96		-60		6.38	16	15.8	
PU122	4.5		1.16		-60		6.38	14.7	14.1	13.4
PU122	6		0.64		18		6.57	13.1	12.8	12.7
PU122	7.5		0.87		95		6.66	12.8	12.3	12.2
PU122	9		0.62		182		6.71	13.4	12.2	12.5
PU123	7.5		1.97		166		7.04	13.3		
PU123	9		1.71		334		6.95	14.5		
PU124	2.7		0.54		-81		7.11	16.3	15.9	14.8
PU124	3.9		1.4		50		7.10	15.1	15.1	14.4
PU124	5.1		1.44		-47		7.02	13.9	14.1	13.7
PU124	6.3		1.79		61		6.91	14.4	13.6	13.1
PU124	7.5		0.95		30		6.87	16.3	13.6	
PU125	2.7		1.87		41		6.94	14.2	13.4	12.5
PU125	3.9		1.77		95		7.49	14.7	12.5	12
PU125	5.1				95		6.92	14.4	12	11.5
PU125	6.3								11.8	11.3
PU125	7.5		1.78		68		6.93	15.6	11.8	

Note: All measurements performed in-situ using field meters and a flow through cell.

Table C-8. Isotope data for: a) $\delta^{15}\text{N-NH}_4^+$ b) $\delta^{15}\text{N-NO}_3^-$ and c) $\delta^{18}\text{O-H}_2\text{O}$, August 28, 2008 - November 15th, 2009

a)

Well	Depth (m)	$^{15}\text{N-NH}_4^+$ (‰)		
		Aug. 28/08	Oct. 31/08	Aug. 20/09
PU83	1.9	35.7		
PU84	1.9	29.6		
PU84	2.3	30.6		
PU84	2.7	37.2		
PU97	1.8		18.4	
PU97	2.2		18.6	
PU97	3		20.9	
PU107	2.3	-	26.1	
PU92	1.4			27.1
PU92	1.8			24.0
PU92	2.2			24.8
PU92	2.6			26.2
PU92	3			30.8
PU95	1.8			37.3
PU95	2.2			39.6
PU95	2.6			36.3
PU96	2.2			26.2
PU96	2.6			25.4
PU96	3			26.8
PU115	2.2			26.1
PU115	2.6			23.5
PU115	3			25.3
PU122	3			21.5
PU122	4.5			17.5
PU122	6			28.4
PU122	7.5			30.1
PU122	9			31.1
PU123	4.5			26.8
PU124	2.7			26
PU124	3.9			31.6
PU125	2.7			29.3
PU125	3.9			31.9

b)

Well	Depth (m)	¹⁵ N-NO ₃ ⁻ (‰) Aug. 20/09
PU121	1.8	35.4
PU121	2.6	31.9
PU123	7.5	20.6
PU124	3.9	40.2
PU124	5.1	29.3
PU124	6.3	30.7
PU124	7.5	29.1
PU125	3.9	30.6
PU125	5.1	27.4
PU125	6.3	29.8
PU125	7.5	29.8

c)

Location	Date	¹⁸ O-H ₂ O (‰)
POND	May 8/09	-4.1
POND	June 15/09	-2.3
POND	Aug. 20/09	-0.9
POND	Sept. 20/09	-1.2
POND	Nov. 13/09	-5.2
PU86-3.1	Aug. 20/09	-13.4
PU86-2.7	Nov. 13/09	-12.6
PU95-2.2	July 14/09	-8.4
PU95-2.2	Aug. 20/09	-6.1
PU95-2.2	Sept. 25/09	-5.3
PU95-2.2	Nov. 13/09	-9.0
PU96-1.4	July 14/09	-12.0
PU96-1.8	Aug. 20/09	-11.7
PU96-2.6	Sept. 25/09	-10.7
PU96-1.8	Nov. 13/09	-10.0

Table C-9. Geochemistry and isotopic data for the manure runoff lagoon, August 2008 - January 2010.

Sample	Date	NH ₄ ⁺ -N mg/L	NO ₃ ⁻ -N mg/L	Cl ⁻ mg/L	EC μS/cm	pH	E _h mV	Al ³⁺ mg/L	Ca ²⁺ mg/L	Fe ²⁺ mg/L	K ⁺ mg/L	Mg ²⁺ mg/L	Na ⁺ mg/L	¹⁵ N-NH ₄ ⁺ ‰
POND1	Aug. 28 2008	58.5	3.5	815				<0.231	74.0	20.6	1309	102	243	45.5
POND2	Sept. 03 2008	53.7	3.8	926	5570									
POND3	Sept. 11 2008	44.0			8620	7.8	25							
POND4	Sept. 23 2008	87.1	2.6	718										
POND5	Oct. 31 2008	150	3.4		7500	7.98	-27	<0.05	71.0	18.9	1343	67.1	336	33.6
POND6	Dec. 01 2008	67.8	1.4	327				<0.05	41.0	8.2	624	36.9	127	29.4
POND7	Mar.03 2009	43.0												
POND8	Mar. 31 2009	236												
POND10	May 11 2009	268			4200									34.7
POND11	June 15 2009	131			5180			<0.005	76.9	19.8	1215	47.8	208	45.2
POND12	July 15 2009	112	2.94					<0.005	62.2	12.6	1213	52.9	214	48.2
POND13	Aug 20 2009	80.1	4		5110	7.66	-23	<0.05	72.1	21.2	1234	67.1	226	53.0
POND14	Sept. 25 2009	79.8	3		3150									47.4
POND16	Nov. 13 2009	32.0	2.83					<0.05	88.9	10.8	970	74.3	182	72.1
POND17	Jan. 07 2010	374												28.2

APPENDIX D

Ammonification Experiments

April - July 2010

Table D-1. Results from ammonification lab batch experiment 2. 2L Pyrex containers were filled 200 mL with core sample (taken from near PU92), and the rest with groundwater from indicated locations. The environment was kept strictly anoxic for 11 days, with periodic sampling as indicated, using helium gas to replace the volume of liquid extracted.

Sample Location	Day	NH ₄ ⁺ -N	NO ₂ ⁻ -N	NO ₃ ⁻ -N	TKN	ON	TN
		mg/L					
PU122 4.5 m	0	155	0.03	0.68	210	54.7	210
	1	155	0.06	0.96	200	45.5	201
	2	154	0	0.97	196	41.8	197
	3	158	0.07	1.95	193	34.7	195
	4	164	0.05	0.94	198	33.9	199
	5	143	0.07	1.84	197	54.4	199
	11	144	0.14	1.21	199	55.2	201
PU95 2.6 m	0	43.4	0.02	0.6	53.5	10.1	54.2
	1	40	0.09	0.98	49.1	9.07	50.1
	2	38.8	0.08	1.86	47.8	9	49.7
	3	37.9	0.11	1.73	47	9.1	48.8
	4	38.1	0.08	0.76	47.21	9.11	48.1
	5	36.7	0.1	0.92	45.63	8.93	46.7
	11	33.2	0.02	0.04	44.83	11.6	44.9
PU92 1.4 m	0	4.65	0.02	0.53	29.02	24.4	29.6
	1	3.99	0.04	1.16	24.87	20.9	26.1
	2	4.51	0.08	2.29	23.99	19.5	26.4
	3	3.8	0.07	2.2	22.73	18.9	25
	4	3.87	0.06	1.16	22.24	18.4	23.5
	5	3.84	0.16	1.13	21.43	17.6	22.7
	11	3.93	0.13	0.97	21.95	18.0	23.1
PU115 2.2 m	0	2.79	0.11	3.17	12.83	10.0	16.1
	1	2.52	0.1	1.71	11.49	8.97	13.3
	2	2.31	0.11	3.5	9.67	7.36	13.3
	3	2.01	0.11	3.46	10.66	8.65	14.2
	4	2.27	0.09	1.64	10.17	7.9	11.9
	5	2.57	0.13	3.4	9.76	7.19	13.3
	11	1.88	0.19	3.59	9.34	7.46	13.1

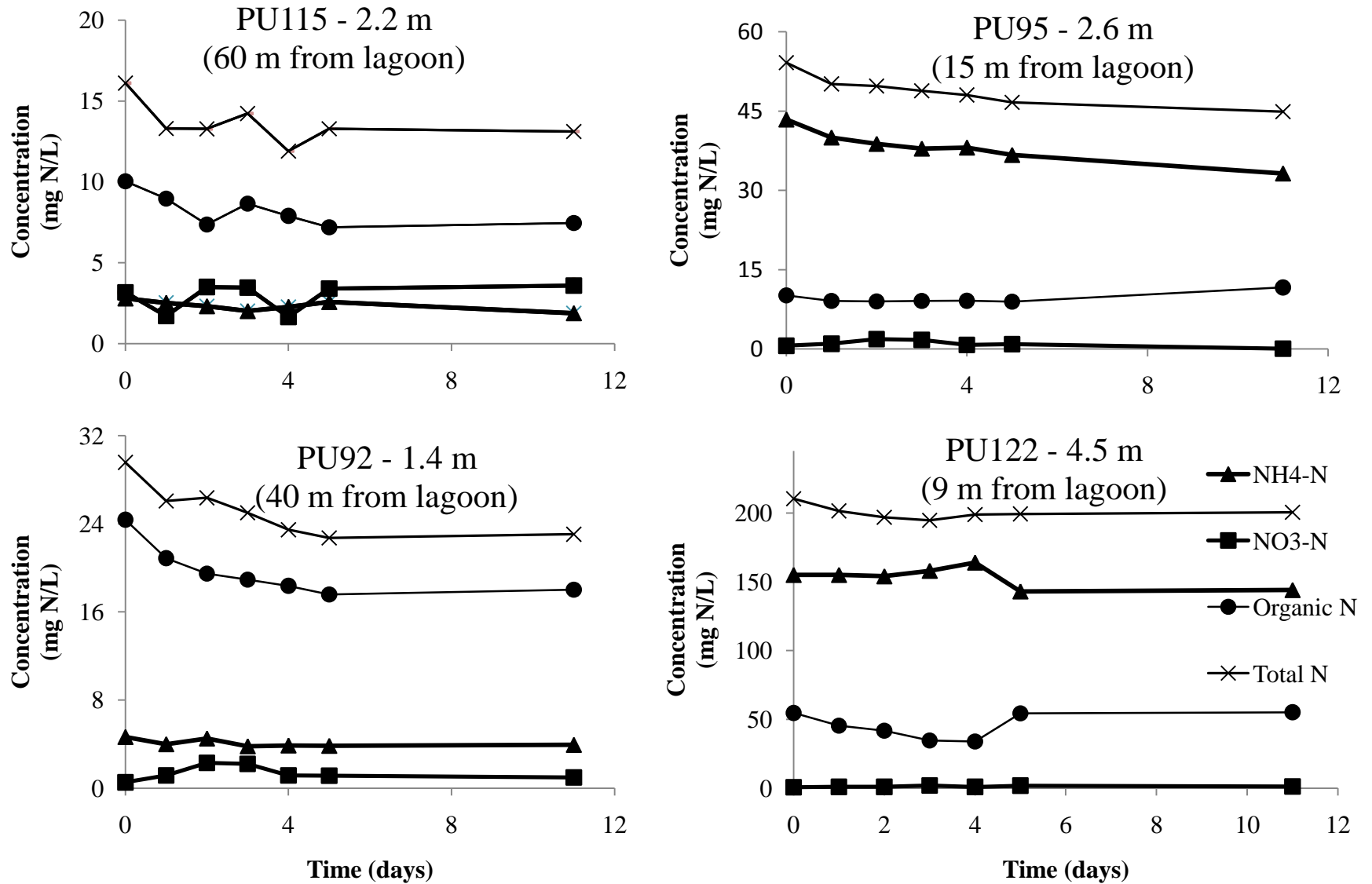


Figure D-1. Temporal trends in nitrogen for lab batch experiment 2, performed in a strictly anoxic environment with a 10:1 mixture of groundwater to sediment, reacting for 11 days.

APPENDIX E

Additional Cross Sections

Na⁺, K⁺, NH₄⁺-N, NO₃⁻-N, EC Distributions October 31, 2008 & July 15, 2009

K⁺, July 15, 2009

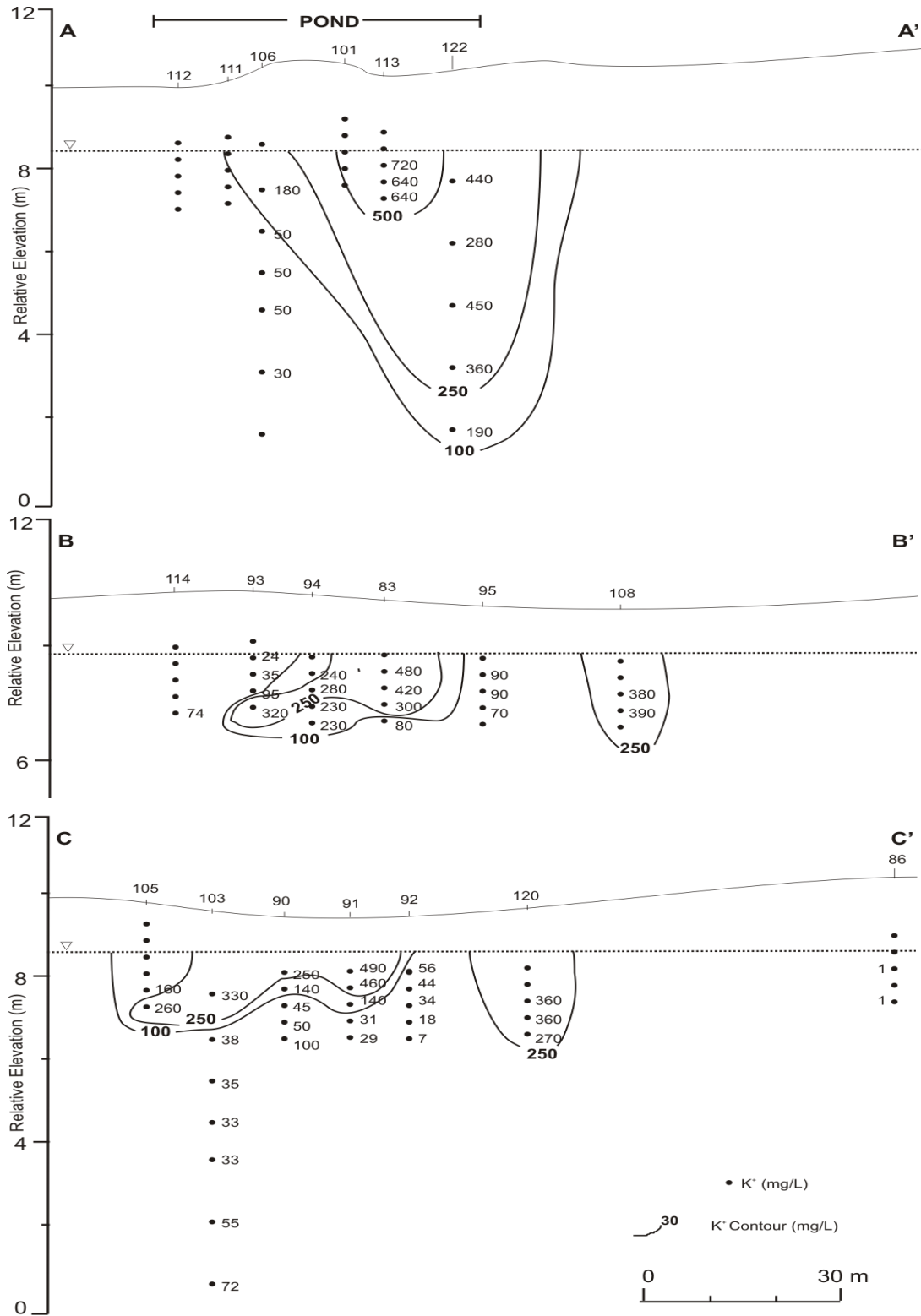


Figure E-1. Distribution of K⁺ along transverse sections A-E, July 15, 2009.

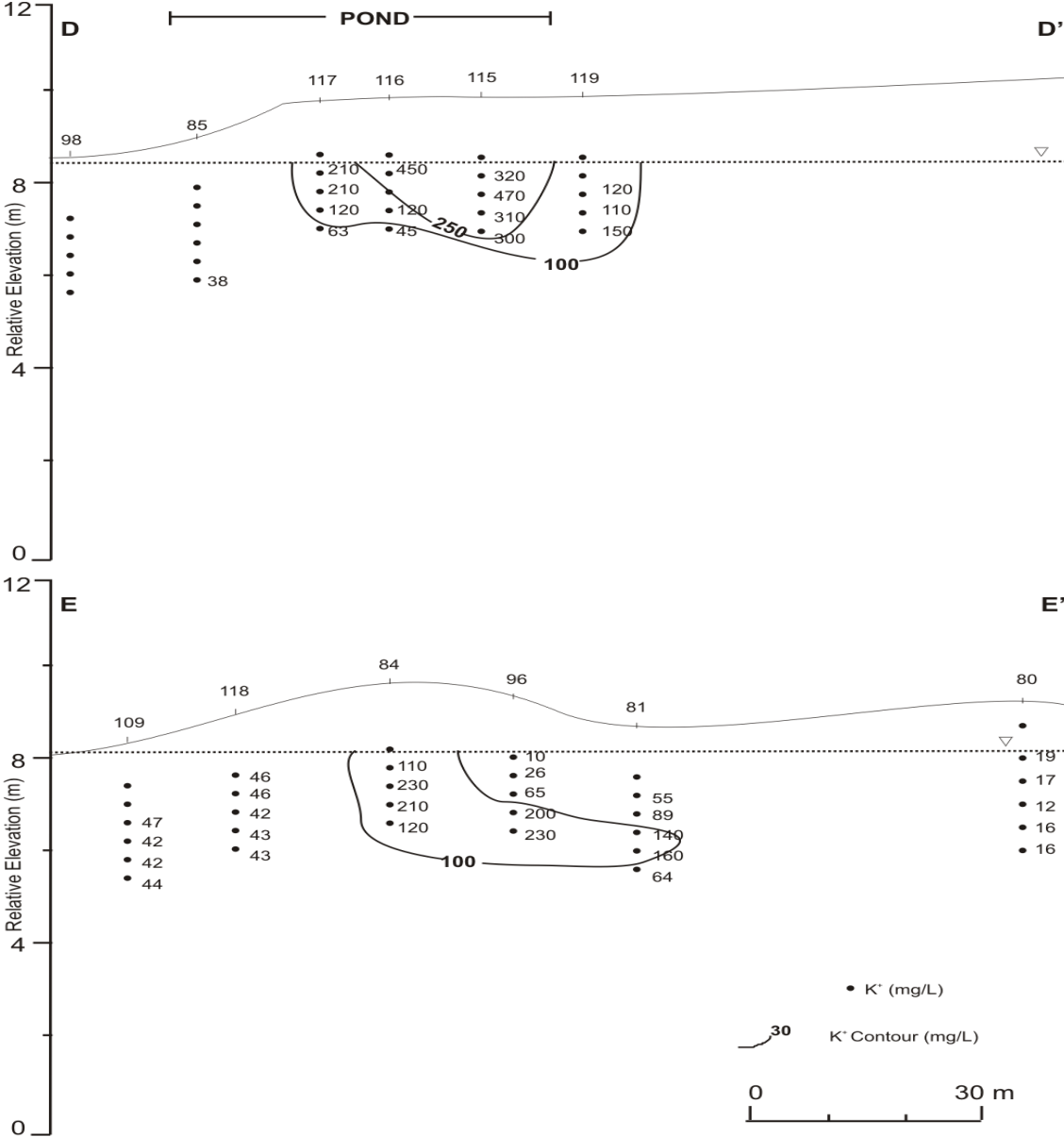


Figure E-1. cont.

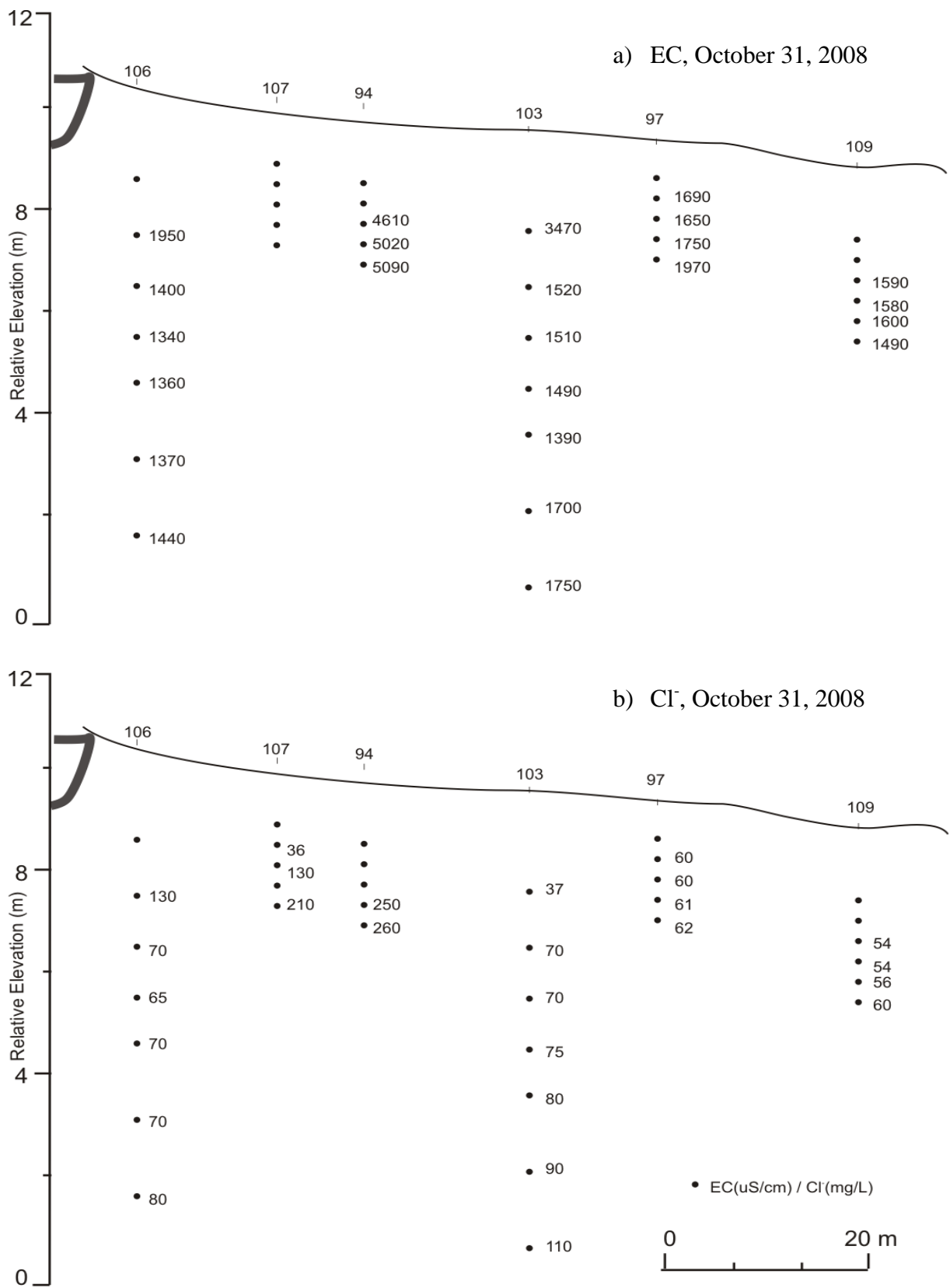


Figure E-2. Distribution of a) EC and b) Cl⁻ along the proposed centre line, October 31, 2008

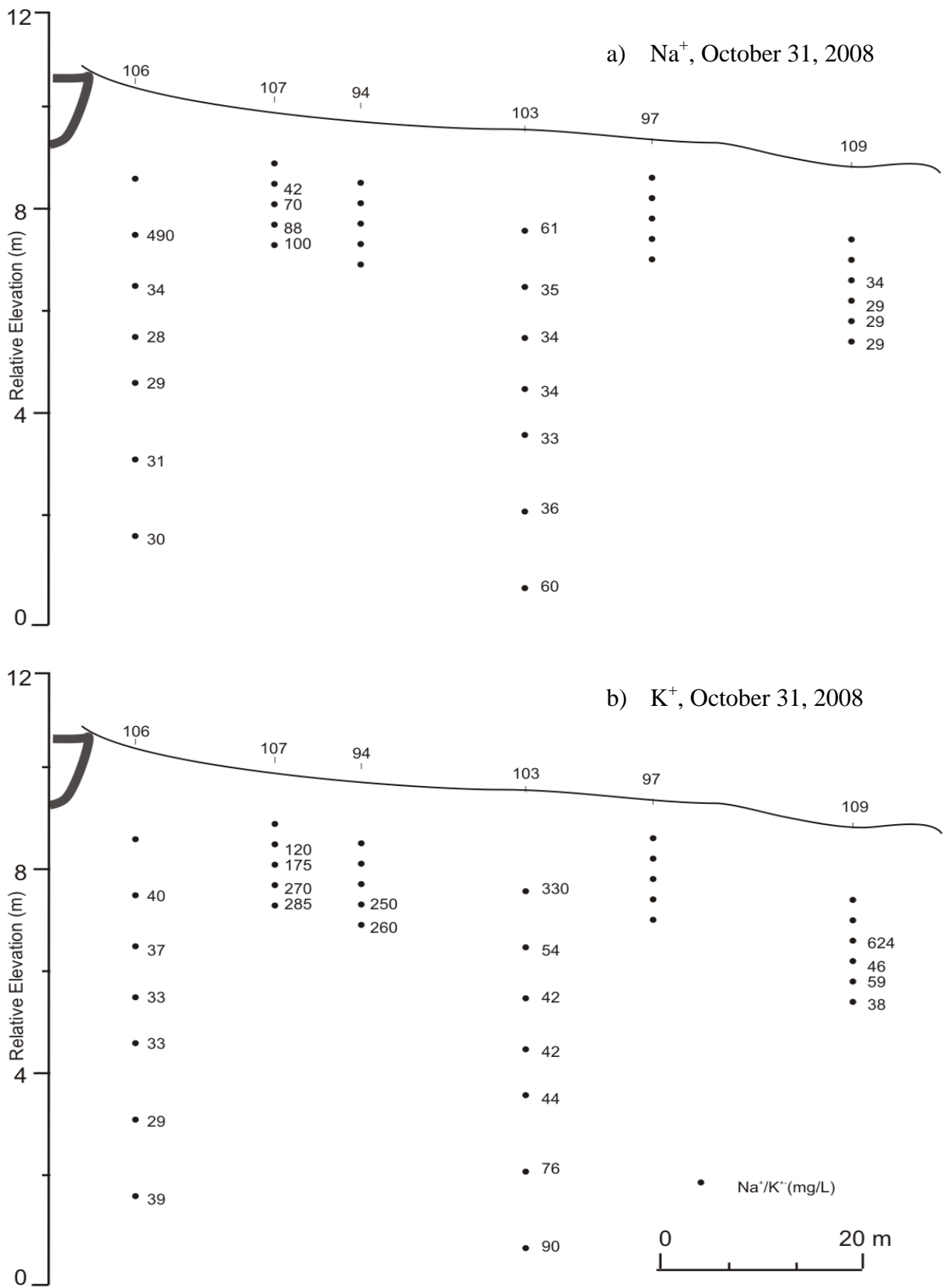


Figure E-3. Distribution of a) Na⁺ and b) K⁺ along the proposed centre line, October 31, 2008

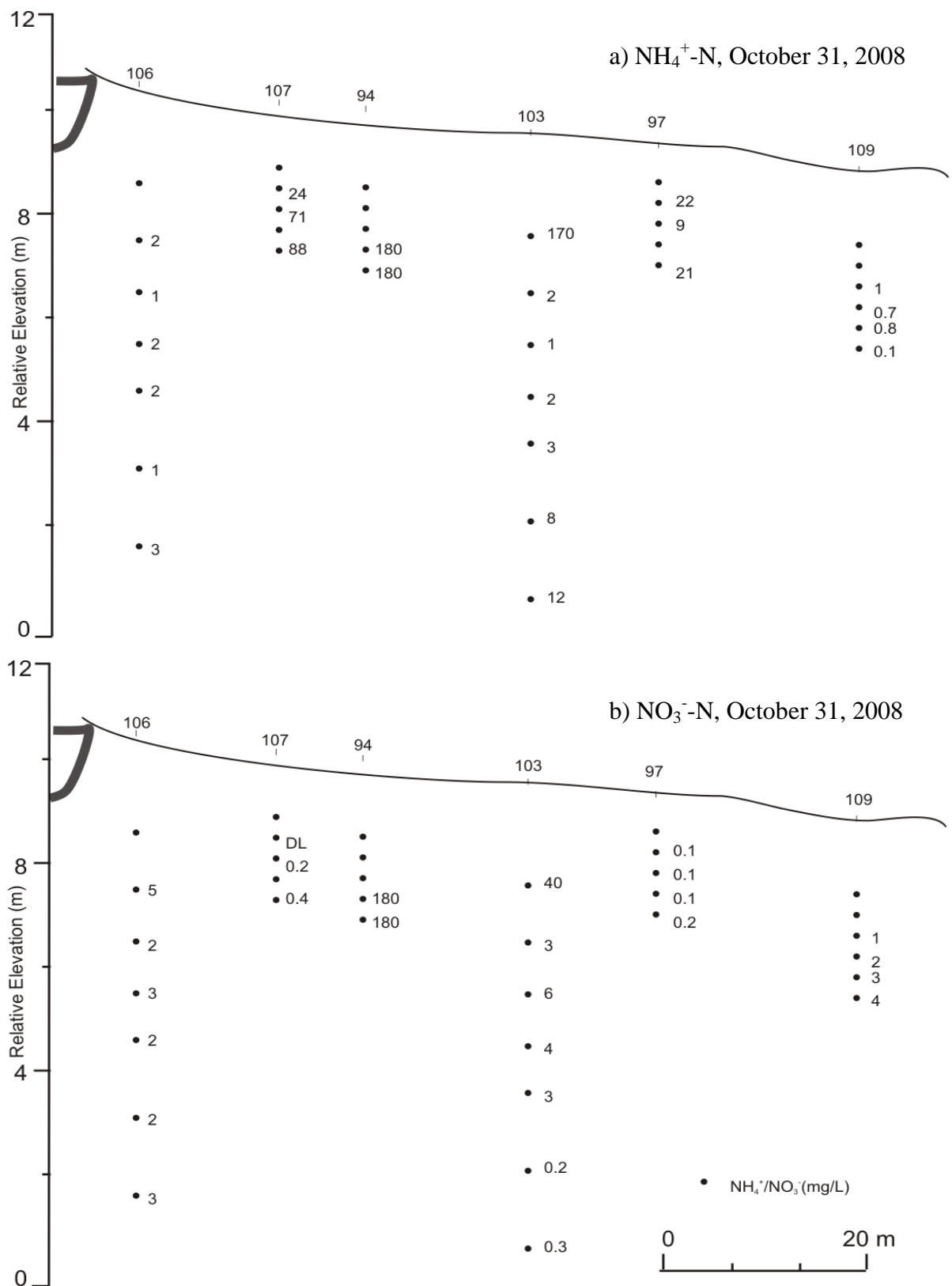


Figure E-4. Distribution of a) $\text{NH}_4^+\text{-N}$ and b) $\text{NO}_3^-\text{-N}$ along the proposed centre line, October 31, 2008.